Journal of the

ENGINEERING MECHANICS DIVISION

Proceedings of the American Society of Civil Engineers

CONTENTS

October, 1958

Papers

Paper 1790 October, 1958 EM 4

Journal of the
ENGINEERING MECHANICS DIVISION
Proceedings of the American Society of Civil Engineers

MINIMUM WEIGHT OF FRAMES UNDER SHAKEDOWN LOADING[a]

Jacques Heyman[1]
(Proc. Paper 1790)

SUMMARY

The first part of the paper discusses the minimum weight design of framed structures under both fixed and independently varying loads. A simple numerical example is given, for which the complete solution is obtained, and the results corresponding to the two types of loading are compared.

An iterative method is then presented for the minimum weight design of a frame of any degree of complexity; this iterative method may lead to results which are slightly inexact.

INTRODUCTION

The type of frame to be considered in this paper is composed of prismatic members, joined together sufficiently rigidly so that the full plastic moment of any member may be developed at such joints. If distributed loads act on a frame, they will be replaced by a suitable combination of concentrated loads; under these conditions, plastic hinges can form only at joints and at loading points, owing to the piecewise linear distribution of bending moments between such critical sections.

The normal assumptions of simple plastic theory will be made, of which the most important are that indefinite rotation can occur at a hinge position under constant moment (the full plastic moment), and that elastic and plastic deflections of the members are negligible compared with the overall dimensions of the frame.

Note: Discussion open until March 1, 1959. To extend the closing date one month, a written request must be filed with the Executive Secretary, ASCE. Paper 1790 is part of the copyrighted Journal of the Engineering Mechanics Division, Proceedings of the American Society of Civil Engineers, Vol. 84, No. EM 4, October, 1958.

a. The results presented in this paper were obtained in the course of research sponsored by the Office of Naval Research under Contract Nonr-562(10) with Brown Univ.

1. Fellow of Peterhouse, Univ. Lecturer in Eng., Univ. of Cambridge, Eng., Visiting Prof., Brown Univ., 1957-58, Providence, R. I.

The total weight of material used in a frame will be taken as proportional to the length and to the full plastic moment of each member; thus, if a typical member has full plastic moment M_K and length ℓ_K, the total weight of material in the frame will be given to some scale by

$$X = \Sigma M_K \ell_K \tag{1}$$

where the summation extends over all the members.

Minimum weight design under these conditions and with fixed loads acting on the frame was first discussed systematically by Foulkes;(1) the basic ideas can perhaps best be presented by means of a simple numerical example.

Design Under Fixed Loads

Consider the two span beam shown in Fig. 1, in which the point loads W_A and W_B act at midspan. Each span has constant section, but the full plastic moments M_A and M_B may have different values. There are four possible modes of collapse of this structure, shown in Fig. 2. Modes (i) and (ii) occur for $M_A < M_B$, and modes (iii) and (iv) for $M_A > M_B$; the actual mode of collapse will depend on the relative magnitudes of $W_A\ell_A$ and $W_B\ell_B$ as well as upon the full plastic moments of the cross-sections.

For example, if collapse occurs by mode (i), then, noting that the work done by the load W_A on a displacement of the collapse mechanisms is $W_A(\frac{1}{2}\ell_A\theta_1)$, while the work dissipated in the hinges is $3M_A\theta_1$, then

$$\text{(i)} \qquad 3M_A = \tfrac{1}{2} W_A \ell_A \tag{2}$$

Similar expressions may be obtained from consideration of the other collapse mechanisms:

$$\text{(ii)} \qquad M_A + 2M_B = \tfrac{1}{2} W_B \ell_B$$

$$\text{(iii)} \qquad 2M_A + M_B = \tfrac{1}{2} W_A \ell_A \tag{2 bis}$$

$$\text{(iv)} \qquad 3M_B = \tfrac{1}{2} W_B \ell_B$$

As a numerical example, suppose the two spans are equal, and that the loads have the magnitudes shown in Fig. 3, so that

$$\begin{aligned} W_A \ell_A &= 1200 \\ W_B \ell_B &= 600 \end{aligned} \tag{3}$$

(Note that it is not necessary to specify the units of length or of load in Eqs. (3)). Eqs. (2) then become

$$\begin{aligned} &\text{(i)} && M_A = 200 \\ &\text{(ii)} && M_A + 2M_B = 300 \\ &\text{(iii)} && 2M_A + M_B = 600 \\ &\text{(iv)} && M_B = 100 \end{aligned} \tag{4}$$

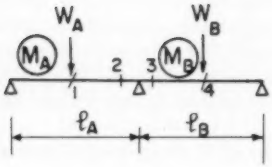

FIG. 1

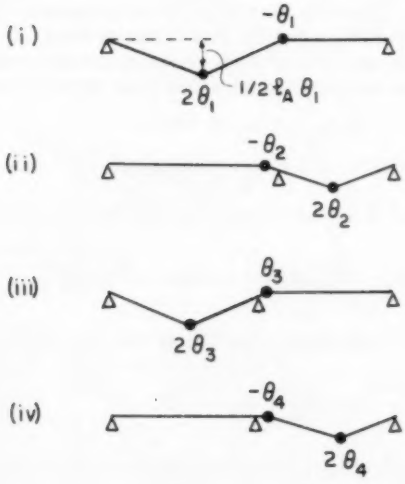

FIG. 2

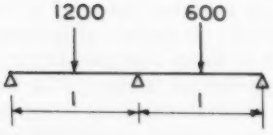

FIG. 3

Eqs. (4) are plotted in the design plane with axes M_A and M_B shown in Fig. 4. According to the principles of simple plastic theory, a point in this plane which lies within the open convex polygon, defined by the mechanism lines, Eqs. (4), and shown shaded in Fig. 4, will represent a safe design of the structure, i.e. one capable of withstanding the given loads. A point on the boundary of the polygon represents a design of the structure which is just collapsing under the given loads; for this particular example, therefore, mode (ii) cannot occur for any values of M_A and M_B. All points on the boundary of the polygon must now be examined to determine which represents the minimum weight design.

From Eq. (1), the weight of the two-beam system is given by

$$X = M_A + M_B \tag{5}$$

This weight line, when plotted in the design plane, is a line of 45° slope whose distance from the origin is proportional to the weight of the structure. Since the minimum weight is required, this will occur when the weight line is just "tangent" to the polygon. Thus the vertex M of the polygon in Fig. 4 represents the minimum weight design for the two-beam system. It will be seen that two mechanisms ((iii) and (iv)) are operating simultaneously; from Eqs. (4), the equations of these two mechanisms lines can be written

$$\begin{aligned} 2\alpha M_A + \alpha M_B &= 600\,\alpha \\ \beta M_B &= 100\,\beta \end{aligned} \tag{6}$$

where multipliers α and β have been taken for the two equations. Adding Eqs. (6),

$$2\alpha M_A + (\alpha+\beta) M_B = 600\,\alpha + 100\,\beta \tag{7}$$

and comparing Eq. (7) with the weight Eq. (5), it will be seen that if $\alpha = 0.5$, $\beta = 0.5$,

$$X = M_A + M_B = 350 \tag{8}$$

This superposition of alternative mechanisms is characteristic of minimum weight design; in the simple example above, positive coefficients α and β could be found such that when these were multiplied into the mechanism equations, the equation resulting from their superposition gave the weight line. Interpreted geometrically, the condition that the coefficients α and β are positive implies that the tangent weight line in Fig. 4 lies within the acute angle formed by the intersection of mechanism lines (iii) and (iv). This condition is necessary if the weight line is to be "tangent" to the convex polygon.

These simple results were extended and proved rigorously by Foulkes for the case in which a frame is being designed to have N different full plastic moments. A geometrical representation can be made in an N-dimensional design space, the former mechanism lines being replaced by hyperplanes or "flats". The mechanism flats for all conceivable modes of collapse define an open convex polyhedron (the permissible region). In general, the weight flat will be "tangent" at a vertex of the permissible region, each vertex being characterized by the intersection of, in general, N mechanism flats. Thus the minimum weight design will be characterized by N alternative mechanisms,

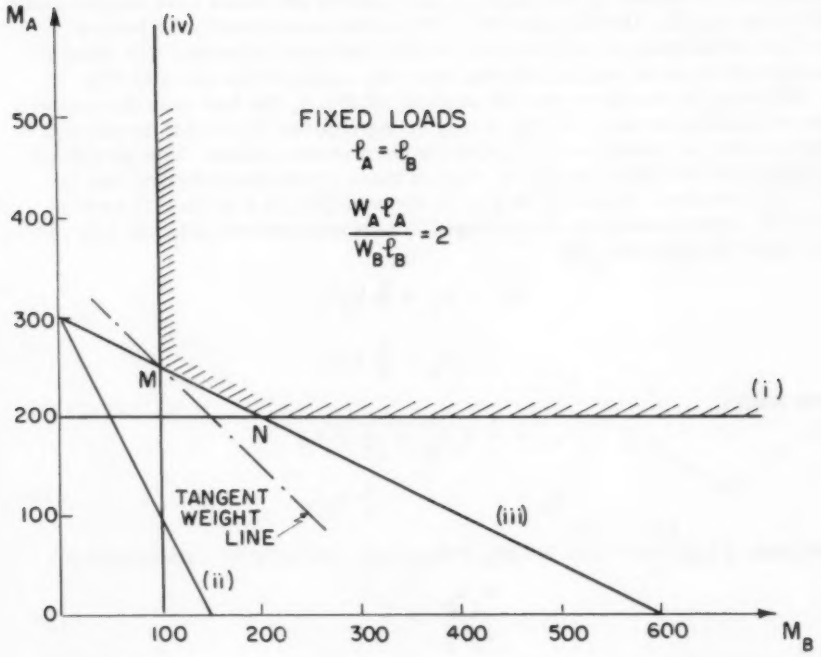
M_A
(iv)
500
400
300
200
100
0
FIXED LOADS
$\rho_A = \rho_B$
$\frac{W_A \rho_A}{W_B \rho_B} = 2$
M
N
(i)
TANGENT WEIGHT LINE
(ii)
(iii)
100
200
300
400
500
600
M_B

FIG. 4

and these may be superposed with positive coefficients to give what may be called a Foulkes mechanism which coincides with the tangent weight flat.

In exceptional cases, a vertex of the permissible region may give more than N alternative mechanisms; such behaviour does not interfere with the calculations. Alternatively, it may happen that one of the faces of the polyhedron is itself parallel to the weight flat; for example, the weight line in Fig. 4 might by accident have been parallel to mechanism line (iii), in which case a design represented by any point on the segment MN would have had the same minimum weight. (Mechanism (iii) in this case would itself have been a Foulkes mechanism; it will be seen readily that such behaviour will arise for the specific case of one span having twice the length of the other in Fig. 1).

Returning to the more general example of Fig. 1, the four possible mechanisms of collapse shown in Fig. 2 may be superposed in pairs in an attempt to characterize all possible vertices of the permissible region. The significant possibilities are shown in Fig. 5, each of these mechanisms having two degrees of freedom. Vertex M in Fig. 4, for example, is a particular case of mode D, corresponding to the superposition of mechanisms (iii) and (iv). For this mode D, from Eqs. (2),

$$\begin{aligned} 2M_A + M_B &= \tfrac{1}{2} W_A \ell_A \\ 3M_B &= \tfrac{1}{2} W_B \ell_B \end{aligned} \tag{9}$$

from which

$$\begin{aligned} M_A &= \tfrac{1}{4} W_A \ell_A - \tfrac{1}{12} W_B \ell_B \\ M_B &= \tfrac{1}{6} W_B \ell_B \end{aligned} \tag{10}$$

Now mode 4 can occur only for $M_A > M_B$; Eqs. (10) give for this condition

$$\frac{W_A \ell_A}{W_B \ell_B} > 1 \tag{11}$$

Further, Eqs. (9) must be combinable with positive coefficients (α and β say) to give the Foulkes mechanism

$$\ell_A M_A + \ell_B M_B = X \tag{12}$$

Thus

$$\begin{aligned} 2\alpha &= \ell_A \\ \alpha + 3\beta &= \ell_B \end{aligned} \tag{13}$$

from which

$$\begin{aligned} \alpha &= \tfrac{1}{2} \ell_A \\ \beta &= -\tfrac{1}{6} \ell_A + \tfrac{1}{3} \ell_B \end{aligned} \tag{14}$$

The condition that β be positive gives

$$\frac{\ell_A}{\ell_B} < 2 \tag{15}$$

A (i)+(ii)

$M_A < M_B$

B (i)+(iii)

$M_A = M_B$

C (ii)+(iv)

$M_A = M_B$

D(iii)+(iv)

$M_A > M_B$

FIG. 5

Inequalities (11) and (15) thus define the region D in Fig. 6 within which all minimum weight designs having $M_A > M_B$ must lie. Similar considerations of the modes A, B and C in Fig. 5 lead to the correspondingly marked regions in Fig. 6. Fig. 6 is complete; knowing the ratios $W_A l_A / W_B l_B$ and l_A / l_B, the minimum weight design can be determined immediately by using the figure.

Shakedown Phenomena

From Eqs. (6) and Fig. 4 for the simple beam example shown in Fig. 3, it is seen that the minimum weight design for this particular static loading condition is

$$M_A = 250$$
$$M_B = 100 \qquad (16)$$

Suppose now that the two loads W_A and W_B are not fixed, but may vary independently within the ranges

$$0 \leq W_A \leq 1200$$
$$0 \leq W_B \leq 600 \qquad (17)$$

that is, the loads have the same respective maximum values as before, but can now take on any lesser positive values. The minimum weight design, Eqs. (16), is now inadequate to carry the system of varying loads, since incremental collapse will for the corresponding load rapidly occur after a few cycles of loading.

The phenomenon of incremental collapse may be explained briefly as follows: Suppose a given frame is acted upon by a set of loads varying between prescribed limits, and that an elastic analysis is made for the effect of each load acting separately. For each critical section, the two combinations of loads can then be determined to give the greatest and least total elastic moment at the section considered. If the greatest and least elastic moments at all critical sections are less in absolute value than the corresponding full plastic moments, then the structure is safe. ("Full plastic moment" in the above sentence should really be replaced by "yield moment", but this does not affect the argument).

Suppose, however, that at one (or more) critical section the maximum elastic moment is greater than the full plastic moment. When the corresponding load combination is applied to the frame, yield will occur at that section, and a redistribution of bending moments will occur accompanied by the generation of a system of residual moments (self-stressing moments) in the frame. Providing this residual system remains unaltered, the next time that the same loading combination is applied no further yield will occur. The response of the frame will be purely elastic, and the structure is said to have shaken down.

However, plastic flow at some other critical section under some other load combination may have altered the residual moments; in this case, a second application of the original load combination may cause further plastic flow at the original section. Thus, as the loads vary independently, there is the possibility of plastic hinge rotations occurring at certain critical sections under one load combination, further hinge rotations occurring at other sections under another load combination, and so on. If this occurs, and if the sections which suffer plastic deformation are so located that they would form a plastic hinge system for a mechanism in the usual sense, then eventually the frame will

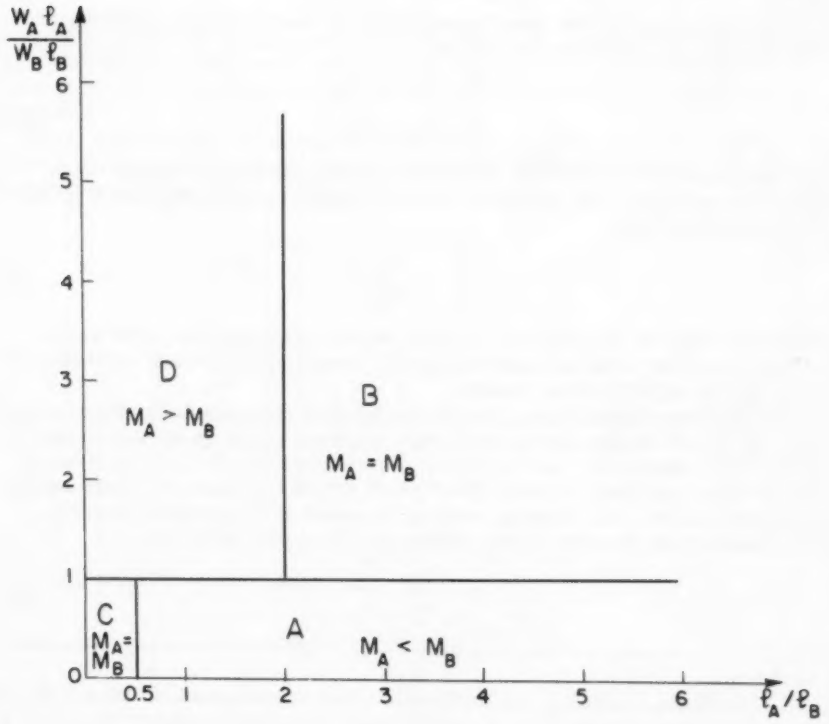
$\frac{W_A \ell_A}{W_B \ell_B}$
6
5
4
3
2
1
0
D
$M_A > M_B$
B
$M_A = M_B$
C
$M_A = M_B$
A
$M_A < M_B$
0.5
1
2
3
4
5
6
ℓ_A / ℓ_B

FIG. 6

suffer severe deformations. Indeed, after only a few cycles of loading, the frame will look as if it had formed a mechanism under static loading. Thus failure by incremental collapse is in effect failure by the formation of a collapse mechanism; the hinges of this mechanism are not formed together, but some under one load combination, and some under another (or others).

Minimum Weight Design Under Shakedown Loading

Consider again the two span beam in Fig. 1, where now the loads W_A and W_B can take any values in the ranges

$$0 \leq W_A \leq P_A$$
$$0 \leq W_B \leq P_B \qquad (18)$$

The moments of inertia of the two beams will be denoted I_A and I_B; these quantities are obviously related to the full plastic moments M_A and M_B, and it will be assumed that

$$\frac{I_A}{I_B} = \left(\frac{M_A}{M_B}\right)^n \qquad (19)$$

A typical value for the exponent n might be 1.4; in most of the work which follows, n will be taken as unity for ease of computation, without seriously restricting the validity of the results.

The following Table I gives the elastic bending moments at the four critical sections (1 to 4 in Fig. 1); the first two lines show the moments due to the loads acting separately, and these are then combined in the last two lines to give greatest and least values $\mathcal{M}$ max and $\mathcal{M}$ min as the loads vary between the prescribed limits (18). Sagging bending moments are considered positive. The quantity k is the ratio of the stiffnesses of the two spans, i.e.

$$k = \frac{\ell_A}{\ell_B} \cdot \frac{I_B}{I_A} \qquad (20)$$

Section	1	2,3	4
Load W_A	$\frac{W_A \ell_A}{32}\left(\frac{8+5k}{1+k}\right)$	$-\frac{W_A \ell_A}{32}\left(\frac{6k}{1+k}\right)$	$-\frac{W_A \ell_A}{32}\left(\frac{3k}{1+k}\right)$
Load W_B	$-\frac{W_B \ell_B}{32}\left(\frac{3}{1+k}\right)$	$-\frac{W_B \ell_B}{32}\left(\frac{6}{1+k}\right)$	$\frac{W_B \ell_B}{32}\left(\frac{5+8k}{1+k}\right)$
$\mathcal{M}^{\max}$	$\frac{P_A \ell_A}{32}\left(\frac{8+5k}{1+k}\right)$	0	$\frac{P_B \ell_B}{32}\left(\frac{5+8k}{1+k}\right)$
$\mathcal{M}^{\min}$	$-\frac{P_B \ell_B}{32}\left(\frac{3}{1+k}\right)$	$-\frac{P_A \ell_A}{32}\left(\frac{6k}{1+k}\right) - \frac{P_B \ell_B}{32}\left(\frac{6}{1+k}\right)$	$-\frac{P_A \ell_A}{32}\left(\frac{3k}{1+k}\right)$

Table I

Now, for any critical section i, the necessary and sufficient condition (2,3) for shakedown to occur is that a residual bending moment m_i can be found such that

$$\mathcal{M}_1^{max} + m_1 \leq M_{K1}$$

$$\mathcal{M}_1^{min} + m_1 \geq -M_{K1} \qquad (21)$$

where M_{Ki} is the full plastic moment of the member at section i. In the limit, the inequalities similar to (21) are replaced by equalities at a sufficient number of critical sections for an incremental collapse mechanism to be formed.

Thus, suppose Fig. 2(i) gives the mode of incremental collapse of the two-span beam under the varying loads, hinges being formed at sections 1 and 2. Reference to Table I shows that

$$\frac{P_A \ell_A}{32}\left(\frac{8+5k}{1+k}\right) + m_1 = M_A$$

$$-\frac{P_A \ell_A}{32}\left(\frac{6k}{1+k}\right) - \frac{P_B \ell_B}{32}\left(\frac{6}{1+k}\right) + m_2 = -M_A \qquad (22)$$

The residual moments m_1 and m_2 must be in equilibrium with zero external load; by virtual work, using the mechanism of Fig. 2(i) again,

$$(2\theta_1)m_1 + (-\theta_1)m_2 = 0$$

$$\text{or} \qquad 2m_1 - m_2 = 0 \qquad (23)$$

Eqs. (22) and (23) solve to give

(i) $$3M_A = \frac{P_A \ell_A}{2} + \frac{P_B \ell_B}{32}\left(\frac{6}{1+k}\right) \qquad (24)$$

and this equation must be satisfied if incremental collapse is just to occur by mode (i). Similar analyses may be made for the other three modes in Fig. 2. (It is not in fact necessary to introduce the residual moments since these are always eliminated. For example, Eq. (24) above could have been found by noting that since

$$\mathcal{M}_1^{max} + m_1 = M_A$$

$$\mathcal{M}_2^{min} + m_2 = -M_A$$

then the sum obtained by adding the first of these equations multiplied by $(2\theta_1)$ to the second multiplied by $(-\theta_1)$ will give precisely Eq. (24), m_1 and m_2 disappearing by virtue of Eq. (23). The quantities $(2\theta_1)$ and $(-\theta_1)$ are the hinge rotations of the mechanism considered, Fig. 2(i)). The other three modes give

(ii) $$M_A + 2M_B = \frac{P_A \ell_A}{32}\left(\frac{6k}{1+k}\right) + \frac{P_B \ell_B}{2}$$

(iii) $$2M_A + M_B = \frac{P_A \ell_A}{2} + \frac{P_B \ell_B}{32}\left(\frac{6}{1+k}\right) \qquad (24 \text{ bis})$$

(iv) $$3M_B = \frac{P_A \ell_A}{32}\left(\frac{6k}{1+k}\right) + \frac{P_B \ell_B}{2}$$

For the simple numerical example, $\ell_A = \ell_B = 1$, suppose again that

$$P_A \ell_A = 1200$$
$$P_B \ell_B = 600 \qquad (25)$$

Then Eqs. (24) give

(i) $$M_A = 200 + \frac{37.5}{1+k}$$

(ii) $$M_A + 2M_B = 225\left(\frac{k}{1+k}\right) + 300 \qquad (26)$$

(iii) $$2M_A + M_B = 600 + \frac{112.5}{1+k}$$

(iv) $$M_B = 75\left(\frac{k}{1+k}\right) + 100$$

where k, for the particular case $\ell_A = \ell_B$, is given from Eqs. (20) and (19):

$$k = \frac{I_B}{I_A} = \left(\frac{M_B}{M_A}\right)^n \qquad (27)$$

For n = 1, Eqs. (26) are plotted in Fig. 7, in a way similar to that for the static loading, Fig. 4. Comparison of the two figures shows the general resemblance of the cases of fixed and of varible loads; minimum weight in Fig. 7 is again represented by the point M at which two alternative mechanisms form, and for which

$$M_A = 277$$
$$M_B = 123$$
$$X = 400 \qquad (28)$$

Note the marked increase in weight X, from 350 in Eq. (8) to 400 for the variable loads having the same maxima as the fixed loads.

The lines giving the boundary of the permissible region in Fig. 7 are slightly curved. There is thus the possibility of the weight line being tangent to the permissible region at a point which is not an apex. Fig. 8 illustrates this. For the particular ratios $\ell_A = 1.621\,\ell_B$, and $P_A \ell_A = 2P_B\ B$, the straight line joining the apices MN of the permissible region is parallel to the weight line. Since the mechanism line (iii) is slightly curved, the true minimum weight will occur at a point on the boundary of the permissible region between M and N. The weight of the designs corresponding to points M and N is 561.7 (for $P_A \ell_A = 1200$, as before); the true minimum weight is given by calculation as 561.1. The curvature of the portion MN of mechanism line (iii) in Fig. 8 is so slight that the point of tangency cannot be distinguished in this figure. Fig. 9 shows the calculated weight X for designs lying on the line MN, and gives the minimum weight for the ratio M_B/M_A equal to about 0.75. Thus confining attention to the apices of the permissible region leads to an error of about 0.1%. In the following, no attempt is made to allow for this slight error, and it is assumed that minimum weight always occurs at an apex of the permissible region.

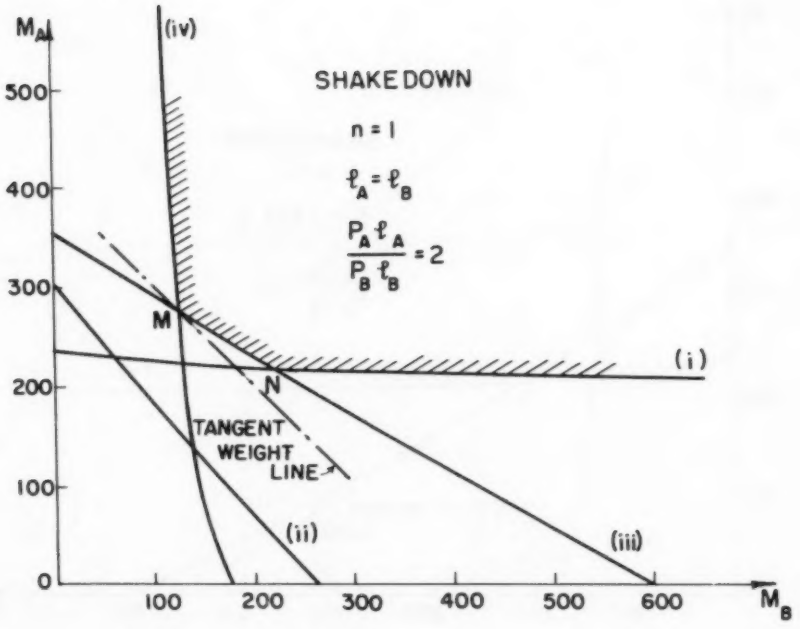
M_A
(iv)
SHAKE DOWN
n = 1
$\ell_A = \ell_B$
$\frac{P_A \ell_A}{P_B \ell_B} = 2$
500
400
300
200
100
0
M
N
(i)
TANGENT
WEIGHT
LINE
(ii)
(iii)
100
200
300
400
500
600
M_B

FIG. 7

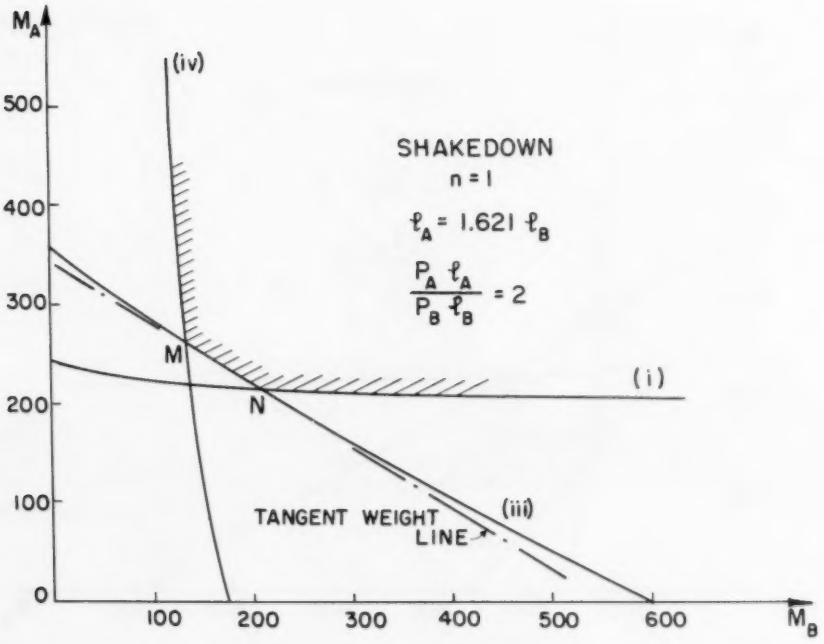
M_A
500
400
300
200
100
0
(iv)
SHAKEDOWN
n = 1
$\ell_A = 1.621\ \ell_B$
$\frac{P_A\ \ell_A}{P_B\ \ell_B} = 2$
M
N
(i)
(iii)
TANGENT WEIGHT LINE
100
200
300
400
500
600
M_B

FIG. 8

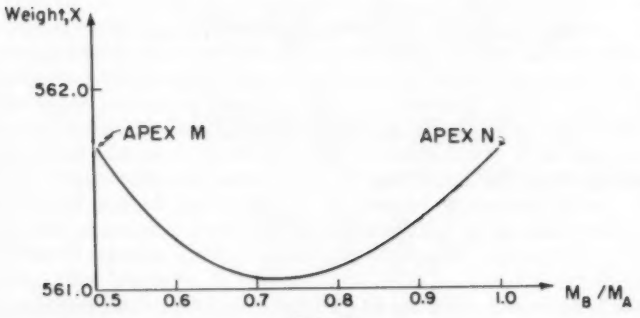
Weight, X
562.0
561.0
APEX M
APEX N
0.5
0.6
0.7
0.8
0.9
1.0
M_B/M_A

FIG. 9

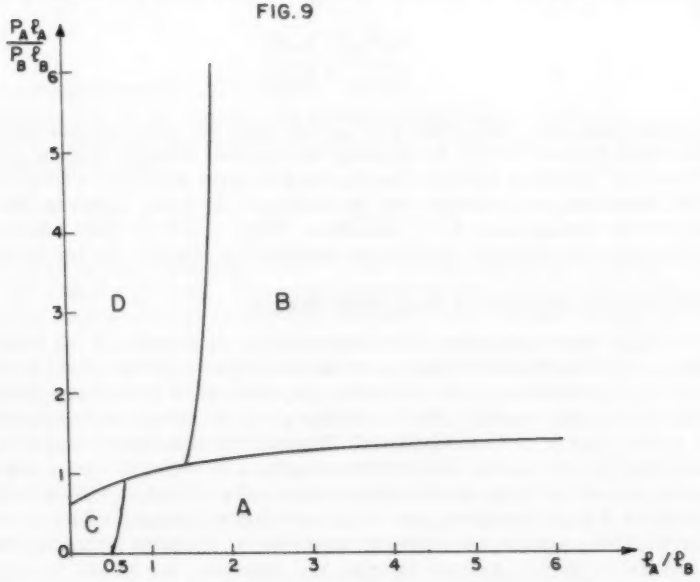
$\frac{P_A \ell_A}{P_B \ell_B}$
6
5
4
3
2
1
0
D
B
A
C
0.5
1
2
3
4
5
6
ℓ_A/ℓ_B

FIG. 10

A brief discussion of the full solution for the two-span beam problem will now be given. As before, Fig. 5 gives the significant possibilities of alternative collapse mechanisms corresponding to apices of the permissible region. For mode D of incremental collapse, for example, (combination of mechanisms (iii) and (iv) as in Fig. 7), Eqs. (24) give

$$M_A = \frac{P_A \ell_A}{96}\left(\frac{24+21k}{1+k}\right) + \frac{P_B \ell_B}{96}\left(\frac{1-8k}{1+k}\right)$$

$$M_B = \frac{P_A \ell_A}{96}\left(\frac{6k}{1+k}\right) + \frac{P_B \ell_B}{96}\left(\frac{16+16k}{1+k}\right) \qquad (29)$$

where k is given by Eqs. (20) and (19),

$$k = \frac{\ell_A}{\ell_B}\frac{I_B}{I_A} = \frac{\ell_A}{\ell_B}\left(\frac{M_B}{M_A}\right)^n \qquad (30)$$

As before, mode D can occur only for $M_A \geq M_B$; from Eqs. (29), this condition gives

$$\frac{P_A \ell_A}{P_B \ell_B} \geq \frac{5+8k}{8+5k} \qquad (31)$$

In the limit when $M_A = M_B$, then $k = \ell_A/\ell_B$ from Eq. (30), and the equality (31) has been plotted in Fig. 10 dividing the regions B and D from A and C. The "vertical" dividing lines in this figure are more difficult to determine, but implicit analytical expressions may be obtained; the lines shown in Fig. 10 are drawn for the exponent n = 1, as usual. Figs. 6 and 10 again bear marked resemblances, the straight lines being replaced by slightly curved lines.

General Iterative Method for Shakedown Design

It will have been noted that shake-down design is essentially an elastic problem, since the elastic response of the structure must be used. Now the elastic bending moments in the structure depend on the stiffnesses of the various members; unfortunately, for the design problem, these stiffnesses are not known at the start of the calculations. Thus the vicious circle obtains in which it is necessary to know the sizes of the members in order to obtain the elastic response, and to know the elastic response in order to determine the sizes of the members for minimum weight. It is true that by employing some device such as a stiffness matrix (written in symbols), a complete formal solution can be obtained; such a solution is unwieldy, however, for all but the very simplest frames.

The iterative method proposed assumes a certain design of the frame. The method of moment distribution, or some other convenient means of elastic analysis, will then enable the elastic response under the given loads to be determined. In particular, $\mathcal{M}_{max}$ and $\mathcal{M}_{min}$ can be calculated for each section. These values of $\mathcal{M}_{max}$ and $\mathcal{M}_{min}$ are then taken to be unvarying, and the minimum weight design is derived under these conditions. This minimum weight design will differ, in general, from that originally assumed. New values of $\mathcal{M}_{max}$ and $\mathcal{M}_{min}$ are then calculated, and the process is repeated, convergence usually being reasonably fast.

The computations will be made in the tabular form proposed recently.(4,5) As an example, the same two-span beam problem will be considered, with $\ell_A = \ell_B = 1$, $P_A \ell_A = 2P_B \ell_B = 1200$, $k = (M_B/M_A)^n$ (see Fig. 7). The computation will be started by assuming that one beam is of negligible strength compared with the other, say $M_B << M_A$, i.e. $k = 0$. The elastic bending moments may then be computed directly, or, for this simple example, $k = 0$ can be substituted in the expressions for $\mathcal{M}^{max}$ and $\mathcal{M}^{min}$ in Table I. The resulting values of $\mathcal{M}^{max}$ and $\mathcal{M}^{min}$ have been entered as Step O in line 4 of Table II, the first four values corresponding to $\mathcal{M}^{max}$ at the sections 1 to 4.

The three preceding lines in Table II, labelled "data", represent the hinge rotations of independent elementary mechanisms from which all conceivable mechanisms can be obtained by linear combination. For example, line 1 in Table II represents the mechanism in Fig. 2(i); line 10 in the same Table, which is the sum of lines 1 and 3, represents the mechanism in Fig. 2(iii). These data equations also give the coefficients of the independent homogeneous equilibrium equations which must be satisfied by any system of residual moments; for example, if residual moments m_1 and m_2 act at sections 1 and 2, then line 1 of the Table states that

$$2m_1 - m_2 = 0 \tag{32}$$

which is identical with Eq. (23) above.

Examining line 4 of Table II, and remembering that it is assumed for the moment that this line represents a fixed elastic response, it will be seen that a beam system having

$$M_A = 300, \qquad M_B = 112.5, \qquad X = 412.5 \tag{33}$$

is safe. (The largest absolute values of the elastic moments in spans A and B are asterisked in line 4). The most general system of residual moments will now be constructed in an attempt to modify line 4 in such a way that the total weight X is reduced, and subject to the following condition: If the maximum moment in span K is M_K, then the sections at which M_K occurs will be "attacked" by residual moments $-m_K$. Thus all "hinges" (sections at which the moment M_K acts) will be maintained while the value of M_K is reduced in an attempt to reduce the total weight of the structure.

For the numerical example, it will be seen that the largest moment in span A occurs at section 1. Thus the residual moment m_1 will be set equal to $-m_A$; similarly, the largest moment in span B occurs at section 3, and m_3 will be set equal to $+m_B$. Data Eq. (3) requires that $m_2 = m_3 = m_B$, while data Eq. (2) gives $m_4 = \frac{1}{2} m_3 = \frac{1}{2} m_B$. These values are displayed in line 5 of Table II. Further, data Eq. (1) requires $2m_A + m_B = 0$, so that line 6 of Table II gives the most general distribution of residual bending moments that can be used to modify line 4. For example, the moment at section 1 can be reduced to $300 - m_A$, representing a saving of material of $1 \times m_A$, while the moment at section 3 is increased to $|112.5 + 2m_A|$, representing an increase in material consumption of $1 \times 2m_A$. Such a change implies a net increase in material consumption; evidently if m_A is taken negative, a saving in material will be made. The maximum saving occurs for $m_A = -6.2$, noted in line 6 of Table II; line 7 gives the residual moment distribution to be added to line 4, and line 8 gives the result of this operation. m_A was limited to the value -6.2 since a

STEP	LINE	PLASTIC MOMENT SECTION	M_A 1	M_A 2	M_B 3	M_B 4	M_A 1	M_A 2	M_B 3	M_B 4	
DATA	1		2	-1							
	2				-1	2					
	3			1	-1						
0	4	k = 0	300*	0	0	93.8	-56.3	-112.5	-112.5*	0	X=412.5
I	5	$2m_A+m_B=0$	$-m_A$	m_B	m_B	$\frac{1}{2}m_B$	$-m_A$	m_B	m_B	$\frac{1}{2}m_B$	
	6	$1\times 6.23=6.2$ | m_A	-1	-2	-2	-1	-1	-2	-2	-1	
	7	$m_A=-6.23$	6.2	12.5	12.5	6.2	6.2	12.5	12.5	6.2	
	8		306.2	12.5	12.5	100*	-50.1	-100	-100	6.2	X=406.2
II	9		+		-	+					
	10	1+3 | α	2		-1						
	11	2 | β			-1	2					
	12		(2α)		$-(\alpha+\beta)$	(2β)					
	13	$\alpha=\frac{1}{2}$, $\beta=\frac{1}{6}$	(1)		$-(\frac{2}{3})$	$(\frac{1}{3})$					
0	14	k =0.326	272.6*	0	0	107.8	-42.5	-140.3	-140.3*	-27.7	X=412.9
I	15	$m_A=-10.83$	10.8	21.7	21.7	10.8	10.8	21.7	21.7	10.8	
	16		283.4	21.7	21.7	118.6*	-31.7	-118.6	-118.6	-16.9	X=402.0
0	17	k =0.418	267.0*	0	0	110.3	-39.7	-145.8	-145.8*	-33.2	X=412.8
I	18	$m_A=-11.83$	11.8	23.7	23.7	11.8	11.8	23.7	23.7	11.8	
	19		278.8	23.7	23.7	122.1*	-27.9	-122.1	-122.1	-21.4	X=400.9
0	20	k =0.438	265.4*	0	0	110.8	-39.1	-146.8	-146.8*	-34.3	X=412.2
I	21	$m_A=-12$	12	24	24	12	12	24	24	12	
	22		277.4	24	24	122.8*	-27.1	-122.8	-122.8	-22.5	X=400.2

TABLE II

new hinge is formed at section 4 for this value. No further change is possible in an attempt to save material, and Step I, occupying lines 5 to 8 in Table II, is terminated. (In general, Step I may be repeated by making suitable modifications; an example is given below).

Step II, lines 9 to 13, checks that the Foulkes mechanism which always appears at the end of Step I is a true Foulkes mechanism. Line 9 gives the signs of the hinge rotations corresponding to line 8; note that the negative hinge has been transferred from the second half of the Table. The original data equations are now combined in such a way that zero coefficients occur at critical sections (i.e. section 2 in this example) where no hinge has been formed. This has been done in lines 10 and 11; line 12 gives the most general combination of the two mechanisms under coefficients α and β. For a true, as opposed to a false, Foulkes mechanism, the quantities in brackets in line 12 must be positive, and, in each span, must sum to the length of the span. Line 13 displays the hinge rotations under these conditions, and it will be seen that the solution is satisfactory. (Had one or more of the quantities in brackets been negative, corresponding to a false Foulkes mechanism, then Step I could be re-initiated by dropping the requirement of maintaining the hinge at one of these false hinge positions.)

From line 8 of Table II it will be seen that subject still to the (false) assumption that the elastic response is invariant and given by the bending moments in line 4, a safe design of the two beams is

$$M_A = 306.2, \quad M_B = 100.0, \quad X = 406.2 \tag{34}$$

These values give k = 100.0/306.2 = 0.326, and this revised value of k will give rise to a modified set of elastic moments in the frame. This new elastic response is entered as a new Step O in line 14 of Table II; as before, the total weight of the beam system is reduced, and the design corresponding to line 16 is

$$M_A = 283.4, \quad M_B = 118.6, \quad X = 402.0 \tag{35}$$

The new value of k is 0.418, and the process is repeated; after four iterations, the values

$$M_A = 277.4, \quad M_B = 122.8, \quad X = 400.2 \tag{36}$$

are derived, compared with the correct values given in Eqs. (28).

If k had been taken as $(M_B/M_A)^n$, where n is not equal to unity, it is evident that no complications would have arisen. The iteration may have been shorter or longer, depending on the starting value of k.

A second example will show that errors can be introduced into the analysis by using the concept that the elastic response is fixed for any one iteration. Consider the same beam system, Fig. 1, but with

$$P_A \ell_A = 2P_B \ell_B = 1200$$

$$\ell_A = 1.8 \tag{37}$$

$$\ell_B = 1$$

Reference to Fig. 10 shows that the design point lies within the area B, for which the two beams have equal sections, and exact calculation gives

$$M_A = M_B = 213.2, \qquad X = 597.0 \tag{38}$$

Now $k = 1.8\, M_B/M_A$: the iterative process will be started assuming a uniform beam, i.e. $k = 1.8$. The working is given in Table III(a), and after three iterations line 10 gives

$$M_A = 260, \qquad M_B = 137, \qquad X = 605 \tag{39}$$

This design is satisfactory in that the corresponding beam system will just fail by incremental collapse under the given loads; however, comparison with Eqs. (38) shows that it is not the minimum weight design, the weight being just over 1% too high.

The iterative method has converged on the wrong vertex of the permissible region; using Fig. 7 for illustrative purposes (this figure is drawn for $\ell_A = \ell_B$ and not $\ell_A = 1.8\, \ell_B$), the iterative method has given vertex M as the minimum weight design whereas the true minimum occurs at vertex N. The error (which, as was seen, was small) has been introduced because of the false assumption that the elastic response may be regarded as fixed while the ratio M_A/M_B is changed. Line 2 of Table III shows the saving consequent on changing m_A by a certain amount; if m_A is given the value unity, for example, a saving of 1.8 units of material will be effected in span A, but an increase of 2 units of material will occur in span B. Thus m_A was chosen negative to give a net saving of 0.2 times the value of m_A. In effect, the iterative method assumes that the slope of mechanism line (iii) in Fig. 7 is constant and equal to 2, that is, greater than 1.8; in fact, the mechanism line is curved, and in the region MN has a slope less than 1.8.

Table III(b) shows the result of choosing m_A positive; line 1 has been transferred to line 11, and line 13 shows $M_A = M_B$, thus concluding the iteration. Between lines 11 and 13 the weight has increased from 594 to 597, but the latter value is less than that given in line 10. The iterative method will tend to break down in this way when the slope of the Foulkes mechanism line (i.e. of the weight line) is close to the slope of one of the lines representing an actual mechanism of failure. Thus a design point in Fig. 10 which lies close to the lines separating region B from D, or A from C, will represent a case for which the iterative method may lead to errors. (The iterative method will replace these curved dividing lines by straight lines at $\ell_A/\ell_B = 2$ and 1/2 respectively). The danger signal is given, as in Table III, by a large change in one of the attacking moments (m_A) producing only a small change in total weight of the structure. If this happens, then the designer should check, as in Table III(b), whether an apparent increase in weight in fact leads to the correct solution.

Final Example

As a final example, consider the simple portal frame shown in Fig. 11 in which the two columns have equal sections, possibly different from that of the beam. If the loads shown are static, then the minimum weight design occurs for

$$X = 30\, M_A + 20\, M_B = 3000$$
$$M_A = M_B = 60 \tag{40}$$

STEP	LINE	PLASTIC MOMENT / SECTION	M_A 1	M_A 2	M_B 3	M_B 4	M_A 1	M_A 2	M_B 3	M_B 4	
0	1	k =1.8	227.4*	0	0	130.0	-20.1	-184.7	-184.7*	-72.3	X=594.0
I	2	0.2x18.23=3.6 m_A	-1	-2	-2	-1	-1	-2	-2	-1	
	3	m_A=-18.23	18.2	36.5	36.5	18.2	18.2	36.5	36.5	18.2	
	4		245.6	36.5	36.5	148.2*	-1.9	-148.2	-148.2	-54.1	X=590.3
0	5	k =1.08	241.8*	0	0	123.0	-27.0	-170.9	-170.9*	-58.4	X=606.1
I	6	m_A=-15.97	16.0	31.9	31.9	16.0	16.0	31.9	31.9	16.0	
	7		257.8	31.9	31.9	139.0*	-11.0	-139.0	-139.0	-42.4	X=603.0
0	8	k =0.97	244.6*	0	0	121.4	-28.5	-167.9	-167.9*	-55.4	X=608.2
I	9	m_A=-15.5	15.5	31.0	31.0	15.5	15.5	31.0	31.0	15.5	
	10		260.1	31.0	31.0	136.9*	-13.0	136.9	-136.9	-39.9	X=605.1

(a)

0	11	k =1.8	227.4*	0	0	130.0	-20.1	-184.7	-184.7*	-72.3	X=594.0
I	12	m_A=14.23	-14.2	-28.5	-28.5	-14.2	-14.2	-28.5	-28.5	-14.2	
	13		213.2	-28.5	-28.5	115.8	-34.3	-213.2*	-213.2	-86.5	X=597.0

(b)

TABLE III

For the shakedown design, the two loads will be assumed to vary independently between zero and the maximum values shown. The stiffness ratio constant will be taken as

$$k = \frac{h}{\ell}\left(\frac{I_B}{I_A}\right)^n = \frac{3}{4}\left(\frac{M_B}{M_A}\right)^{1.4} \qquad (41)$$

The iteration will be started with a uniform frame, i.e. k = 3/4. Table IV gives the working. This table is split into two halves, as usual, the left hand half dealing with the maximum and the right hand half with the minimum elastic moments.

The four independent mechanisms of collapse are displayed as line 1 to 4 of the Table; line 1 gives the sidesway and line 2 the beam mechanism, while lines 3 and 4 correspond to joint rotations at the two corners of the frame. Line 5, Step O, gives the maximum and minimum elastic moments for a frame with equal beam and columns (i.e. k = 3/4). The two asterisked moments are the largest which occur in the respective spans for either half of the Table. In line 6 is constructed the most general system of residual moments which can be used to modify the moments in line 5. A moment $+m_A$ "attacks" section 3, where the largest negative moment in span A occurs, and $-m_B$ attacks section 6 in span B. Since the frame has three redundancies, a supplementary moment x is required to complete the residual distribution. Lines 7, 8 and 9 form an operations table; each line may be used independently of the others. Thus a unit change in m_A will save 30 units of material, while a

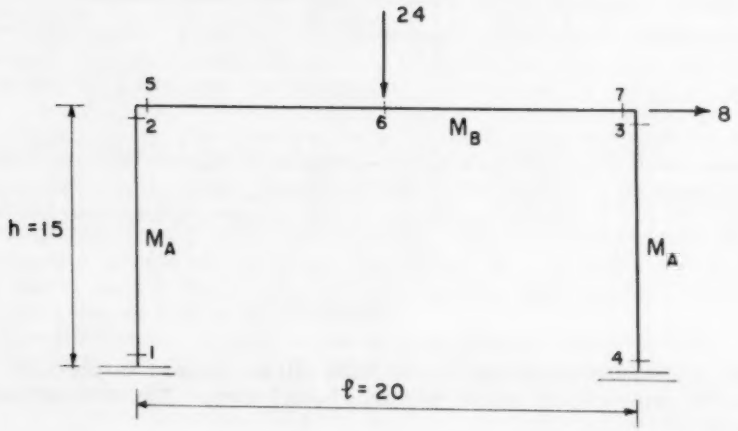

FIG. 11

unit change in m_B will save 20 units. If m_B is taken as 5.45, line 10, and this line is superposed on line 5, line 11 results, which shows that a new hinge is formed at section 4. The total material saving is 109 units, which has been noted in line 8. Had line 7 been used, this also would have resulted in the same saving of 109 units.

Step I requires that all hinges formed during the operation should be maintained. Thus the newly formed hinge at section 4 must be attacked by $-m_A$. Now the total residual moment at section 4 is $(2m_A + 2m_B + x)$; thus

$$2m_A + 2m_B + x = -m_A \tag{42}$$

Eq. (42) enables one of the residual moments to be eliminated from the operations table; lines 12 and 13 show the result of eliminating the supplementary moment x. Step I can now proceed; use of line 12 saves 206 units of material, and hence is more efficient than use of line 13, which saves only 56 units. A new hinge is formed in line 15, m_B is eliminated in line 16, and finally no further move can be made by Step I at line 18.

Lines 19 to 23 check that a true Foulkes mechanism has been formed, and it will be seen that all the hinge rotations in line 23 are of the right sign. As mentioned earlier, had one of the numbers in brackets been negative, Step I could have been reinitiated by dropping the requirement that this false hinge be maintained.

Line 18 gives the following minimum weight design, on the assumption that $k = 3/4$:

$$M_A = 58.7, \quad M_B = 73.6, \quad X = 3233 \tag{43}$$

From values (43), however, k from Eq. (41) is found to have the value 1.03. Remembering the general behaviour exhibited in the example worked in Table II, the next iteration is made for $k = 1.1$. Lines 24 to 36 of Table IV summarize the calculations, and lead to

$$M_A = 56.7, \quad M_B = 76.3, \quad X = 3227, \quad k = 1.13 \tag{44}$$

Evidently the iterations are converging to the final design:

$$M_A = 56.6, \quad M_B = 76.4, \quad X = 3226, \quad k = 1.14 \tag{45}$$

No errors have been introduced in this particular solution by the non-linearity of the basic equations. The minimum weight design under shakedown conditions uses 7-1/2% more material than the corresponding design under static loads.

REFERENCES

1. Foulkes, J. D., The Minimum Weight Design of Structural Frames, Proc. Roy. Soc. A, vol. 223 (1954).

2. Melan, E., Theorie statisch unbestimmter Systeme, Preliminary Publication, International Association for Bridge and Structural Engineering, 2nd Congress, Berlin (1936).

STEP	LINE	PLASTIC MOMENT SECTION		M_A 1	2	3	4	M_B 5	6	7	M_A 1	2	3	4	M_B 5	6	7	
DATA	1			-1	1	-1	1											
	2							-1	2	-1								
	3				-1			1										
	4					-1				1								
0	5	$k = 3/4$		21.8	24.5	0	57.3	24.5	76.4*	0	-55.5	-43.6	-68.2*	0	-43.6	0	-68.2	X_0=5974
	6			X	$-m_A$ $-2m_B$	m_A	$2m_A$ $+2m_B$ $+X$	$-m_A$ $-2m_B$	$-m_B$	m_A								
	7	30×5.63=109	m_A		-1	1	2	-1		1		-1	1	2	-1		1	
	8	20×5.45=109	m_B		-2		2	-2	-1			-2		2	-2	-1		
	9	X		1			1				1			1				
	10	m_A=5.45			-10.9		10.9	-10.9	-5.4			-10.9		10.9	-10.9	-5.4		
I	11			21.8	13.6	0	68.2*	13.6	71.0	0	-55.5	-54.5	-68.2	10.9	-54.5	-5.4	-68.2	X_0=5466
	12	30×6.89=206	m_A	-3	-1	1	-1	-1		1	-3	-1	1	-1	-1		1	
	13	20×2.8=56	m_B	-2	-2			-2	-1		-2	-2			-2	-1		
	14	m_A=6.85		-20.6	-6.8	6.9	-6.9	-6.8		6.9	-20.6	-6.8	6.9	-6.9	-6.8		6.9	
	15			1.2	6.8	6.9	61.3	6.8	71.0	6.9	-56.1	-61.3*	-61.3	4.0	-61.3	-5.4	-61.3	X_0=3259
	16	10×26=26	m_A	-1	1	1	-1	1	1	1	-1	1	1	-1	1	1	1	
	17	m_A=2.6		-2.6	2.6	2.6	-2.6	2.6	2.6	2.6	-2.6	2.6	2.6	-2.6	2.6	2.6	2.6	
	18			-1.4	9.4	9.5	58.7	9.4	73.6	9.5	-58.7	-58.7*	-58.7	1.4	-58.7	-2.8	-58.7	X_0=3259
	19			-	-	-	+		+									
	20	1	α	-1	1	-1	1											
II	21	$2+5+4$	β		-1	-1			2									
	22			$-(\alpha)$	$-(\beta-\alpha)$	$-(\alpha+\beta)$	(α)		(2β)									
	23	$\alpha=5$, $\beta=10$		-(5)	-(5)	-(15)	(5)		(20)									
0	24	$k = 1.1$		19.3	26.0	0	55.2	26.0	81.3*	0	-53.9	-58.7	-64.7*	0	-58.7	0	-64.7	X_0=3467
	25	30×5.85=115	m_A		-1	1	2	-1		1		-1	1	2	-1		1	
	26	20×5.75=115	m_B		-2		2	-2	-1			-2		2	-2	-1		
	27	X		1			1				1			1				
	28	m_A=5.85			-5.8	5.8	7.7	-5.8		5.8		-5.8	5.8	7.7	-5.8		5.8	
	29			14.3	22.2	5.8	60.9*	22.2	81.3	5.8	-55.9	-62.5	-60.9	7.7	-62.5	0	-60.9	X_0=3455
I	30	30×6.75=203	m_A	-3	-1	1	-1	-1		1	-3	-1	1	-1	-1		1	
	31	20×9.2=184	m_B	-2	-2			-2	-1		-2	-2			-2	-1		
	32	m_A=6.75		-20.3	-6.7	6.7	-6.7	-6.7		6.7	-20.3	-6.7	6.7	-6.7	-6.7		6.7	
	33			-1.0	15.5	10.5	54.2	15.5	81.3	10.5	-54.2*	-49.2	-54.2	1.0	-49.2	0	-54.2	X_0=3252
	34	10×2.9=29	m_A	1	3	1	-1	3	2	1	1	3	1	-1	3	2	1	
	35	m_A=-2.5		-2.5	-7.5	-2.5	2.5	-7.5	-5.0	-2.5	-2.5	-7.5	-2.5	2.5	-7.5	-5.0	-2.5	
	36			-3.5	8.0	8.0	56.7	8.0	76.3	8.0	-56.7	-56.7*	-56.7	3.5	-56.7	-5.0	-56.7	X_0=3227

TABLE IV

3. Koiter, W. T., A New General Theorem on Shake-down of Elastic-Plastic Structures. Koninkl. Nederl. Akademie van Wetenschappen, Series B, vol. 59, no. 1 (1956).

4. Heyman, J. and Prager, W., Automatic Minimum Weight Design of Steel Frames. To be published, Franklin Inst.

5. Heyman, J., Automatic Plastic Analysis of Steel Framed Structures under Fixed and Varying Loads. Tech. Report IBM 2038/2, Brown University.

Paper 1791 October, 1958 EM 4

Journal of the
ENGINEERING MECHANICS DIVISION
Proceedings of the American Society of Civil Engineers

EFFECT OF END-FIXITY ON THE VIBRATION OF RODS

D. Burgreen,[1]
(Proc. Paper 1791)

A study is made of the free vibration of rods with end supports of equal elasticity. Expressions are derived relating the end-fixity to frequency and mode of vibration. With the proper type of negative springs attached to the ends of the rod, it is shown that vibrations can be completely surpressed. The relationship of this phenomenon to the instability of beams with negative end-fixity is discussed.

NOMENCLATURE

- E = Young's modulus of elasticity
- I = moment of enertia of bar
- ρ = mass density of bar
- A = cross-sectional area of bar
- X_n = $f(x)_n$ = equation of mode
- ω_n = natural frequency of vibration
- β_n = $(\rho A \omega_n^2 / EI)^{1/4}$
- L = length of bar
- α = proportionality constant defining end fixity used in the expression $X'' = X'$
- t = depth or thickness of bar
- δ = maximum amplitude of vibration, or maximum deflection

Note: Discussion open until March 1, 1959. To extend the closing date one month, a written request must be filed with the Executive Secretary, ASCE. Paper 1791 is part of the copyrighted Journal of the Engineering Mechanics Division, Proceedings of the American Society of Civil Engineers, Vol. 84, No. EM 4, October, 1958.

1. Eng. Advisor, Nuclear Development Corp. of America, White Plains, N.Y.

ϵ_o = maximum extreme fibre strain

k_o = amplitude-strain factor defined by $\frac{\delta}{\epsilon_o} = k_o L^2/t$

w = distributed beam load

In a vibration program dealing with the effects of high velocity water flowing parallel to long thin rods, one of the problems that arose and required investigation was the effect of the end connections of a prismatic test rod on the natural frequencies and modes of vibration. Specifically, the questions that required an answer were:

1. If the fundamental frequency of vibration of the rod with an equal amount of end-fixity at each end, is known, what are the higher natural frequencies of vibration?
2. If the extreme fibre strain in the rod is known, what is the amplitude of vibration?

Texts on vibration discuss the problem of vibration of prismatic bars with specific end conditions such as pin ends, built in ends, or free ends, and generally list some of the lower natural frequencies of vibration of these bars. In practice, however, most bars or beams are neither pin-ended nor built in, but have end connections with some amount of elasticity in them. If the amount of elasticity in the end connections is known, then the natural frequencies and modes of vibration can be determined.

It will be shown that a knowledge of the amount of end-fixity in the rod supports is not necessary in order to answer the above questions. The end-fixity is simply the parameter which relates the desired quantities. There are, however, occasions when the end-fixity as determined by a measurement of the fundamental frequency of vibration or from strain deflection data may be of direct use. For example, it may be desired to determine accurately the load carrying capacity of a beam in a structure—which depends upon the amount of end-fixity of the member. This can be done by the use of the curves in Fig. 2 wherein the end-fixity is plotted against the natural frequency of vibration. Some characteristics of elastically restrained beams that are of practical interest are discussed in the text that follows.

The equation for the vibration of the prismatic bar with elastically built in ends, shown in Fig. 1 is

$$EI \frac{\partial^4 y}{\partial x^4} + \rho A \frac{\partial^2 y}{\partial t^2} = 0. \tag{1}$$

The solution to this equation is taken as

$$y = \sum_{n=1}^{\infty} X_n \sin \omega_n t, \tag{2}$$

which gives the equation for the mode of vibration as

$$X_n'''' - \frac{\rho A \omega_n^2}{EI} X_n = 0. \tag{3}$$

With the notation

$$\beta_n^4 = \frac{\rho A \omega_n^2}{EI},$$

Equation (3) becomes

$$X_n'''' - \beta_n^4 X_n = 0. \tag{4}$$

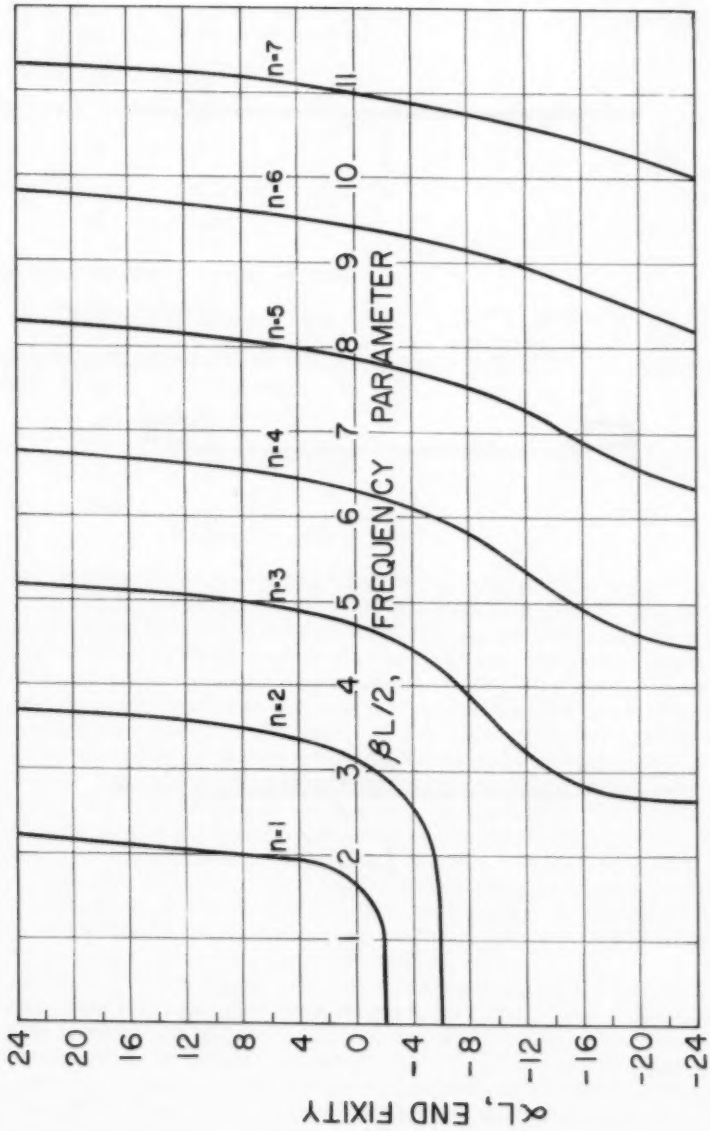
αL, END FIXITY
24
20
16
12
8
4
0
-4
-8
-12
-16
-20
-24
βL/2, FREQUENCY PARAMETER
1
2
3
4
5
6
7
8
9
10
11
n=1
n=2
n=3
n=4
n=5
n=6
n=7

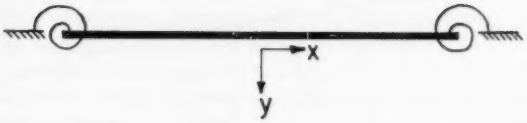
x
y

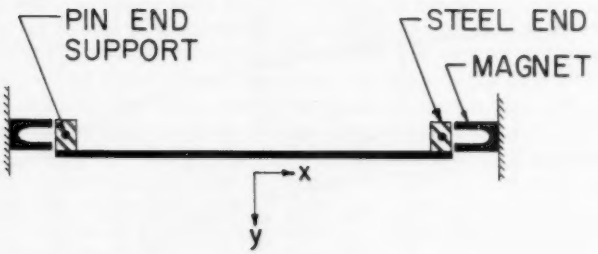
PIN END
SUPPORT
STEEL END
MAGNET
x
y

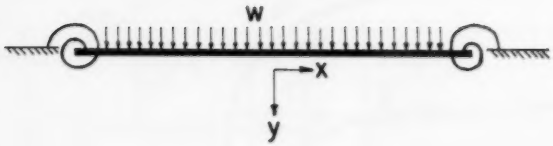
w
x
y

The solution to Equation 4 is

$$X = A \sin \beta x + B \cos \beta x + C \sinh \beta x + D \cosh \beta x \tag{5}$$

The ends of the bar are assumed to be elastically built in with the angle of rotation proportional to the applied moment. This is the common type of linear torsional elasticity expressed as

$$M = \text{constant } \theta.$$

The boundary conditions representing this are expressed as

$$X''_{-L/2} = \alpha X'_{-L/2} \tag{6}$$

and

$$X''_{L/2} = -\alpha X'_{L/2}$$

The other boundary conditions are

$$X_{\pm L/2} = 0 \tag{7}$$

Setting Boundary Conditions (6) and (7) into Equation (5), the following frequency equations are obtained:

$$\alpha L = \frac{-2\beta L}{\tan \beta L/2 + \tanh \beta L/2} \tag{8}$$

$$\alpha L = \frac{2\beta L}{\cot \beta L/2 - \coth \beta L/2} \tag{9}$$

The above expressions refer respectively to the symmetrical and to the anti-symmetrical modes of vibration and are plotted in Fig. 2. These curves give the relationship between the end-fixity and the natural frequencies of vibration. The curve designated as n=1 refers to the first symmetrical mode of vibration of a prismatic bar whose end-fixity is α. The special case of a pin ended beam with zero end-fixity is included here as the point of intersection of the curve with the βL axis. At this point αL is zero and $\beta L = \pi$, which corresponds to the known fundamental frequency of vibration of a pin ended beam. The higher natural frequencies of vibration of a pin ended beam are given by the intersection of the βL axis with the successive curves.

The upper part of curve n=1 approaches an asymptote at $\beta L = 4.73$; that is, as αL approaches infinity, signifying a bar with infinite end restraint or built in ends, βL, the root of the Frequency Equation (8), gives the frequency of vibration of a built in beam. The asymptotes, as αL approaches infinity, on the higher numbered curves, similarly give the higher frequencies of vibration of prismatic bars with built in ends.

On curve n=1, which refers to the first symmetrical mode of vibration, it may be noted that low order wave shapes are included up to that of a beam with built in ends (one full wave). Curve n=3 which represents the second symmetrical mode of vibration starts at $\alpha L \to -\infty$ with the mode shape of a beam with built in ends, or one full wave, gradually changes its shape with increasing βL to become a pin ended beam in its second symmetrical mode with one and a half waves, at $\alpha L = 0$, and finally at $\alpha L \to \infty$ assumes the shape of the second symmetrical mode of a beam with built in ends, or a beam having two full waves. The progress of change in shape with end-fixity and

frequency may be traced in the same manner for the even numbered anti-symmetrical modes.

Of particular interest is the significance of the negative values of the end-fixity. This is the case in which the springs at the extremeties of the bar, instead of offering restraint and acting as a restoring force against the inertia forces of the vibrating bar, actually assists the inertia forces and act in opposition to the restoring forces due to the bending rigidity of the bar.

A bar with built in extremities offers the greatest end restraint. As the end-fixity is gradually relaxed by attaching the ends to successively softer springs, the restoring forces at the bar ends is diminished until the limiting case of a bar with zero end restraint, or one with pin ends, is attained. Any lesser end restraint must now be a negative end restraint. It may be possible to attach devices to the extremities of the bar which can be called negative springs, which cause the bar to have greater end slopes, in the absolute sense, than it would have if it were pin ended. Such devices assist the motion when the bar is moving from its straight line position and hold it back when it is moving toward its straight line position, and therefore have the effect of reducing the frequency of vibration.

A method of attaining a negative end-fixity is shown in Fig. 3. Steel pieces are attached to the ends of the rod, supported by pins, as shown. For the purposes of the illustration, the mass and moment of inertia of the steel attachments must be disregarded. Two stationary magnets are places in close proximity to the end fittings, so that the bar in its straight line position, as shown in the figure, will not have any tendency to deflect either upward or downward. It can be seen in this arrangement that when the bar deflects downward, the effect of the magnets is to increase this deflection, and when the bar deflects upward, the effect of the nagnets is to increase the upward deflection still further. The magnets also restrain the movement toward the straight line position. It is seen then that this behavior is exactly in opposition to the behavior of normal springs. It is apparent that when strong magnets are used a small deflection from the straight position may cause the bar to buckle. That is, there may be a critical magnet strength associated with instability of the bar in Fig. 3.

When βL is set equal to zero in Equations (8) and (9), signifying zero frequency of vibration, $\alpha L=-2$ and $\alpha L=-6$ are found to be the end-fixities associated with zero frequency of vibration in the symmetrical and anti-symmetrical modes of vibration. It is well known that the conditions for zero frequency of vibration are often the same as the conditions required for instability. This phenomenon is usually associated with axial loads rather than negative springs. It is of interest to determine whether this correspondence exists also for negative springs.

Consider the bar in Fig. 4, which is the same as the bar under discussion, except that now it is uniformly loaded. Using the same boundary conditions as before, the equation for the deflected bar is

$$EIy = \frac{wx^4}{24} - \frac{wL^2x^2}{48}\left(\frac{6+\alpha L}{2+\alpha L}\right) + \frac{wL^4}{384}\left(\frac{10+\alpha L}{2+\alpha L}\right) \qquad (10)$$

Note in the above equation that when $\alpha=0$, the deflection equation for a pin ended bar is obtained, and when $\alpha \to \infty$, the deflection equation for a built in bar is obtained. The particular feature in the above equation that is of interest is the indication of instability when αL approaches -2. This is the

critical value of the magnet strength that would produce an instability condition. In Fig. 5, the same bar is shown with an antisymmetrical loading expressed as

$$W = w \sin \frac{2\pi x}{L}$$

and the resulting deflection equation is

$$EIy = \frac{wL^4}{16\pi^4} \sin \frac{2\pi x}{L} \quad \frac{\alpha w L x^3}{4\pi^3} \left(\frac{1}{6 + \alpha L} \right) - \frac{\alpha w L^3 x}{16\pi^3} \left(\frac{1}{6 + \alpha L} \right) \quad (11)$$

The critical vaule of the end-fixity in this equation is $\alpha L = -6$, indicating that this value of end-fixity refers to an anti-symmetrical type of instability. The correspondence of instability due to negative spring supports, of end-fixity $\alpha L = -6$ when a bar is antisymmetrically loaded, and of end-fixity of $\alpha L = -2$ when the bar is symmetrically loaded, to zero frequency is thus shown.

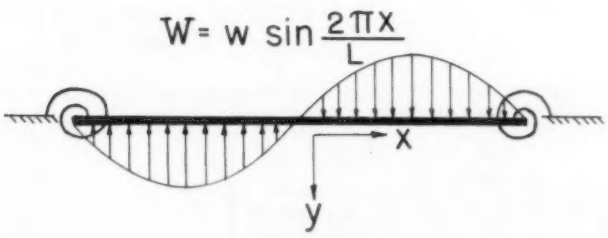

This may also be seen from the n=1 curve in Fig. 2. When the end-fixity of a bar vibrating in its first symmetrical mode reaches the limit $\alpha L = -2$, then no vibration is possible. The second curve, n=2, in Fig. 2, shows that the natural frequency of vibration in the first antisymmetrical mode approaches zero as the end-fixity αL approaches the instability value -6. The higher numbered curves corresponding to higher mode shapes do not have any limiting values of negative end-fixity which exclude the possibility of vibration. The negative values of end-fixity of the higher modes have, however, limited physical significance, since it is not generally possible to get past the lowest end-fixity that causes instability, that is, $\alpha L = -2$.

Of practical interest in the study of bars with elastically supported ends is the relationship between amplitude of vibration and strain. The constant k, which relates amplitude and extreme fibre strain is given as

$$\frac{1}{k} = \frac{\epsilon}{\delta} \frac{L^2}{t}$$

k may also be expressed as, $k = 2X/L^2X''$. In experimental tests, data is sometimes recorded by means of strain gages in terms of extreme fibre strain, which must be converted to amplitude. The above relationship which is valid for loaded bars as well as for vibrating bars is useful in experimental work. If the value of k at the center of the bar is defined as k_o, then for a uniformly loaded beam with elastic end supports it is given as

$$k_{ou} = \frac{\alpha L + 10}{8\alpha L + 48} \quad (12)$$

and for a beam with elastic end supports having a concentrated load at the center of the span it becomes

$$k_{oc} = \frac{\alpha L + 8}{12\alpha L + 48} \tag{13}$$

the above expression may be used, for example, in determing the amplitude-strain relationships of a uniformly loaded beam with undetermined end-fixity when calibrations are made with a concentrated load. For a bar which is vibrating freely, a similar expression may be derived. The equation for the symmetrical mode has the form

$$X = D\ (\cosh \beta x - \frac{\cosh \beta L/2}{\cos \beta L/2} \cos \beta x) \tag{14}$$

which satisfies the condition of zero displacement at the ends. For the center of the beam this gives

$$\left| k_o \right| = \frac{2}{L^2} \frac{X_{x=o}}{X''_{x=o}} = \frac{\frac{\cosh \beta L/2}{\cos \beta L/2} - 1}{2(\beta L/2)^2 \left(1 + \frac{\cosh \beta L/2}{\cos \beta L/2}\right)} \tag{15}$$

and relates the amplitude of vibration with the extreme fibre strain at the center of the beam as given below

$$\frac{\delta}{\epsilon_o} = \left[\frac{\frac{\cosh \beta L/2}{\cosh \beta L/2} - 1}{2(\beta L/2)^2 \ 1 + \frac{\cosh \beta L/2}{\cos \beta L/2}} \right] \frac{L^2}{t} \tag{16}$$

The above expression for k_o does not include the end-fixity α directly as in the case of beams. The deflection-strain relationship obviously depends upon the rigidity of the end supports and its dependence upon α is seen in Equation (8) wherein βL is given as an implicit function of αL. Equation (15) is plotted in Fig. 6. It may be observed that the ratio of deflection to extreme fibre strain becomes smaller as the frequency of vibration (or βL) increases. It signifies the crowding of a large number of waves into the rod length, which must necessarily produce high curvatures and small deflections. A limiting case is represented by a pin ended beam which vibrates in a half sine wave. The amplitude-strain factor for a sine wave is $2/\pi^2$. Fig. 6 gives $\beta L = \pi$ for this value of k_o, and it corresponds to the known fundamental frequency of vibration of a pin ended beam. The curve also shows that k_o approaches a limit of 1/4 as the frequency approaches zero. It was shown that the natural frequency of vibration of the first symmetrical mode of a bar approaches zero when the end-fixity approaches its instability value of $\alpha L = -2$. Since no vibration occurs when $\alpha L = 2$, the bar may simply be considered uniformly loaded by its own weight. Equation (12) which shows the variation of k_o with the end-fixity α, for a uniformly loaded beam verifies that the value of the amplitude-strain factor becomes 1/4, as αL approaches -2. In Fig. 6, it is seen that 1/4 is the largest value that k_o may attain, indicating that the shape in which the bar becomes unstable is that of least curvature at its center.

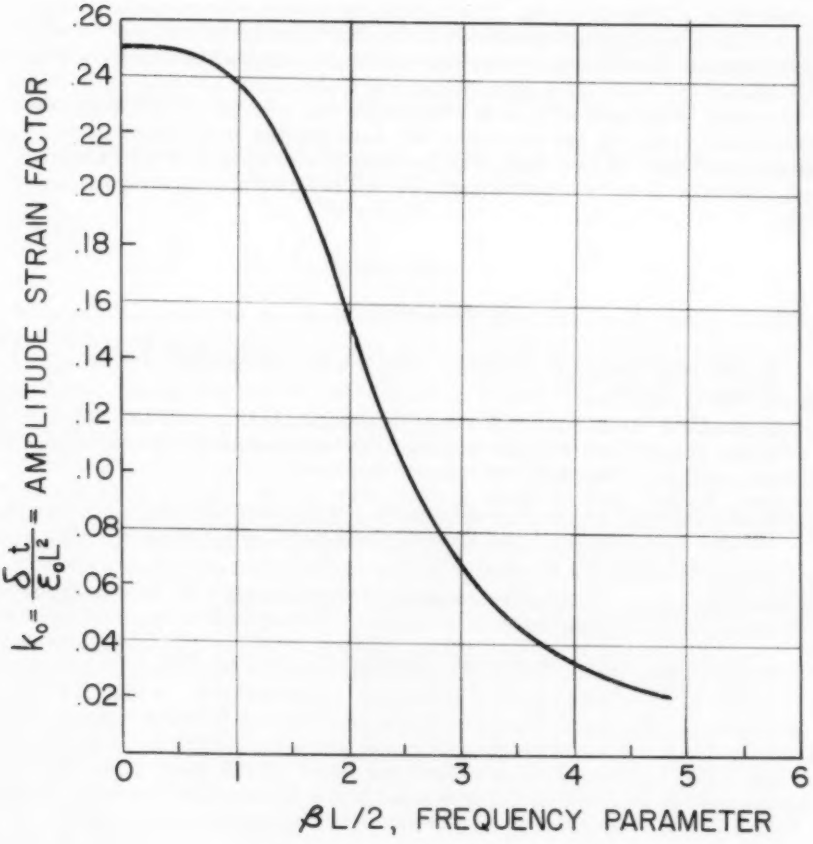
$k_o = \frac{\delta t}{\varepsilon_o L^2}$ = AMPLITUDE STRAIN FACTOR
.26
.24
.22
.20
.18
.16
.14
.12
.10
.08
.06
.04
.02
0
1
2
3
4
5
6
βL/2, FREQUENCY PARAMETER

In the practical application of strain to amplitude conversion it will be found that the strain-amplitude ratio is not particularly sensitive to mode shape, permitting any reasonable fundamental type mode to be assumed. It must, of course, be ascertained, that the loading or forcing function is not of the type that would preferentially cause higher type mode-forms to be developed. With strain gages mounted at the center of the rod the second mode would not be picked up. Also, since the energy required to produce a mode with a given amplitude varies as the fourth power of the mode number it is apparent that a large energy input would be required to maintain vibrations of any significant amplitude in the higher mode shapes.

In order to present as clearly as possible the behavior of vibrating rods with elastic supports, the discussion has been limited to rods with equal elastic restraints at each end. The problem of vibrating rods with unequal end restraints is an interesting one, and will be presented at some future date.

REFERENCES

1. K. Hohenemser and W. Prager, "Dynamik der Stabwerke", Julius Springer, Berlin, 1933.

2. W. Mudrak, "Bestimmung der Eigenschwingungszahlen von Durchlaufenden Tragern und Rahmen", Zeitschrift fur Augewandte Mathematik und Mechanik, Vol. 28, 1948, pp. 258-263.

3. N. M. Newmark and A. S. Veletsos, "A Simple Approximation of the Natural Frequencies of Partly Restrained Bars", Journal of Applied Mechanics, Vol. 19, No. 4, p. 563.

4. Timoshenko, S: "Vibration Problems in Engineering", D. Van Nostrand Company, New York, 1928.

5. Den Hartog, J. P.: "Mechanical Vibrations", McGraw Hill, 1947.

Paper 1792 October, 1958 EM 4

Journal of the
ENGINEERING MECHANICS DIVISION
Proceedings of the American Society of Civil Engineers

ECCENTRICALLY LOADED, HINGED STEEL COLUMNS

Richard E. Mason,[1] Gordon P. Fisher,[2] A. M. ASCE and
George Winter,[3] M. ASCE
(Proc. Paper 1792)

SUMMARY

This paper reports an experimental investigation of eccentrically loaded hinged-end steel columns bent about a minor axis parallel to the flanges.(1) In this respect it differs from, and supplements most existing experimental column investigations which are chiefly of two kinds: I-shaped columns tested (1) with bending applied about a minor axis parallel to the web, so that maximum stresses appear only at the flange tips, or (2) with bending applied about a major axis parallel to the flanges, in which case flexural failure is normally accompanied by torsion. The present tests, in which bending is about a minor axis parallel to the flanges, preclude torsion while at the same time producing maximum stresses over the entire width of the flanges.

Twenty-four eccentrically loaded and six concentrically loaded columns have been tested. In addition to initial yielding and ultimate loads, information has been obtained on load-deflection performance not only up to, but considerably beyond the ultimate loads, a matter which is of some consequence for plastic strength analysis of structures. No new theories or formulas for strength prediction are developed, but results are compared with predicted failure loads calculated by a variety of methods, including the secant formula, a plastic strength formula, and two interaction type formulas.

In addition to these 30 new tests, the results of 28 tests on eccentrically loaded, elastically end restrained columns which have been reported previously are compared in the Appendix with values calculated by the same two interaction formulas.

Note: Discussion open until March 1, 1959. To extend the closing date one month, a written request must be filed with the Executive Secretary, ASCE. Paper 1792 is part of the copyrighted Journal of the Engineering Mechanics Division, Proceedings of the American Society of Civil Engineers, Vol. 84, No. EM 4, October, 1958.

1. Asst. Prof., Dept. of Structural Eng., Cornell Univ., Ithaca, N. Y.
2. Associate Prof., Dept. of Structural Eng., Cornell Univ., Ithaca, N. Y.
3. Prof. and Head, Dept. of Structural Eng., Cornell Univ., Ithaca, N. Y.

INTRODUCTION

Presently available experimental data on the strength of eccentrically-loaded two-flange columns, predominantly I-sections, are incomplete in two respects. First, there is considerable experimental data on the strength of two-flange sections eccentrically loaded to produce bending about an axis perpendicular to the flanges which, for the usual I-sections, is the minor axis. In this case maximum stresses occur at the tips of the flanges only, and observed ultimate loads appreciably exceed the strength computed by initial-yield formulas such as the secant formula. Second, in other tests bending was induced about the major axis of unbraced I-shaped columns. Such bending is almost always accompanied by twist, and test results cannot be interpreted by the usual formulas which exclude this effect. However, many structures incorporate I-shaped columns bent about the major axis, but so braced against minor-axis buckling that twist does not occur.

Therefore, available test data are neither wholly adequate for comparison with present column formulas, nor are they wholly applicable to the commonly-occurring condition in many structures where I-shaped columns are bent about the major axis parallel to the flanges and at the same time braced against buckling about the minor axis, effectively excluding twisting. Likewise, twisting does not occur for box-shaped members bent about either axis.

In order to overcome these deficiencies, hat-shaped sections, formed by connecting two rolled Z-sections flange-to-flange, were fabricated to produce a minor axis parallel to the flanges and were loaded eccentrically to produce bending about this axis. Consequently, the maximum compression stress was uniform over the entire width of the compression flange, and since bending was about the minor axis, there was no tendency of the entire column to twist. Therefore, results could be evaluated by methods applying to non-torsional flexural column action.

In addition to failure loads, the behavior of such members beyond the ultimate load is of significance in relation to ultimate strength design, and for this purpose load-deflection observations were made far into the descending branch of the load-deflection curves. Width-to-thickness ratio of flanges was varied to investigate the effect of flange dimensions on this post-ultimate behavior and on the ultimate strength.

Specimens

Test specimens consisted of a pair of Z-sections placed to form a hat-shaped cross-section, with outstanding flanges connected by batten plates and connected flanges stitch-welded intermittently. See Fig. 1. Thirty columns were fabricated and tested, using three different weights of rolled Z-sections. Three lengths of columns were made of each weight, and eccentricity ratios ec/r^2 were varied from zero to 1.5. Specimen properties are given in Table 1.

The following compression yield points were used in evaluating test results for the column specimens:

1/4 x 3 (3 x 2 3/4, 6.7#)	42,500 psi.
1/4 x 4 (4 x 3, 8.2#)	44,500 psi.
1/2 x 3 (3 x 2 3/4, 12.6#)	39,000 psi.

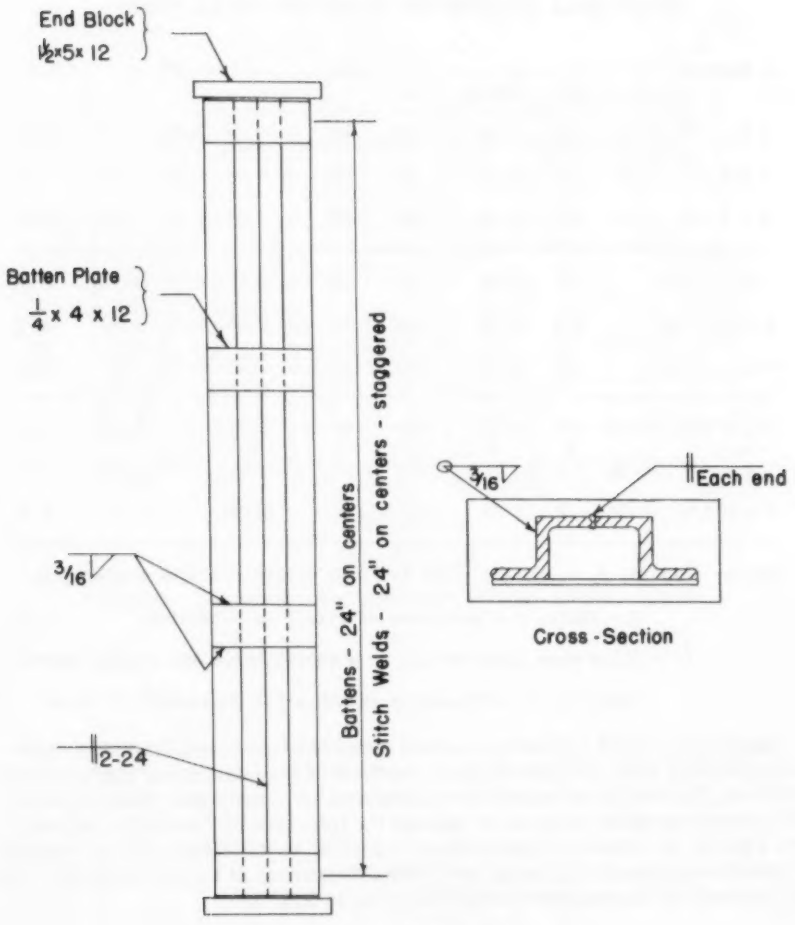

Figure 1

Double Zee Hat Section
Column Specimens

TABLE 1

PROPERTIES OF SPECIMENS AND ECCENTRICITY RATIOS TESTED

Z-Section	t in.	A sq.in.	L in.	L/r	ec/r^2	b/t
3 x 2 3/4, 6.7#	1/4	3.94	59	49	0; 0.25; 0.75; 1.50	10.8
3 x 2 3/4, 6.7#	1/4	3.94	83	69	0; 0.25; 0.75; 1.50	10.8
3 x 2 3/4, 6.7#	1/4	3.94	131	108	0; 0.25; 0.75; 1.50	10.8
4 x 3, 8.2#	1/4	4.82	59	36	0; 0.25; 0.75; 1.50	12.3
4 x 3, 8.2#	1/4	4.82	107	66	0; 0.25; 0.75; 1.50	12.3
4 x 3, 8.2#	1/4	4.82	181	110.5	0; 0.25; 0.75; 1.22	12.3
3 x 2 3/4, 12.6#	1/2	7.38	59	53	0.25; 1.50	5.4
3 x 2 3/4, 12.6#	1/2	7.38	83	74	0.25; 1.50	5.4
3 x 2 3/4, 12.6#	1/2	7.38	131	117	0.25; 1.50	5.4

Notes: (1) A, r, c, b, and t are based on nominal section properties. b = width, t = thickness of flange of Z-section.

(2) Areas were spot-checked on a weight basis and nominal areas found to be sufficiently reliable for evaluation of tests.

These were based on average values observed from compression stress-strain tests of short lengths of whole sections in the unannealed (as-received) condition, the results of which were compared for consistency with (a) similar tests on annealed material to assess the influence of residual stresses, (see Fig. 2), (b) tensile coupon tests of material as-received, and (c) residual stress measurements following the method described in Lehigh tests.[3] Typical residual stress measurements are given in Fig. 3.

Testing Procedure

The column testing arrangement, instrumentation, and centering procedure were similar to those described in previous papers except for end fixtures.[2,4] Briefly, the columns were supported on simple knife-edge fixtures parallel to the minor axis, were equipped with set screws to permit eccentricity adjustments, and were loaded so that maximum compression occurred in the outstanding flanges.

Dial gages were located at mid-height and quarter-points of the column, and at the upper head of the testing machine. Tuckerman optical strain gages were placed at both quarter-points for centering, then at the mid-height only for testing. Four gages were used at each quarter-point, one pair on the

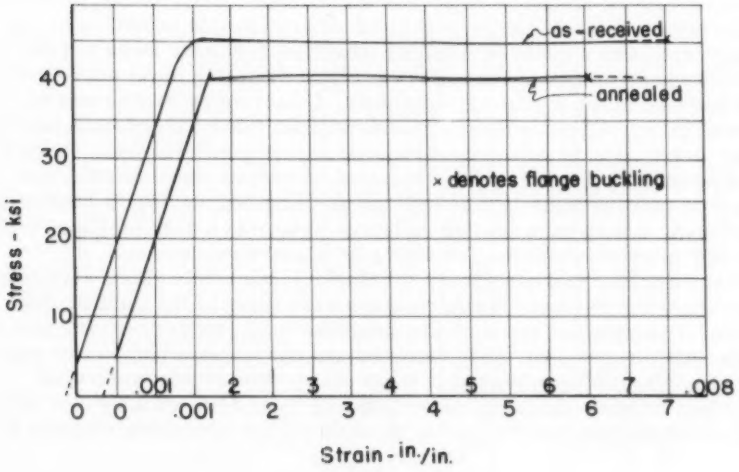

Figure 2

Typical Sectional Compressive Stress-Strain Curve

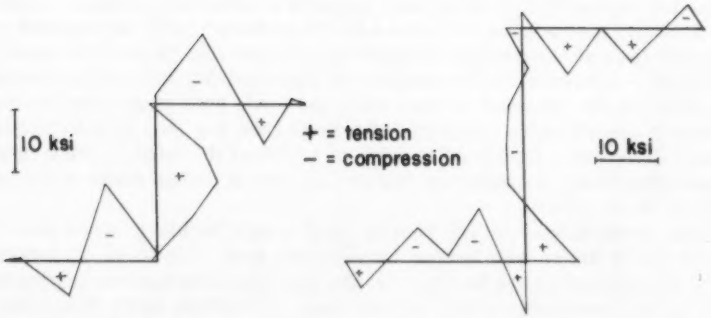

Figure 3

Typical Residual Stress Distributions

outer edges of the compression flanges and one pair on the edges of the tension face; at midheight, six gages were used: one pair each at inner and outer edges of the compression flanges and one pair at the outer edges of the tension face.

For column centering, control was achieved with two aids: (a) computed charts of load-vs-midheight deflection for various eccentricities, based on elastic behavior and (b) theoretical yield loads computed according to the secant formula as a guide for limiting maximum centering loads and selecting load increments to be used in the tests. Final centering loads were about 60 to 65 per cent of the computed yield loads. Centering procedure was as follows: (1) preset end eccentricities to desired value, (2) equalize lateral stress distribution by balancing strains on opposing quarter-point strain gages and shimming the column ends as required, (3) adjust end eccentricities slightly to produce midheight deflections as computed, and equal quarter-point deflections. It may be noted that deflection centering using dial gages is significantly more accurate than centering by use of strain gages.

When centering was considered satisfactory, the strain gages were moved to midheight for the test. Strain readings were taken to the limit of range of the Tuckerman gages. Location and progression of yielding, as indicated by a white-wash stress coat, were recorded and particular attention was paid to flange buckling, noting when and if it did occur. Deflections were read throughout the test, straining being continued beyond the ultimate load until the equilibrium load had dropped to about 65-75 per cent of the ultimate load.

Behavior Under Load

Deflections agreed satisfactorily with those predicted by elastic analysis nearly to the computed yield load. First yielding occurred at loads somewhat less than the predicted values, attributable to the high residual stresses observed. Ultimate equilibrium loads were usually slightly above the yield loads predicted by secant formula. (See Table 2).

Behavior beyond the ultimate load followed a consistent pattern. Loads dropped off quite slowly for columns with large eccentricity as opposed to more rapid loss of capacity for concentric columns and those with small eccentricity. Likewise, loads dropped off more quickly for low slenderness ratios whereas for the most slender columns loads held at or near the maximum over a considerable range of deflections (see Fig. 4). At ultimate loads midheight deflections amounted to 0.2% to 1.15% of the length, which is a moderate magnitude, considering that deflections at design loads would be a fraction of these values.

Column strength was not affected by local flange buckling, since when it occurred at all, it did so well beyond the ultimate load. Likewise, no influence could be detected of flange buckling on the post-ultimate load-deflection behavior. It had been conjectured that for large b/t-ratios, early flange buckling at loads just past the ultimate might lead to quicker collapse, i.e. a steeper load-deflection curve, than for stockier sections, but no such trend of significant magnitude was observed within the range of dimensions investigated, i.e. within w/t from 4.4 to 11.3, where t = thickness, w = projection of outstanding flange.

The point of initial yield, not reliably indicated by the white-wash stress coat, was determined by a semi-empirical method described in a previous

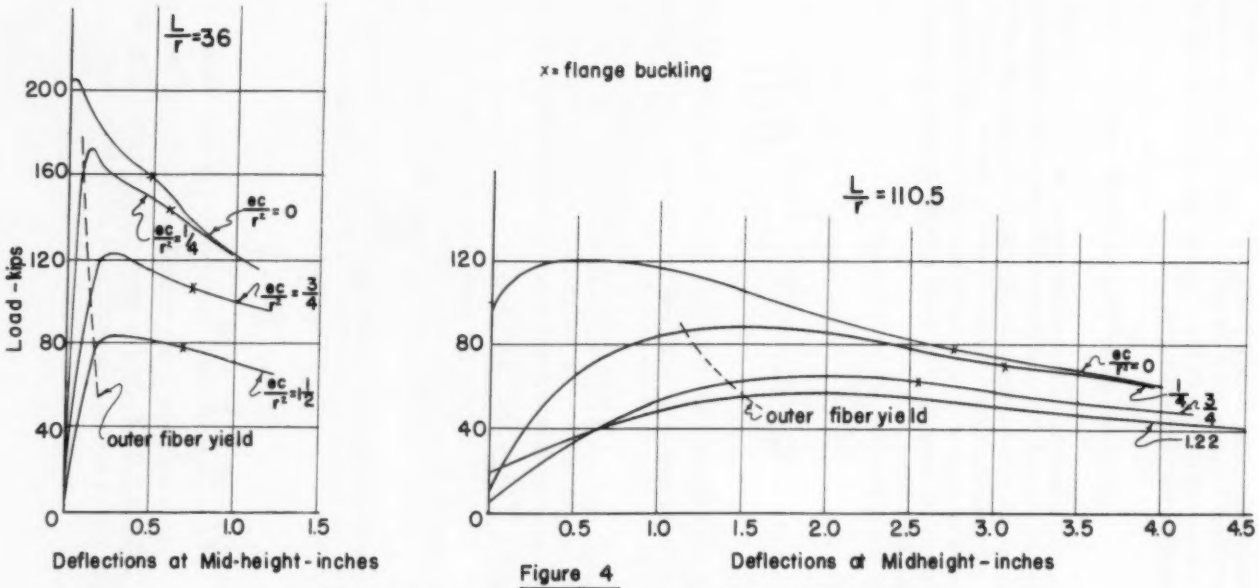

Figure 4

Mid-height Deflection Curves, Zee 4x3x8.2#

paper.(2) This consisted of computing the midheight bending moment from the load and the corresponding total midheight eccentricity, computing therefrom the maximum fiber stress, and plotting this stress against the observed strain to obtain a linearized stress-strain curve. Initial yield load occurs where this plot first deviates from linearity. Initial yielding so determined is indicated by the dashed curves of Fig. 4 and is seen to occur typically at loads but slightly smaller than the ultimates.

Ultimate Loads: Test vs. Prediction

Experimental ultimate loads have been compared with predicted values by the secant formula, by the Bijlaard method,(2) and by two interaction formulas. For hinged-end columns the ultimate load by the Bijlaard method is quite simply obtained since the effective length is known. A shape factor $\mu = 1.4$ was used as suggested in the previous publication(2) for bending about an axis parallel to the flanges. The mean eccentric buckling stress is expressed by the formula:

$$\sigma_a = \frac{\sigma_{ess}}{\gamma}$$

where

$$\sigma_{ess} = \sigma_{ys} - 50{,}000 \left\{ \frac{\frac{L}{r}}{\left(\frac{L}{r}\right)_E} + \left[\frac{\frac{L}{r}}{\left(\frac{L}{r}\right)_E} \right]^2 \right\}$$

$\left(\frac{L}{r}\right)_E$ is the slenderness ratio for which the buckling stress is equal to the proportional limit (assumed to be 10,000 psi less than the yield point).

$$\left(\frac{L}{r}\right)_E = \left(\frac{3 \times 10^6}{\sigma_{ys} - 10{,}000}\right)^{\frac{1}{2}}$$

and where the reduction factor γ which accounts for eccentricity is obtained as follows, where $\left(\frac{L}{r}\right)_C = 157 - 0.0014\ \sigma_{ys}$:

for $200 > \frac{L}{r} > \left(\frac{L}{r}\right)_C$

$$\gamma = 1 + (21\,000 - 0.23\ \sigma_{ys}) \frac{\left(\frac{\mu e}{K_c}\right)^{\frac{2}{3}}}{\left(\frac{L}{r}\right)^2}$$

for $\left(\frac{L}{r}\right)_C - 30 > \frac{L}{r} > 20$

$$\gamma = 1 + 0.52\ \frac{\mu e}{K_c} + \frac{\left(\frac{\mu e}{K_c}\right)^{\frac{1}{2}}}{370 - 0.005\ \sigma_{ys}} \left(\frac{L}{r} - 20\right)$$

for $\left(\frac{L}{r}\right)_c > \left(\frac{L}{r}\right)_c - 30$ interpolate linearly between γ values for $\left(\frac{L}{r}\right)_c - 30$ and $\left(\frac{L}{r}\right)_c$

A = cross-sectional area of column

e = eccentricity of load

k_c = core radius

L = length of column

r = radius of gyration of cross-section

γ = division factor for eccentricity

μ = shape factor

σ_a = mean equilibrium stress

σ_{cES} = Engesser-Shanley buckling stress (by Bijlaard method)

σ_{ys} = yield point stress

Then, the predicted ultimate load is

$$P_{ult} = \sigma_a \times A$$

Table 2 compares measured ultimate loads with those calculated by the secant formula and the Bijlaard method. The latter is seen to be slightly more conservative than the former, but both are satisfactorily accurate in predicting the capacities of these columns.

From Table 2, the Bijlaard method is seen to give good correlation for columns of short and intermediate lengths, while the predicted ultimate loads for the long specimens are consistently below the experimental values. Thus it would appear that the value for the effective proportional limit which has been assumed in determining the Engesser-Shanley buckling stress is too conservative when applied to these double Z-section columns.

From the same table it can be seen that the secant formula gives very satisfactory correlation with experimental values for ultimate loads for all slenderness-ratios.

Failure loads have also been evaluated according to two types of interaction formulas. The simpler type is the one current in several widely used design codes, namely "Interaction Formula Type I":

$$\frac{P}{P'} + \frac{M}{M'} = 1 \qquad (I)$$

where P = actual load at failure under combined action

M = bending moment at failure under combined action

P' = axial load at failure under concentric compression, the Engesser-Shanley load (when determined by the Bijlaard method, $P' = \sigma_{cES}A$)

TABLE 2

ULTIMATE LOADS - TEST VS. THEORY

Specimen t x b (in.)	$L/_r$	$\frac{ec}{r^2}$	(1) P_{ult} Test (kips)	(2) P_{ult} Secant (kips)	Ratio (1)/(2)	(3) P_{ult} Bijlaard (kips)	Ratio (1)/(3)
1/4 x 3	49	0.25	122	123	0.992	118	1.034
1/4 x 3	69	0.25	110	111	0.991	105	1.047
1/4 x 3	108	0.25	75	74.4	1.007	66.4	1.129
1/4 x 3	49	0.75	89.3	85.5	1.044	87.8	1.017
1/4 x 3	69	0.75	77.6	76.8	1.011	76.5	1.014
1/4 x 3	108	0.75	57.2	56.7	1.008	49.4	1.158
1/4 x 3	49	1.50	65.9	60.7	1.085	64.5	1.022
1/4 x 3	69	1.50	58.4	54.8	1.066	56.2	1.039
1/4 x 3	108	1.50	43.2	42.5	1.016	38.1	1.134
1/4 x 4	36	0.25	171.8	164	1.048	162	1.060
1/4 x 4	66	0.25	143.8	143	1.006	135	1.065
1/4 x 4	110.5	0.25	87.8	90.1	0.974	81.2	1.081
1/4 x 4	36	0.75	123.2	115	1.070	121.5	1.014
1/4 x 4	66	0.75	100.1	99.0	1.012	99.0	1.012
1/4 x 4	110.5	0.75	66.2	68.5	0.967	61.7	1.073
1/4 x 4	36	1.50	84.2	81.0	1.039	89.7	0.939
1/4 x 4	66	1.50	71.0	71.2	0.997	72.7	0.977
1/4 x 4	110.5	1.215	58.1	57.9	1.004	52.4	1.108
1/2 x 3	53	0.25	214.2	211	1.015	200	1.071
1/2 x 3	74	0.25	188.6	187.5	1.005	173	1.090
1/2 x 3	117	0.25	122.3	122	1.002	109.5	1.117
1/2 x 3	53	1.50	117.2	103	1.138	109.5	1.070
1/2 x 3	74	1.50	101.2	93.0	1.088	91.8	1.103
1/2 x 3	117	1.50	76.1	71.0	1.071	64.4	1.182

M' = bending moment at failure under bending only. For simple bending, it is the plastic hinge moment, or if lateral buckling occurs, the critical lateral buckling moment.

The "Interaction Formula Type II", is:

$$\frac{P}{P'} + \frac{M}{M'\ (1 - P/P_E)} = 1 \qquad \text{(II)}$$

where P_E = the Euler elastic buckling load.

Comparisons are given in Table 3 and Figs. 5 and 6.

Inspection of Fig. 5 reveals that the "simple", widely used interaction formula of Type I is unconservative. Of all eccentric tests, only one reached an ultimate load barely exceeding that predicted by this formula. In all other cases the formula overestimates the actual strength, frequently by 15 to 20 per cent and more, and also results in rather wide scattering. On the other hand, Fig. 6 shows that the interaction formula of Type II, is safe in nearly all cases, is never excessively conservative, and results in rather narrow scattering.

This comparison is somewhat distorted because the values for P' (for zero eccentricity), computed by the Bijlaard method from the Engesser-Shanley stress σ_{cES} (see above), are somewhat too conservative in that they overestimate, for these sections, the influence of residual stresses in lowering the effective proportional limit. This was mentioned previously, is apparent from Table 4, and is reflected in the interaction plots where for M = 0 all test results fall above 1 (one). If a less conservative approach had been used in computing P', interaction formula I would have been more unsafe, while formula II would have resulted in a straight line very close to the middle of the narrow scattering band.

A statistical study of the correlation of test data with the various theories is summarized in Table 5. For the secant formula and the Bijlaard method, the ratio of the experimental ultimate load to the predicted value was used as the "observation"; the sum $P/P' + M/M'$ was used for interaction formula I, and the sum $\frac{P}{P'} + \frac{M}{M'(1 + P/P_E)}$ for interaction formula II. Arithmetic means, standard deviations, and coefficients of variation have been computed for an assumed normal distribution, since the number of tests was too small to justify further refinement.

The results of the statistical study, as given in Table 5, show quite definitely that for these columns, bent about an axis parallel to the flanges, and without tendency to torsional instability, the secant formula gives the most satisfactory correlation of predicted and actual ultimate loads. Next in agreement are the interaction formula of Type II and the Bijlaard method, both of which show satisfactory and practically identical coefficients of variation, and both of which err slightly and systematically on the conservative side, for reasons previously discussed. The customary interaction formula, Type I, shows the largest coefficient of variation, i.e., the largest scattering range, is the only one which consistently errs on the unsafe side, and must be regarded as unsatisfactory.

TABLE 3

INTERACTION FORMULAS

Specimen t x b	L/r	$\frac{ec}{r^2}$	(1) $\frac{P}{P'}$	(2) $\frac{M}{M'}$	Sum (1) + (2)	(3) $\frac{M}{M'(1 - P/P_e)}$	Sum (1) + (3)
1/4 x 3	49	0.25	0.802	0.156	0.958	0.210	1.012
1/4 x 3	69	0.25	0.769	0.141	0.910	0.257	1.026
1/4 x 3	108	0.25	0.768	0.096	0.864	0.412	1.180
1/4 x 3	49	0.75	0.587	0.343	0.930	0.423	1.010
1/4 x 3	69	0.75	0.542	0.298	0.840	0.438	0.980
1/4 x 3	108	0.75	0.586	0.220	0.806	0.528	1.114
1/4 x 3	49	1.50	0.433	0.508	0.941	0.589	1.022
1/4 x 3	69	1.50	0.408	0.449	0.857	0.591	0.999
1/4 x 3	108	1.50	0.443	0.333	0.776	0.598	1.041
1/4 x 4	36	0.25	0.850	0.174	1.024	0.208	1.058
1/4 x 4	66	0.25	0.778	0.145	0.923	0.263	1.041
1/4 x 4	110.5	0.25	0.763	0.089	0.852	0.376	1.139
1/4 x 4	36	0.75	0.610	0.375	0.985	0.424	1.034
1/4 x 4	66	0.75	0.541	0.305	0.846	0.442	0.983
1/4 x 4	110.5	0.75	0.576	0.202	0.778	0.476	1.052
1/4 x 4	36	1.50	0.417	0.514	0.931	0.557	0.974
1/4 x 4	66	1.50	0.384	0.432	0.816	0.555	0.939
1/4 x 4	110.5	1.215	0.505	0.287	0.792	0.579	1.084
1/2 x 3	53	0.25	0.828	0.149	0.977	0.206	1.034
1/2 x 3	74	0.25	0.783	0.131	0.914	0.248	1.031
1/2 x 3	117	0.25	0.779	0.085	0.864	0.385	1.164
1/2 x 3	53	1.50	0.453	0.488	0.941	0.577	1.030
1/2 x 3	74	1.50	0.420	0.422	0.842	0.566	0.988
1/2 x 3	117	1.50	0.485	0.317	0.802	0.615	1.100

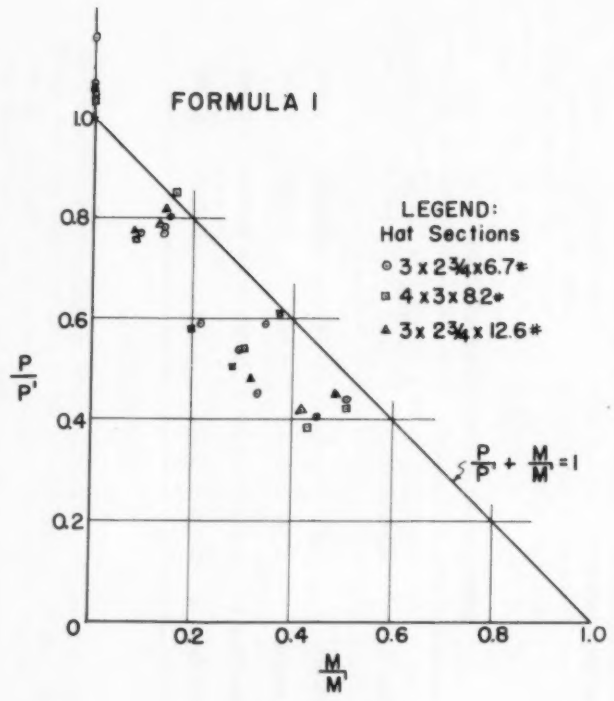

Figure 5

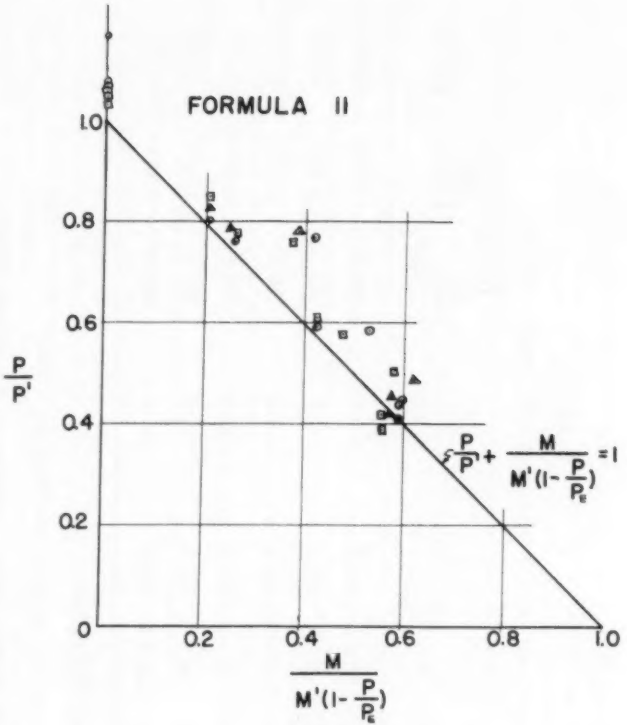

Figure 6

Comparison of Failure Loads with Interaction Formulas

TABLE 4

CONCENTRIC SPECIMENS

Specimen	$L/_r$	(1) Equilibrium* P_{ult}, kips	(2) Maximum** P, Kips	(3) Theor. P', Kips	(4) (1)/(3)	(5) (2)/(3)
1/4 x 3	49	156.8	162.6	152.2	1.030	1.068
1/4 x 3	69	163.4	166.5	143.0	1.143	1.163
1/4 x 3	108	102.0	104.1	98.0	1.041	1.062
1/4 x 4	36	203.5	208.5	202.0	1.007	1.032
1/4 x 4	66	189.0	193.7	185.0	1.022	1.047
1/4 x 4	110.5	119.7	121.2	115.0	1.040	1.054

* Highest Stable Load

** Maximum load reached, but load not stable

Note: Stiffening effect of batten plates and end blocks has been neglected.

TABLE 5

COMPARISON OF VARIOUS FAILURE THEORIES

Type of Observation	Range of Observations	Arithmetic Mean	Standard Deviation	Coefficient of Variation
Secant Formula	0.967 to 1.138	1.027	0.0398	3.87%
Bijlaard Method	0.939 to 1.182	1.065	0.0562	5.28%
Interaction Type I	0.776 to 1.024	0.882	0.0658	7.47%
Interaction Type II	0.939 to 1.180	1.043	0.0593	5.68%

Discussion

It is seen that the ultimate loads of these columns were predicted with almost equal accuracy by the secant formula (i.e. based on elastic calculations), by the Bijlaard method (based on plastic calculations), and by the interaction formula of Type II. The only method which proved definitely unsatisfactory is the interaction formula of Type I.

In regard to the three satisfactory methods, the following may be said in regard to their validity for columns of types other than those tested:

The secant formula (or any determination based on an initial-yield criterion) is accurate only for bending about an axis parallel to the flanges, and provided that such bending is not accompanied by torsion. It has been shown in Ref. 2 that in the case of bending about an axis parallel to the web the initial-yield criterion underestimates the column capacity considerably, up to 100% in those tests. On the other hand it is well known (see e.g. Ref. 5) that for columns bent about a major axis parallel to the flanges, torsion can reduce the ultimate load considerably below that predicted by an initial-yield criterion.

As to the Bijlaard method, the combined results of the present tests and those reported in Ref. 2 indicate that this method is satisfactorily accurate no matter whether bending is about an axis parallel or perpendicular to the flanges, and no matter whether the columns are hinged or elastically restrained. The principal limitation is that it does not apply in the case of flexural-torsional buckling. That is, in case of application to bending about a major axis parallel to the flanges, it is restricted to the case where torsion is prevented as by appropriate minor-axis bracing.

The interaction formula of Type II has been proposed by various investigators.[6,7] In the present paper and its Appendix it is shown that the results of this formula are satisfactorily accurate for bending about axes either parallel or perpendicular to the flanges when torsion is prevented, and for end-restrained as well as for hinged columns. In addition, however, it has been shown previously by others[7,8] that this formula is also satisfactory for aluminum columns subject to flexural-torsional as well as purely flexural failure. Finally, by means of an extensive series of tests, C. Massonnet and F. Campus[9] have shown that for steel columns also this formula is likewise satisfactory both for flexural and for torsional-flexural failure, including the case of unequal as well as opposite end moments. In the case of torsional-flexural failure (major-axis bending of unbraced I-shaped columns) the critical moment for lateral beam buckling is substituted for M', and for unequal end moments an equivalent moment is used for M which is obtained from a very simple formula.

To summarize: While it is possible to devise satisfactory formulas for various special cases of eccentrically loaded columns, of those so far proposed the only simple equation which seems to apply satisfactorily to all situations is the interaction formula of Type II.

CONCLUSIONS

1. Although flange-projection-to-thickness ratios ranged from 4.4 to 11.3, flange buckling occurred only in the plastic region, did not affect column strength, and had no discernible effect on the behavior of the columns past the ultimate load, in that region of large deflections which is important in connection with ultimate strength design.

2. For these columns bent about an axis parallel to the flanges the secant formula showed best correlation with experimental data. It is concluded that for columns bent so that the entire flange width is stressed uniformly, the ultimate load is practically identical with that for which the elastically computed flange stress becomes equal to the yield point, provided torsional-flexural failure is precluded.
3. The Bijlaard method also was satisfactory for these particular Z-section columns. Correlation was not quite as good as with the secant formula, but improvement would be possible by adjustment of the assumed proportional limit stress, in order to reflect more nearly the small influence of residual stresses in these tests.
4. The simple interaction formula, $\frac{P}{P'} + \frac{M}{M'} = 1$ is definitely unconservative for eccentrically loaded columns. For all but one of 24 specimens this formula predicted larger strengths than were obtained by test.
5. The interaction formula, $\frac{P}{P'} + \frac{M}{M'(1 - P/P_E)} = 1$ showed very satisfactory correlation with test data. Scattering was small and only six specimens failed at loads lower than the predicted values, the largest error in this direction being 6 per cent and the rest of the "unsafe" observations erring by 2-1/2 per cent or less.
6. Evidence presented in the Appendix shows that the better interaction formula is also satisfactory for end-restrained columns, although it does not provide a significant simplification in this case.
7. Reviewing the evidence of other investigators it is concluded that only the interaction formula of 5, above is equally satisfactory for all investigated cases of eccentric columns: those of steel or aluminum, hinged or restrained, with equal or unequal eccentricities, with bending parallel or perpendicular to the flange, and failing flexurally or by combined torsion and flexure.

ACKNOWLEDGEMENT

This paper reports on part of the results of a research project on buckling of rigid joint structures sponsored at Cornell University, (Ithaca, N. Y.) by the Column Research Council and the Bureau of Public Roads, United States Department of Commerce.

REFERENCES

1. R. E. Mason, G. P. Fisher, and George Winter, "Tests and Analysis of Eccentrically Loaded Columns," 4th Progress Report, Investigation on Buckling of Rigid Joint Structures, Cornell University, Ithaca, New York, April 1956.
2. P. P. Bijlaard, G. P. Fisher, and George Winter, "Eccentrically Loaded End Restrained Columns," Trans. ASCE, Vol. 120, pp. 1070 and 1105, 1955.
3. A. W. Huber and L. S. Beedle, "Residual Stresses and the Compressive Strength of Steel", Lehigh Inst. of Research, 1953.

4. G. P. Fisher, Third Progress Report on Investigation of Flexural Buckling of Rigid Joint Structures, Cornell University, Ithaca, New York, Dec. 1953.

5. B. G. Johnston and L. Cheney, "Steel Columns of Rolled Wide Flange Sections," 2nd Progress Report, Am. Inst. of Steel Construction, 1952.

6. H. N. Hill and J. W. Clark, "Lateral Buckling of Eccentrically Loaded I- and H-Section Columns", Proc. 1st Nat. Cong. Appl. Mech., 1951, p. 407.

7. J. Zickel and D. C. Drucker, "Investigation of Interaction Formula", Report No. 1, Column Research Council, Brown Univ., Providence, R. I., April 1951.

8. J. W. Clark, "Eccentrically Loaded Aluminum Columns", Trans. ASCE, Vol. 120, p. 1116, 1955.

9. F. Campus and C. Massonnett, "Recherches sur le flambement de Colonnes en acier A37, a profil en double Te, sollicitées obliquement." Comptes Rendus de Recherches, I.R.S.I.A., No. 17, Brussels, April, 1956. For summary in English, see C. Massonnet, "Evaluation of the Plastic Design Method of Steel Structures in the Light of Some Recent Belgian Researches", Ingeniøren, 15 April 1957, pp. 355-367. (Copenhagen)

10. George Winter, P. T. Hsu, B. Koo and M. H. Loh, "Buckling of Trusses and Rigid Frames", Cornell Univ. Eng. Exp. Station Bull. No. 36, 1948.

Appendix

End-Restrained Columns

An extensive experimental and theoretical investigation on elastically end-restrained, eccentrically loaded columns was reported in Ref. 2. Column specimens consisted of square-bar sections and of I-sections bent about the minor axis, parallel to the web. It was shown that the Bijlaard method, as applied to these restrained columns, predicted the failure loads very accurately. On the other hand, it was shown that the measured ultimate loads exceeded greatly (up to 100%) the calculated incipient-yield loads of these columns (i.e. the loads calculated for these restrained columns on the same basis on which secant-formula loads are calculated for hinged columns.)

In view of the simplicity of interaction formulas, and in view of the versatility of the interaction formula of Type II as explained in the body of the paper, it seemed of interest to evaluate the results of that investigation in terms of these two interaction formulas. This is done in the present appendix.

As indicated in Ref. 2, elastically-restrained eccentric columns of length L and eccentricity e are successfully analyzed by replacing them by equivalent eccentric hinged-hinged columns of length cL and with effective eccentricity e_e. The correct determination of cL and e_e involves the calculation of the plastic reduction factor η, which is computed by successive approximation. Figs. 7 and 8 were constructed on this basis. That is, in these figures

P is the ultimate test load

P' is the concentric Engesser-Shanley buckling load determined from Eq. (20) of Ref. 2 for the equivalent column of length cL, where this

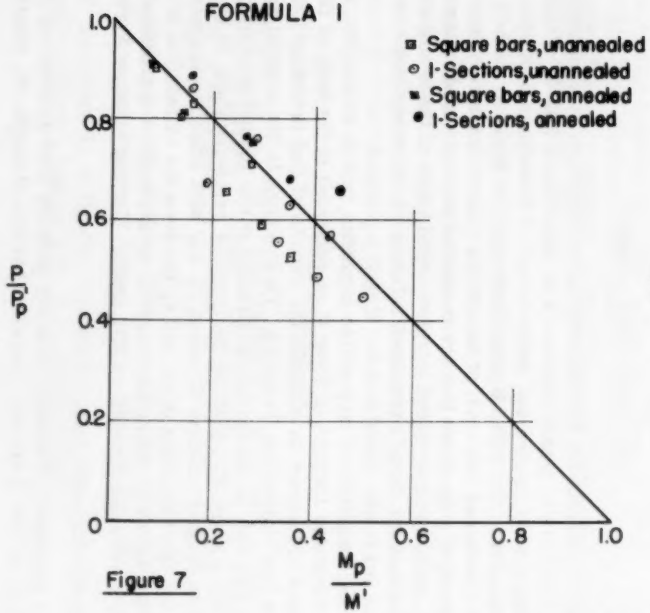

Figure 7

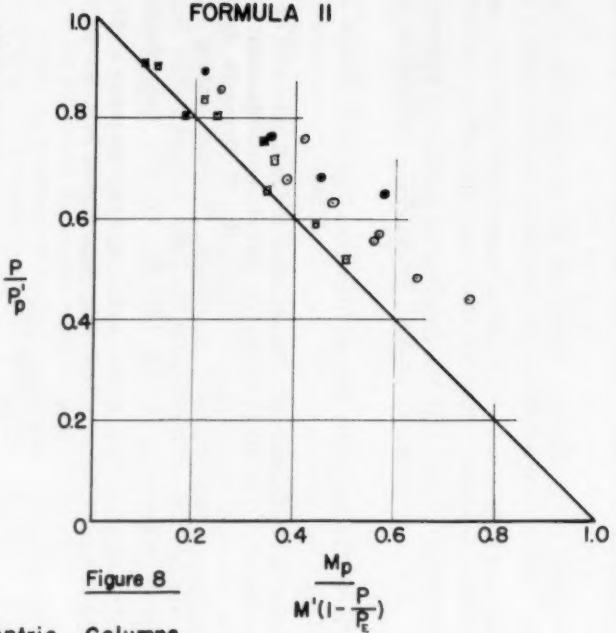

Figure 8

End-restrained Eccentric Columns
Failure Loads vs. Interaction Formulas

length is calculated on the basis of the appropriate plastic reduction factor η.

M_p is the portion of the total bending moment Pe which at failure, is resisted by the column, i.e. $M_p = Pe_e$, where the equivalent eccentricity e_e is again determined by means of the plastic reduction factor η, as indicated in Step 5, p. 1086 of Ref. 2.

M' is the plastic hinge moment of the member about the axis about which bending was applied (the minor axis for the I-sections), computed by the simple plastic theory from the dimensions of the section and the yield point obtained from the compression tests.

P_E is the elastic Euler load of a column of length c'L, where c'L is determined for fully elastic conditions, i.e. for $\eta = 1$. (Methods for this determination are given in Ref. 10).

The above method is intrinsically consistent with the analytical approach developed in Ref. 2. Its practical disadvantage, in connection with an interaction formula, consists in the fact that use is made of the plastic reduction factor η, which must be determined by successive approximation. Hence, the use of an interaction formula, if successful, merely replaces Step 7, p. 1088 of Ref. 2, which happens to be the simplest and most direct of the various steps there given. For this reason interaction formulas have little real advantage in this case. Their validity is explored in this Appendix chiefly to verify whether they apply to restrained columns.

Fig. 8 indicates that the use of the more accurate interaction formula, Eq. II, results in a grouping of test values close to and above the straight line representing this equation. Hence, if this equation is used in connection with the correct plastic reduction factor η, a safe and reasonably accurate determination of failure loads results.

Fig. 7 indicates that the simpler interaction formula, Type I, used in conjunction with the correct plastic reduction factor η, gives significantly unconservative determinations for a sizeable number of the tests. This is in agreement with the findings of other investigators and with the evidence presented in the body of the present paper.

Paper 1793 October, 1958 EM 4

Journal of the
ENGINEERING MECHANICS DIVISION
Proceedings of the American Society of Civil Engineers

APPROXIMATE BUCKLING LOADS OF OPEN COLUMNS

Yu-kweng M. Lin,[1] A. M. ASCE
(Proc. Paper 1793)

SYNOPSIS

A general equation for buckling loads of open thin-walled columns is presented in this paper. The equation is applicable to any boundary conditions. The coupling effect between torsional buckling and bending bucklings is considered. It is found that a most general case of triple coupling may be treated as two double coupling cases without introducing significant errors. Equations are also given for columns restrained by flexible skin.

NOTATIONS

A	Cross-sectional area
C_u	Uniform torsion constant (corresponding to the Saint-Venant Theory of Torsion)
C_w	Warping constant, $= \int_A (D - w_s)^2 \, dA$
D	Average warping of a section due to unit twist
E	Modulus of elasticity
G	Modulus of elasticity in shear
I	Moment of inertia
J	Polar moment of inertia
M	External end moment
P	Resultant end thrust
U	Strain energy

Note: Discussion open until March 1, 1959. To extend the closing date one month, a written request must be filed with the Executive Secretary, ASCE. Paper 1793 is part of the copyrighted Journal of the Engineering Mechanics Division, Proceedings of the American Society of Civil Engineers, Vol. 84, No. EM 4, October, 1958.

1. Prof. of Civ. Eng., Imperial College of Engineering, Addis Ababa, Ethiopia.

W	Work
X	Dimensionless function of x, representing mode shape
ℓ	Length of column
m	Mode shape factor
w_s	Warping at any point of a section due to unit twist
v, w	Translations in the y, z directions respectively (referred to the shear center without subscription
x, y, z	Coordinate axes through shear center, or the corresponding coordinate values
γ	Coupling factor
η, ζ	Centroidal coordinate axes (η and ζ are parallel to y and z respectively)
κ	A section property
ϕ	Angle of twist
δ	Unit compressive stress

The following symbols are used for subscripts

C	Centroid
M, N	Line of attachment to skin
O	Shear center
Q	Point of application of resultant thrust
m	Modified

INTRODUCTION

A prismatic member of thin-walled open section may have small rigidity against torsion. When used as a column, it may buckle in torsion, or in coupled bending and torsion. In general, the solution of the critical load, at which the buckling occurs, involves three simultaneous differential equations, and usually is difficult to solve except in the case of a column with simple supports at both ends. Further difficulty arises when a mixed boundary is in question, such as an end condition providing a simple support for torsion but a clamped support for bending. Using the Rayleigh-Ritz method these complications can be avoided, and the solution can be extended to cover all boundary conditions.

Energy Consideration

The Rayleigh-Ritz method is based on the principle of conservation of energy of a system. Let us consider a column of arbitrary thin-walled open shape as shown in Fig. 1. C is the centroid, and 0 is the shear center of the section. η and ζ are the centroidal principal axes corresponding to the

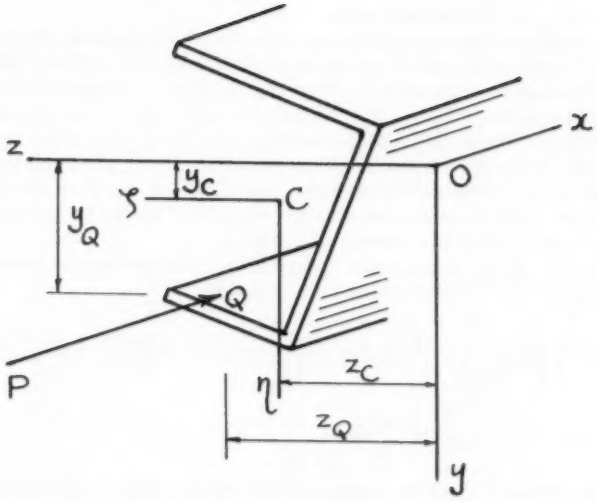
z
x
O
y_c
ζ
C
y_Q
Q
P
η
z_c
z_Q
y

Fig. 1

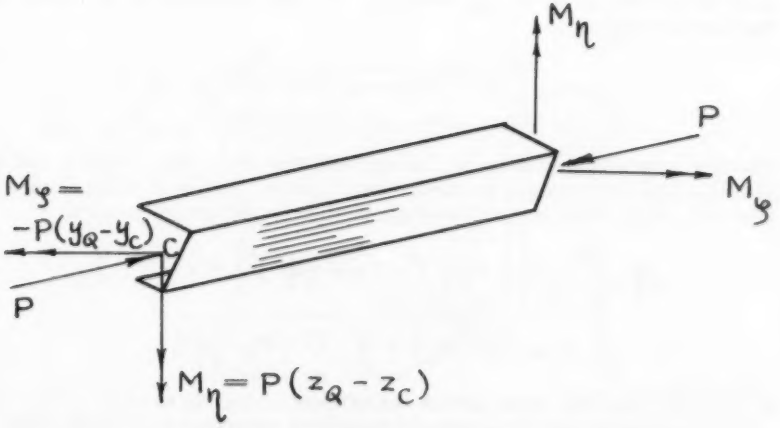
M_η
P
M_ζ
$M_\zeta =$
$-P(y_Q - y_c)$
C
P
$M_\eta = P(z_Q - z_c)$

Fig. 2

minimum and maximum moments of inertia. We take the coordinate system with the origin at the shear center 0 of an end section, and with the y and z axes parallel to η and ζ respectively. In this way, the x axis will coincide with the locus of shear center when the column is undeformed.

The column is loaded at each end with a thrust P through point Q. For convenience of investigation, P will be replaced by an equivalent force system as shown in Fig. 2, where P now passes through C, and M_η, M_ζ, are moments about the and axes, respectively.

Any displaced position of a cross section can be completely defined by the translation components v and w of the shear center of the section (the displaced shear center is indicated as 0' in Fig. 3) and a rotation ϕ around 0'. Owing to the end moments M_η, M_ζ, there are some initial deformations before the buckling. These initial deformations will be disregarded in the following study of energy transformation associated with the buckling only. More precisely, the components of displacement, v, w and ϕ in the discussions to follow are the additional displacements measured from the initially deformed shape just before the instant of buckling.

The additional strain energy due to additional displacements associated with the buckling may be expressed as follows:[2]

$$\Delta U = \frac{1}{2}\left[EI_\zeta\int_0^\ell (v'')^2 dx + EI_\eta\int_0^\ell (w'')^2 dx + GC_u\int_0^\ell (\phi')^2 dx + EC_w\int_0^\ell (\phi'')^2 dx\right] \quad (1)$$

where the primes represent the order of derivation with respect to x. It is seen that Eq. (1) does not include the energy contributed by the direct shear (distinguished from torsional shear) and the additional shear due to warping. This is permissible provided that the column is not extremely short.[3]

The increment of energy given in Eq. (1) results from the additional work done by the end thrust during buckling. The end thrust on an elemental fiber has an intensity of

$$\sigma = \frac{P}{A} + \frac{M_\eta}{I_\eta}(z - z_C) - \frac{M_\zeta}{I_\zeta}(y - y_C) \quad (2)$$

The sign convention used in Eq. (2) is consistent with Figs. 1 and 2, and a positive sign corresponds to compressive stress. When buckling occurs, the two ends of the fiber move toward each other by an amount equal to

$$\Delta\ell = \int_0^\ell \left[\frac{1}{2}\left\{(v' - z\phi')^2 + (w' + y\phi')^2\right\} + v''(y - y_C) + w''(z - z_C) + \phi''(D - w_S)\right] dx \quad (3)$$

2. Ref. (1), Eq. (29), after setting the product of inertia equal to zero. Reference numbers refer to similarly numbered references in bibliography at the end of the paper.
3. For a very short column, failure would usually be a local crippling type with original shape of cross-section distorted. See Ref. (2).

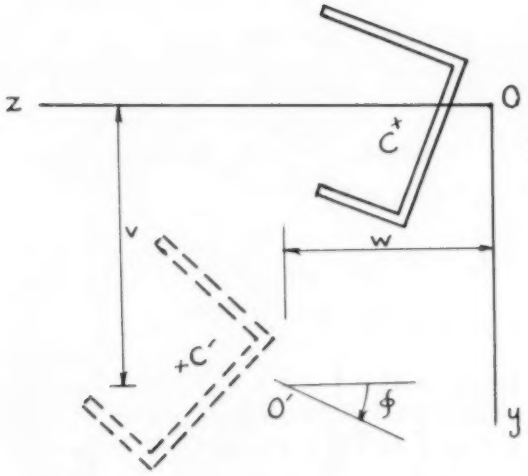

Fig. 3

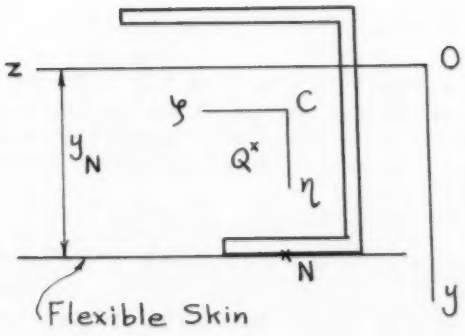

Fig. 4

The total additional work is

$$\Delta W = \int_A \Delta \ell \cdot \sigma \cdot dA \quad --- \tag{4}$$

Observing that

$$\int_A z\, dA = z_C\, A$$

$$\int_A y\, dA = y_C\, A$$

$$\int_A (y^2 + z^2)\, dA = J_O$$

$$\int_A (y - y_C)\, dA = 0$$

$$\int_A (z - z_C)\, dA = 0$$

$$\int_A z (z - z_C)\, dA = \int_A (z - z_C)^2\, dA = I_\eta$$

$$\int_A y (y - y_C)\, dA = \int_A (y - y_C)^2\, dA = I_\zeta$$

$$\int_A y (z - z_C)\, dA = \int_A (y - y_C)(z - z_C)\, dA = I_{\eta\zeta} = 0$$

$$\int_A z (y - y_C)\, dA = \int_A (z - z_C)(y - y_C)\, dA = I_{\eta\zeta} = 0$$

$$\int_A (D - w_s)\, dA = 0 \ ^4$$

$$\int_A (z - z_C)(D - w_s)\, dA = \int_A (y - y_C)(D - w_s)\, dA = 0 \ ^5$$

and denoting

$$k_\eta = \int_A (y^2 + z^2)(z - z_C)\, dA = \int_A z (y^2 + z^2)\, dA - z_C\, J_O$$

$$k_\zeta = \int_A (y^2 + z^2)(y - y_C)\, dA = \int_A y (y^2 + z^2)\, dA - y_C\, J_O$$

4. By definition, D is the average value of w_s of a section, and so the relation is self evident.
5. See Ref. (1), Appendix III.

we obtain

$$\Delta W=\frac{1}{2}P\left[\int_0^\ell (v')^2dx-2\left(z_C+\frac{M_\eta}{P}\right)\int_0^\ell v'\phi'dx+2\left(y_C-\frac{M_\varphi}{P}\right)\int_0^\ell w'\phi'dx\right.$$
$$+\int_0^\ell (w')^2dx+\left(\frac{J_0}{A}+\frac{M_\eta}{P}\cdot\frac{k_\eta}{I_\eta}-\frac{M_\varphi}{P}\cdot\frac{k_\varphi}{I_\varphi}\right)\int_0^\ell(\phi')^2dx \qquad (4')$$
$$\left.+2\frac{M_\eta}{P}\int_0^\ell w''dx-2\frac{M_\varphi}{P}\int_0^\ell v''dx\right] \text{ - - - - - -}$$

Substituting

$$M_\eta = P\,(z_Q - z_C)$$
$$M_\zeta = -P\,(y_Q - y_C)$$

Eq. (4') may be written as follows

$$\Delta W=\frac{P}{2}\left[\int_0^\ell (v')^2dx-2z_Q\int_0^\ell v'\phi'dx+2y_Q\int_0^\ell w'\phi'dx+\int_0^\ell (w')^2dx\right.$$
$$\left.+\frac{J_m}{A}\int_0^\ell(\phi')^2dx+2(z_Q-z_C)\int_0^\ell w''dx+2(y_Q-y_C)\int_0^\ell v''dx\right] \qquad (4'')$$

where

$$\frac{J_m}{A}=\frac{J_0}{A}+(z_Q-z_C)\frac{k_\eta}{I_\eta}+(y_Q-y_C)\frac{k_\varphi}{I_\varphi}$$

In general, we may express

$$\left.\begin{aligned} v &= v_0\,X_v \\ w &= w_0\,X_w \\ \phi &= \phi_0\,X_\phi \end{aligned}\right\} \qquad (5)$$

where v_0, w_0, ϕ_0 are amplitudes, and X_v, X_w, X_ϕ, are dimensionless functions of x, representing the buckled shapes of the first mode[6] in three directions respectively. Substituting (5) into Eqs. (1) and (4''), we get

$$\Delta U=\frac{1}{2}\left[v_0^2EI_\varphi\int_0^\ell(X_v'')^2dx+w_0^2EI_\eta\int_0^\ell(X_w'')^2dx\right.$$
$$\left.+\phi_0^2GC_u\int_0^\ell(X_\phi')^2dx+\phi_0^2EC_w\int_0^\ell(X_\phi'')^2dx\right] \qquad (6)$$

6. The lowest mode order corresponds to the smallest of the eigen values of the critical load which is the only one of practical importance.

or

$$\Delta U = \frac{1}{2}\alpha \tag{6}$$

and

$$\Delta W = \frac{P}{2}\left[v_0^2\int_0^\ell (X_v')^2 dx - 2v_0\phi_0 z_Q\int_0^\ell X_v' X_\phi' dx + 2w_0\phi_0 y_Q\int_0^\ell X_w' X_\phi' dx \right.$$
$$+ w_0^2\int_0^\ell (X_w')^2 dx + \phi_0^2\frac{J_m}{A}\int_0^\ell (X_\phi')^2 dx + 2w_0(z_Q - z_C)\int_0^\ell (X_w'')dx$$
$$\left. + 2v_0(y_Q - y_C)\int_0^\ell (X_v'')dx\right] \tag{7}$$

or

$$\Delta W = \frac{P}{2}\beta \tag{7}$$

where α and β represent the expressions inside the brackets of (6) and (7) respectively.

Critical Loads for Coupled Buckling

The critical load at which buckling will occur may be obtained by equating (6) and (7), which gives

$$P = \frac{\alpha}{\beta} \tag{8}$$

It is seen that both α and β contain arbitrary amplitudes v_0, w_0, ϕ_0. The true values of these amplitudes should render a minimum value for P. This condition is satisfied when

$$\left.\begin{aligned} \frac{\partial P}{\partial v_0} &= 0 \\ \frac{\partial P}{\partial w_0} &= 0 \\ \frac{\partial P}{\partial \phi_0} &= 0 \end{aligned}\right\} \tag{9}$$

Applying (9) to (8) and multiplying the resultant expression by β we obtain

$$\left.\begin{aligned}\frac{\partial\alpha}{\partial v_0}-P\frac{\partial\beta}{\partial v_0}&=0\\ \frac{\partial\alpha}{\partial w_0}-P\frac{\partial\beta}{\partial w_0}&=0\\ \frac{\partial\alpha}{\partial\phi_0}-P\frac{\partial\beta}{\partial\phi_0}&=0\end{aligned}\right\}\qquad(10)$$

Substitution of the expressions for α and β into Eqs. (10) leads to three simultaneous equations for v_0, w_0, and ϕ_0, namely

$$2v_0EI_\eta\int_0^\ell(X_v'')^2dx-P\left[2v_0\int_0^\ell(X_v')^2dx-2\phi_0z_Q\int_0^\ell X_v'X_\phi'dx+2(y_Q-y_C)\int_0^\ell(X_v'')\,dx\right]=0\qquad\text{---------- (a)}$$

$$2w_0EI_\eta\int_0^\ell(X_w'')^2dx-P\left[2w_0\int_0^\ell(X_w')^2dx+2\phi_0y_Q\int_0^\ell X_w'X_\phi'dx+2(z_Q-z_C)\int_0^\ell(X_w'')dx\right]=0\qquad\text{---------- (b)}$$

$$2\phi_0\left[GC_u\int_0^\ell(X_\phi')^2dx+EC_w\int_0^\ell(X_\phi'')^2dx\right]-P\left[-2v_0z_Q\int_0^\ell X_v'X_\phi'dx+2w_0y_Q\int_0^\ell X_w'X_\phi'dx+2\phi_0\frac{J_m}{A}\int_0^\ell(X_\phi')^2dx\right]=0\qquad\text{-- (c)}$$

After rearrangement of terms, we get

$$\left[EI_\eta\int_0^\ell(X_v'')^2dx-P\int_0^\ell(X_v')^2dx\right]v_0+\left[Pz_Q\int_0^\ell X_v'X_\phi'dx\right]\phi_0=P(y_Q-y_C)\int_0^\ell X_v''dx\qquad\text{--------- (a')}$$

$$\left[EI_\eta\int_0^\ell(X_w'')^2dx-P\int_0^\ell(X_w')^2dx\right]w_0-\left[Py_Q\int_0^\ell X_w'X_\phi'dx\right]\phi_0=P(z_Q-z_C)\int_0^\ell X_w''dx\qquad\text{---------- (b')}$$

$$\left[Pz_Q\int_0^\ell X_v'X_\phi'dx\right]v_0-\left[Py_Q\int_0^\ell X_w'X_\phi'dx\right]w_0+\left[GC_u\int_0^\ell(X_\phi')^2dx+EC_w\int_0^\ell(X_\phi'')^2dx-P\frac{J_m}{A}\int_0^\ell(X_\phi')^2dx\right]\phi_0=0\qquad\text{---------- (c')}$$

The values of v_0, w_0, and ϕ_0 become indefinite (mathematical interpretation of instability or buckling) when the following determinate vanishes

$$\begin{vmatrix} EI_\varphi\int_0^\ell (X_v'')^2dx - P\int_0^\ell (X_v')^2dx & 0 & Pz_Q\int_0^\ell X_v'X_\varphi'dx \\ 0 & EI_\eta\int_0^\ell (X_w'')^2dx - P\int_0^\ell (X_w')^2dx & -Py_Q\int_0^\ell X_w'X_\varphi'dx \\ Pz_Q\int_0^\ell X_v'X_\varphi'dx & -Py_Q\int_0^\ell X_w'X_\varphi'dx & GC_u\int_0^\ell (X_\varphi')^2dx + EC_w\int_0^\ell (X_\varphi'')^2dx - P\frac{J_m}{A}\int_0^\ell (X_\varphi')^2dx \end{vmatrix} = 0 \quad (11)$$

Eq. (11) is a cubic equation for p. The terms containing $\int_0^\ell X_v'X_\varphi'dx$ and $\int_0^\ell X_w'X_\varphi'dx$ demonstrate the interaction (or coupling) between bending and torsional bucklings. The equation gives three positive roots corresponding to three possible ways of coupling. However, the smallest root is the only one of practical significance.

Let us now consider a special case, in which $y_Q = z_Q = 0$ (resultant thrust P passes through the shear center 0). Examining Eq. (11), the interacting terms will no longer exist, and the three roots are evidently

$$\left.\begin{aligned} P_v &= \frac{EI_\varphi\int_0^\ell (X_v'')^2dx}{\int_0^\ell (X_v')^2dx} \\ P_w &= \frac{EI_\eta\int_0^\ell (X_w'')^2dx}{\int_0^\ell (X_w')^2dx} \\ P_\varphi &= \frac{GC_u\int_0^\ell (X_\varphi')^2dx + EC_w\int_0^\ell (X_\varphi'')^2dx}{\frac{J_m}{A}\int_0^\ell (X_\varphi')^2dx} \end{aligned}\right\} \quad (12)$$

The first two roots in (12) are critical loads corresponding to the noncoupled bending (or Euler) type, and the third root is the critical load corresponding

to the noncoupled torsional (or Wagner) type of buckling. We shall call P_v, P_w and P_ϕ the noncoupled critical loads in the v, w and ϕ directions respectively.

Generally speaking, the coupling effect will alter the mode shapes in some degree, if the noncoupled bending mode shape are different from the noncoupled torsional mode shape for the specific boundary conditions. However such an alteration is usually small, if there is any, because the boundary conditions remain the same. In most cases, the noncoupled bending modes and the noncoupled torsional mode are identical,[7] then there will be no alteration of either shape. Even if there is some alteration of shapes, Eqs. (12) may still be considered as good approximate relations between the coupled mode shapes and the noncoupled critical loads.

Using relations (12) in Eq. (11), and after expanding the determinant and simplifying, we obtain

$$P^3\left(1-\gamma_{v\phi}m_{v\phi}-\gamma_{w\phi}m_{w\phi}\right)-P^2\left(P_v+P_w+P_\phi -P_v\cdot\gamma_{w\phi}m_{w\phi}-P_w\cdot\gamma_{v\phi}m_{v\phi}\right) +P\left(P_vP_\phi+P_wP_\phi+P_vP_w\right)-P_vP_wP_\phi=0 \cdots \tag{13}$$

where

$$\left.\begin{aligned} \gamma_{v\phi}&=\frac{Az_Q^2}{J_m}=\text{a coupling factor}\\ \gamma_{w\phi}&=\frac{Ay_Q^2}{J_m}=\text{a coupling factor}\\ m_{v\phi}&=\frac{\left\{\int_0^\ell X_v'X_\phi'dx\right\}^2}{\int_0^\ell(X_v')^2dx\int_0^\ell(X_w')^2dx}=\text{a mode shape factor}\\ m_{w\phi}&=\frac{\left\{\int_0^\ell X_w'X_\phi'dx\right\}^2}{\int_0^\ell(X_w')^2dx\int_0^\ell(X_\phi')^2dx}=\text{a mode shape factor} \end{aligned}\right\} \tag{14}$$

When the noncoupled mode shapes in bending and torsion are identical (i.e. $X_v = X_w = X_\phi$), it is seen that $m_{v\phi} = m_{w\phi} = 1$. And,

$$P^3\left(1-\gamma_{v\phi}-\gamma_{w\phi}\right)-P^2\left(P_v+P_w+P_\phi-P_v\gamma_{w\phi}-P_w\gamma_{v\phi}\right) +P\left(P_vP_\phi+P_wP_\phi+P_vP_w\right)-P_vP_wP_\phi=0 \cdots \tag{15}$$

is an exact equation for P for this case. But when X_v, X_w and X_ϕ are not identical, $m_{v\phi}$ and $m_{w\phi}$ are less than unity (in view of Schwarz's theorem of inequality). Their values can be approximated by substituting the noncoupled

7. See Tables I and II in the following paragraph.

mode shapes (use Tables I and II in the following paragraph) in relations (14). In that case, Eq. (13) is to be used and the result is an approximate one. Fortunately, a slight change of the values of m affects very little the smallest root of Eq. (13) which is the only root important to engineers; therefore the approximate formula (13) is usually accurate enough for practical purposes.

Eq. (15) has been given by several previous investigators in different notations and forms.[8] They were derived for columns of simple supports at both ends with centroidal thrust. Here, we have proved that the same equation (or similar equation if Eq. (13) is used) may be applied to a column of other end conditions with a resultant end thrust at any arbitrary point. The only precautions are: (1) P_v, P_w, P_ϕ represent the noncoupled critical loads corresponding to their respective boundary conditions; (2) A modified polar moment of inertia J_m is used instead of the polar moment of inertia with respect to the shear center.

Some conclusions drawn by the previous investigators for columns of simple supports and centroidal thrust[9] may also be applied as well here. The smallest root of Eq. (15) or Eq. (13) is smaller than any of the noncoupled values P_v, P_w and P_ϕ, therefore disregarding the coupling effect is unconservative. However, if one of the noncoupled P's is much smaller than the others, we can practically take that value as the smallest root, and the solution of the cubic equation (13) or (15) becomes unnecessary. For example, if $P_\phi << P_v < P_w$, we shall find that the smallest $P \approx P_\phi$. The buckling is said to be torsionally predominant. On the other hand, if $P_v < P_w << P_\phi$, we may take the smallest $P \approx P_v$. The buckling is said to be bending predominant (more precisely, in the v direction). If the three noncoupled P's are very close to each other, the coupling effect will be large.

Noncoupled Critical Loads and Mode Shapes

For application of Eqs. (13) to (15) knowledge of the noncoupled critical loads and sometimes the noncoupled mode shapes is necessary. The noncoupled critical loads in bending (usually called Euler's loads) are commonly known. They are given with the mode shapes in Table I corresponding to their boundary conditions.

TABLE I

Noncoupled Buckling In Bending

Boundary Conditions	Mode Shape (X_v or X_w)	P_v or P_w
Simple - Simple	$\sin \frac{\pi x}{\ell}$	$\frac{\pi^2 E I}{\ell^2}$
Fixed - Fixed	$1 - \cos \frac{2\pi x}{\ell}$	$\frac{\pi^2 E I}{(0.5\ell)^2}$
Simple - Fixed	$\sin \frac{4.493\, x}{\ell} - \frac{x}{\ell} \sin 4.493$	$\frac{\pi^2 E I}{(0.7\ell)^2}$
Fixed - Free (Cantilever)	$1 - \cos \frac{\pi x}{2\ell}$	$\frac{\pi^2 E I}{4\ell^2}$

8. See, for examples Ref. (1), Eq. (20); Ref. 3, Eq. (84) and Ref. 4, Eq. (61).
9. See, for example, Ref. (4).

The noncoupled torsional buckling was first investigated by H. Wagner.[10] The differential equation for this type of buckling is

$$EC_w\phi^{IV} + \left(\frac{PJ_m}{A} - GC_u\right)\phi'' = 0 \qquad (16)[11]$$

Its general solution is found to be

$$\phi = C_1 \sin \lambda x + C_2 \cos \lambda x + C_3 x + C_4 \qquad (17)$$

where

$$\lambda = \sqrt{\frac{PJ_m}{EC_wA} - \frac{GC_u}{EC_w}}$$

There are four boundary conditions at two ends of a column, from which we can determine the value λ and three arbitrary constants in (17). One of the constants remains arbitrary.

A specific interpretation for the boundary conditions in torsion is needed. A simply supported end means the column is prevented from twisting about any longitudinal axis, but is free to warp (or warping stresses are zero). When written in mathematical language, the two conditions correspond to

$$\phi = 0$$

$$\phi'' = 0$$

By a fixed end in torsion, it is implied that both rotation and warping are prohibited, and

$$\phi = 0$$

$$\phi' = 0$$

are the mathematical expressions. For a free end, there is no restraint of any kind, and the following conditions must be satisfied

$$\phi'' = 0$$

$$GC_u\phi' - EC_w\phi''' = 0$$

The second condition means that the total torque about any longitudinal axis at the end should vanish.[12]

Applying the above-mentioned boundary conditions to (17), we obtain, similar to Table I, the noncoupled critical loads and the noncoupled mode shapes in torsion as shown in Table II.

In Table II, the interesting result is observed, that for a cantilever column the mode shape in torsion is zero, yet there is a definite value for the critical load. The fact is the free end offers no means to counteract any twisting, and the instability is probably of a local nature.

---

10. Ref. (5).
11. As stated before, noncoupled torsional buckling can only occur when the resultant thrust passes through the shear center, and $J_m = J_0$. However, for convenience of later substitution, the notation J_m is purposely retained.
12. See Ref. (5), Eq. (5a).

TABLE II

Noncoupled Buckling In Torsion

Boundary Condition	Mode Shape (X_ϕ)	P_ϕ
Simple-Simple	$\sin \frac{\pi x}{\ell}$	$\frac{GC_uA}{J_m} + \frac{\pi^2 EC_wA}{J_m \ell^2}$
Fixed-Fixed	$1 - \cos \frac{2\pi x}{\ell}$	$\frac{GC_uA}{J_m} + \frac{\pi^2 EC_wA}{J_m (0.5\ell)^2}$
Simple-Fixed	$\sin \frac{4.493\, x}{\ell} - \frac{x}{\ell} \sin 4.493$	$\frac{GC_uA}{J_m} + \frac{\pi^2 EC_wA}{J_m (0.7\ell)^2}$
Fixed-Free (Cantilever)	0	$\frac{GC_uA}{J_m}$

Some Comments on Eqs. (13) and (15)

It is noted from Table I and II that the noncoupled bending modes and torsional modes for the same boundary conditions are identical except in the case of a cantilever. As a result, Eq. (15) may be used most of the time, except in some mixed combinations such as an end condition providing a simple support for torsion but a clamped support for bending.[13] For those cases, $m_{v\phi}$ and $m_{w\phi}$ will have to be actually introduced and the approximate equation (13) used. If the resultant thrust P passes through the z axis, i.e. $y_Q = 0$, and consequently $\gamma_{w\phi} = 0$, Eq. (13) is then reduced to

$$(P-P_w)\left[P^2(1-\gamma_{v\phi}\, m_{v\phi}) - P(P_v+P_\phi) + P_v P_\phi\right] = 0 \qquad (18)$$

It is evident that Eq. (18) has an independent root $P = P_w$ which is the noncoupled critical load in bending in the w direction. The remaining two other directions of buckling, v and ϕ are coupled together. The coupled critical loads are represented by the roots of the following equation

$$P^2(1-\gamma_{v\phi}\, m_{v\phi}) - P(P_v+P_\phi) + P_v P_\phi = 0 \qquad (19)$$

This special case is sometimes called the "Double Coupling" compared with the most general case of "Triple Coupling" when all three directions of buckling are coupled together. If the resultant thrust P passes through the shear center 0, i.e. $y_Q = 0$, $z_Q = 0$, Eq. (13) is reduced to

$$(P-P_v)(P-P_w)(P-P_\phi) = 0 \qquad (20)$$

The roots are already given in (12) and they are all independent of one another.

13. This is possible because the interpretation of boundary conditions in torsion is completely independent of that of bending.

Approximate Solution for a Triple Coupling by Two Double Couplings

A study of Eq. (13) reveals that $\gamma_{w\phi}$ has very little effect on the v direction. As shown in the last paragraph, Eq. (13) reduces to Eq. (18) when $\gamma_{w\phi} = 0$. Similarly, when $\gamma_{v\phi} = 0$, Eq. (13) reduces to

$$(P-P_v)\left[P^2\left(1-\gamma_{w\phi}\, m_{w\phi}\right)-P\left(P_w+P_\phi\right)+P_w P_\phi\right]=0 \qquad (18')$$

A close approximation for the critical load P may be obtained by disregarding first $\gamma_{w\phi}$ and then $\gamma_{v\phi}$, one at a time, i.e. by solving only the quadratic portions of Eqs. (18) and (18'). The smallest of all the four roots may be taken as the critical load P sought. This procedure avoids the trial and error solution of a cubic equation.

It should be noted, however, that the above-mentioned approximation is an upper-bound one. Fortunately, the error associated with the approximation rarely exceeds 2% for a column of ordinary proportions. In the most extreme cases, the error may reach about 10%. At any rate, the approximate value will provide a starting point for the trial and error solution of a cubic equation, if a very accurate result is desired.

Column Attached to a Thin Sheet

The open section columns are often used as stiffeners in aircraft structures and attached to the skin. The skin provides very large resistance on the line of attachment against movement in the plane of skin, but practically no resistance perpendicular to the skin.[14] We can idealize the problem as such that the movement parallel to the plane of skin is zero on the line of attachment.

As shown in Fig. 4, the origin of the coordinate axes is still taken at the shear center of an end section, but the y- and z-axes are now taken as perpendicular and parallel to the flexible skin. The η and ζ are still centroidal axes and parallel to the y and z respectively, but are not necessary in the principal directions. Q is the point of application of the resultant thrust and N indicates the position of the line of attachment.

Referring to these coordinate axes, the increment of strain energy and the additional work done by the end thrust are, respectively

$$\Delta U=\frac{1}{2}\left[EI_\zeta\int_0^l (v'')^2dx+2EI_{\eta\zeta}\int_0^l v''w''dx+EI_\eta\int_0^l (w'')^2dx\right.$$
$$\left.+GC_u\int_0^l(\phi')^2dx+EC_w\int_0^l(\phi'')^2dx\right] \qquad (21)$$

14. All displacements considered are small in magnitude.

$$\Delta W=\frac{P}{2}\Big[\int_0^\ell (v')^2dx-2z_Q\int_0^\ell v'\phi'dx+2y_Q\int_0^\ell w'\phi'dx+\int_0^\ell (w')^2dx+\Big\{\frac{J_0}{A}$$
$$+\frac{I_\varphi(z_Q-z_C)-I_{\eta\varphi}(y_Q-y_C)}{I_\eta I_\varphi-I_{\eta\varphi}^2}k_\eta+\frac{I_\eta(y_Q-y_C)-I_{\eta\varphi}(z_Q-z_C)}{I_\eta I_\varphi-I_{\eta\varphi}^2}k_\varphi$$
$$\Big\}\int_0^\ell(\phi')^2dx+2(y_Q-y_C)\int_0^\ell v''dx+2(z_Q-z_C)\int_0^\ell w''dx\Big] \quad ---- \quad (22)$$

Eq. (21) includes one more term containing the product of inertia $I_{\eta\zeta}$ as compared with Eq. (1). Furthermore, Eqs. (22) and (4'') are essentially the same except for the constant coefficient of the $\int_0^\ell(\phi')^2dx$ term.

Attaching the column to the skin provides certain restraint, namely

$$w_N = w + y_N\phi = 0$$

or

$$w = - y_N\phi \qquad (23)$$

Eq. (23) may be used to eliminate one unknown displacement, w. Doing so, we obtain

$$\Delta U=\frac{1}{2}\Big[EI_\varphi\int_0^\ell(v'')^2dx-2EI_{\eta\varphi}y_N\int_0^\ell v''\phi''dx+GC_u\int_0^\ell(\phi')^2dx$$
$$+(EC_w+y_N^2EI_\eta)\int_0^\ell(\phi'')^2dx\Big] \quad ---------- \quad (24)$$

$$\Delta W=\frac{P}{2}\Big[\int_0^\ell(v')^2dx-2z_Q\int_0^\ell v'\phi'dx+\Big\{y_N^2-2y_Ny_Q+\frac{J_0}{A}$$
$$+\frac{I_\varphi(z_Q-z_C)-I_{\eta\varphi}(y_Q-y_C)}{I_\eta I_\varphi-I_{\eta\varphi}^2}k_\eta$$
$$+\frac{I_\eta(y_Q-y_C)-I_{\eta\varphi}(z_Q-z_C)}{I_\eta I_\varphi-I_{\eta\varphi}^2}k_\varphi\Big\}\int_0^\ell(\phi')^2dx$$
$$+2(y_Q-y_C)\int_0^\ell v''dx-2(z_Q-z_C)y_N\int_0^\ell\phi''dx\Big] \qquad (25)$$

Substituting

$$v = v_0 X_v$$
$$\phi = \phi_0 X_\phi$$

into (24), (25) and denoting

$$\frac{J_{m'}}{A} = \frac{J_o}{A} + y_N^2 - 2y_N y_Q + \frac{I_\zeta(z_Q - z_C) - I_{\eta\zeta}(y_Q - y_C)}{I_\eta I_\zeta - I_{\eta\zeta}^2} \kappa_\eta + \frac{I_\eta(y_Q - y_C) - I_{\eta\zeta}(z_Q - z_C)}{I_\eta I_\zeta - I_{\eta\zeta}^2} \kappa_\zeta$$

we obtain

$$\Delta U = \frac{1}{2}\left[v_o^2 E I_\zeta \int_o^l (X_v'')^2 dx - 2v_o \phi_o E I_{\eta\zeta} y_N \int_o^l X_v'' X_\phi'' dx + \phi_o^2 G C_u \int_o^l (X_\phi')^2 dx + \phi_o^2 (E C_w + y_N^2 E I_\eta) \int_o^l (X_\phi'')^2 dx\right] \quad (26)$$

$$\Delta W = \frac{P}{2}\left[v_o^2 \int_o^l (X_v')^2 dx - 2v_o \phi_o z_Q \int_o^l X_v' X_\phi' dx + \phi_o^2 \frac{J_{m'}}{A} \int_o^l (X_\phi')^2 dx + 2v_o (y_Q - y_C) \int_o^l X_v'' dx - 2\phi_o (z_Q - z_C) y_N \int_o^l X_\phi'' dx\right] \quad (27)$$

Adoption of the same reasoning as for the case of free buckling and application of (10) lead to the following simultaneous equations:

$$\left[E I_\zeta \int_o^l (X_v'')^2 dx - P \int_o^l (X_v')^2 dx\right] v_o - \left[E I_{\eta\zeta} y_N \int_o^l X_v'' X_\phi'' dx - P z_Q \int_o^l X_v' X_\phi' dx\right] \phi_o = P(y_Q - y_C) \int_o^l X_v'' dx \quad \text{(a)}$$

$$-\left[E I_{\eta\zeta} y_N \int_o^l X_v'' X_\phi'' dx - P z_Q \int_o^l X_v' X_\phi' dx\right] v_o + \left[G C_u \int_o^l (X_\phi')^2 dx + (E C_w + y_N^2 E I_\eta) \int_o^l (X_\phi'')^2 dx - P \frac{J_{m'}}{A} \int_o^l (X_\phi')^2 dx\right] \phi_o = -P(z_Q - z_C) y_N \int_o^l X_\phi'' dx \quad \text{(b)}$$

The amplitudes of deflection, v_0, ϕ_0 become indefinite when

$$\begin{vmatrix} E I_\zeta \int_o^l (X_v'')^2 dx - P \int_o^l (X_v')^2 dx & -\left[E I_{\eta\zeta} y_N \int_o^l X_v'' X_\phi'' dx - P z_Q \int_o^l X_v' X_\phi' dx\right] \\ -\left[E I_{\eta\zeta} y_N \int_o^l X_v'' X_\phi'' dx - P z_Q \int_o^l X_v' X_\phi' dx\right] & \left[G C_u \int_o^l (X_\phi')^2 dx + (E C_w + y_N^2 E I_\eta) \int_o^l (X_\phi'')^2 dx - P \frac{J_{m'}}{A} \int_o^l (X_\phi')^2 dx\right] \end{vmatrix} = 0 \quad (28)$$

Considering $(E C_w)_m = E C_w + y_N^2 E I_\eta$ = modified warping rigidity, and using the notations (12), we may transform (28) into

$$\begin{vmatrix} P_v - P & -\dfrac{EI_{\eta\varphi} y_N \int_0^\ell X_v'' X_\varphi'' dx - Pz_Q \int_0^\ell X_v' X_\varphi' dx}{\int_0^\ell (X_v')^2 dx} \\ -\dfrac{EI_{\eta\varphi} y_N \int_0^\ell X_v'' X_\varphi'' dx - Pz_Q \int_0^\ell X_v' X_\varphi' dx}{\frac{J_{m'}}{A} \int_0^\ell (X_\varphi')^2 dx} & P_\varphi - P \end{vmatrix} = 0 \quad \text{---} \tag{29}$$

Upon expansion, we get

$$P^2\left(1 - \gamma'_{v\varphi} m_{v\varphi}\right) - P\left(P_v + P_\varphi - 2EI_{\eta\varphi} y_N z_Q \frac{A}{J_{m'}} \cdot \frac{\int_0^\ell X_v' X_\varphi' dx \int_0^\ell X_v'' X_\varphi'' dx}{\int_0^\ell (X_v')^2 dx \int_0^\ell (X_\varphi')^2 dx}\right)$$
$$+ P_v P_\varphi - E^2 I_{\eta\varphi}^2 y_N^2 \left(\frac{A}{J_{m'}}\right) \frac{\left(\int_0^\ell X_v'' X_\varphi'' dx\right)^2}{\int_0^\ell (X_v')^2 dx \int_0^\ell (X_\varphi')^2 dx} = 0 \tag{29'}$$

where

$$\gamma'_{v\varphi} = \frac{A z_Q^2}{J_{m'}}$$

In most instances $X_v = X_\varphi$ and $m_{v\varphi} = 1$, then

$$P^2\left(1 - \gamma'_{v\varphi}\right) - P\left(P_v + P_\varphi - 2EI_{\eta\varphi} y_N z_Q \frac{A}{J_{m'}} \cdot \frac{\int_0^\ell (X'')^2 dx}{\int_0^\ell (X')^2 dx}\right)$$
$$+ P_v P_\varphi - E^2 I_{\eta\varphi}^2 y_N^2 \frac{A}{J_{m'}} \cdot \frac{\left\{\int_0^\ell (X'')^2 dx\right\}^2}{\left\{\int_0^\ell (X')^2 dx\right\}^2} = 0 \text{ ---------} \tag{30}$$

If the axis η or ζ is an axis of symmetry, then $I_{\eta\zeta} = 0$, and Eq. (29') reduces to

$$P^2\left(1 - \gamma'_{v\varphi} m_{v\varphi}\right) - P\left(P_v + P_\varphi\right) + P_v P_\varphi = 0 \tag{31}$$

Eq. (31) is identical to Eq. (19), except $J_{m'}$ is used instead of J_m to compute the coupling factor γ.

In application of (29') to (31) care must also be exercised that P_ϕ is calculated from the modified $(E C_w)_m$ and J_m'.

Column with Known Axis of Rotation

An example of this category is shown in Fig. 5. As a corner column attached to skin in two perpendicular directions, the column is enforced to rotate about the axis M during buckling. This restriction provides the following relations:

$$v_M = v - z_M \phi = 0$$
$$w_M = w + y_M \phi = 0$$

$$\left.\begin{aligned} v &= z_M \phi \\ w &= - y_M \phi \end{aligned}\right\} \tag{32}$$

Applying the similar procedure to that illustrated in the previous paragraph, we shall conclude that the uncoupled torsional buckling formula

$$P = \frac{G C_u \int_0^\ell (X_\phi')^2 dx + (E C_w)_m \int_0^\ell (X_\phi'')^2 dx}{\frac{J_{m'}}{A} \int_0^\ell (X_\phi')^2 dx} \tag{33}$$

may still be used to determine the critical load, provided the following modified constants are employed:

$$(E C_w)_m = E \left(C_w + I_\varphi z_M^2 + I_\eta y_M^2 \right)$$

$$\frac{J_{m'}}{A} = \frac{J_o}{A} + (z_Q - z_C) \frac{k_\eta}{I_\eta} + (y_Q - y_C) \frac{k_\varphi}{I_\varphi}$$
$$+ y_M^2 - 2 y_Q y_M - 2 z_Q z_M + z_M^2$$

As seen in Fig. 5, η and ζ are the centroidal principal axes throughout the discussion of this paragraph.

Experimental Evidences

A series of experiments has been conducted by A. S. Niles for columns with simple supports at both ends. The results were published in Ref. (2), and they agreed closely to the theoretical values. It is reasonable to predict the similar agreements for other end conditions. However, further experiments pertaining to different boundary conditions with and without skin attachments are highly desirable.

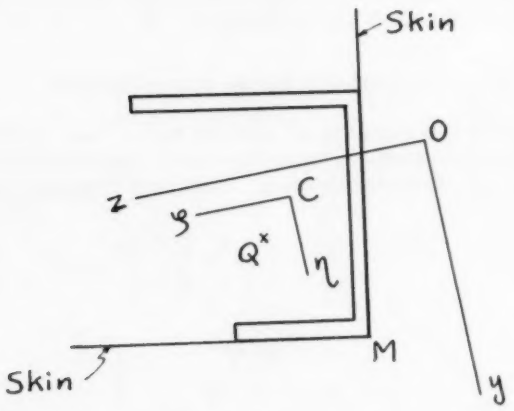

Fig. 5

BIBLIOGRAPHY

1. J. N. Goodier: "The Buckling of Compressed Bars by Torsion and Flexure", Cornell University Engineering Experiment Station Bulletin No. 27, Dec., 1941.

2. A. S. Niles: "Experimental Study of Torsional Column Failure", NACA-TN 733, 1939.

3. R. Kappus: "Twisting Failure of Centrally Loaded Open-section Columns in the Elastic Range", NACA-TM 851, 1938.

4. S. P. Timoshenko: "Theory of Bending, Torsion and Buckling of Thin-walled Members of Open Cross Section", Journal of the Franklin Institute, Vol. 239 (3, 4, 5), 1945.

5. H. Wagner: "Torsion and Buckling of Open Sections", NACA-TM 807, 1936.

6. J. N. Goodier: "Flexure-Torsional Buckling of Bars of Open Sections", Cornell University Engineering Experiment Station Bulletin No. 28, January, 1942.

7. H. N. Hill: "Torsion of Flanged Members with Cross Sections Restrained Against Warping", NACA-TN 888, 1943.

APPENDIX

Formulas for C_w, k_η and k_ζ values for some commonly used sections:

(1) Equal-legged Angle

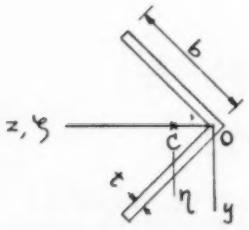

$$C_w = 0$$

$$k_\eta = \frac{t b^4}{2\sqrt{2}} - z_c J_0$$

$$k_\zeta = 0$$

(2) I Section

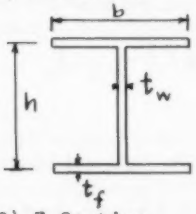

$$C_w = \frac{t_f h^2 b^3}{24}$$

$$k_\eta = k_\zeta = 0$$

(3) Z Section

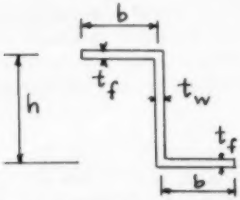

$$C_w = \frac{t_f h^2 b^3}{12} \cdot \frac{2ht_w + bt_f}{ht_w + 2bt_f}$$

$$k_\eta = k_\zeta = 0$$

(4) Channel Section

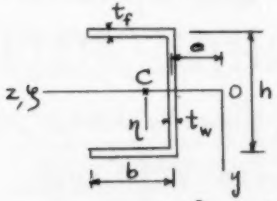

$$e = \frac{b^2 h^2 t_f}{4 I_\zeta}$$

$$C_w = \frac{b^3 h^2 t_f}{12}\left(2 - 3\frac{e}{b}\right)$$

$$k_\zeta = 0$$

$$k_\eta = e t_w h\left(\frac{h^2}{12} + e^2\right) + \frac{t_f(2be + b^2)}{2}\left(\frac{h^2}{2} + 2e^2 + 2be + b^2\right) - z_c J_0$$

(4) C Section of Uniform Thickness

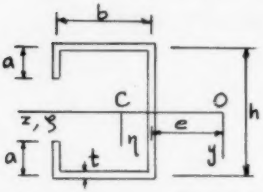

$$\frac{e}{h} = \frac{\left(\frac{b}{h}\right)\left(\frac{a}{h}\right) - \frac{4}{3}\left(\frac{a}{h}\right)^3\left(\frac{b}{h}\right) + \frac{1}{2}\left(\frac{b}{h}\right)^2}{\frac{1}{6} + \frac{b}{h} + \frac{a}{h} - 2\left(\frac{a}{h}\right)^2 + \frac{4}{3}\left(\frac{a}{h}\right)^3}$$

$$C_w = K t h^5$$

$$K = 2\left(\frac{e}{h}\right)^2\left[\frac{1}{3}\left(\frac{a}{h}\right)^3 - \frac{1}{2}\left(\frac{a}{h}\right)^2 + \frac{1}{4}\left(\frac{a}{h}\right) + \frac{1}{4}\left(\frac{b}{h}\right) + \frac{1}{24}\right]$$
$$+2\left(\frac{e}{h}\right)\left[\frac{2}{3}\left(\frac{b}{h}\right)\left(\frac{a}{h}\right)^3 - \frac{1}{2}\left(\frac{b}{h}\right)\left(\frac{a}{h}\right) - \frac{1}{4}\left(\frac{b}{h}\right)^2\right]$$
$$+2\left[\frac{1}{3}\left(\frac{b}{h}\right)^2\left(\frac{a}{h}\right)^3 + \frac{1}{2}\left(\frac{b}{h}\right)^2\left(\frac{a}{h}\right)^2 + \frac{1}{4}\left(\frac{b}{h}\right)^2\left(\frac{a}{h}\right) + \frac{1}{12}\left(\frac{b}{h}\right)^3\right]$$

$$k_\eta = e t h\left(\frac{h^2}{12} + e^2\right) + \frac{t(2be + b^2)}{4}\left(\frac{h^2}{2} + 2e^2 + 2be + b^2\right)$$
$$+2(e+b)ta\left[\frac{h^2}{4} - \frac{ha}{2} + \frac{a^2}{3} + (e+b)^2\right] - z_c J_o$$

$$k_\zeta = 0$$

(5) Hat Section of Uniform Thickness

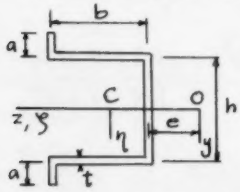

$$\frac{e}{h} = \frac{\left(\frac{b}{h}\right)\left(\frac{a}{h}\right) - \frac{4}{3}\left(\frac{a}{h}\right)^3\left(\frac{b}{h}\right) + \frac{1}{2}\left(\frac{b}{h}\right)^2}{\frac{1}{6} + \frac{b}{h} + \frac{a}{h} + 2\left(\frac{a}{h}\right)^2 + \frac{4}{3}\left(\frac{a}{h}\right)^3}$$

$$C_w = K t h^5$$

$$K = 2\left(\frac{e}{h}\right)^2\left[\frac{1}{3}\left(\frac{a}{h}\right)^3 + \frac{1}{2}\left(\frac{a}{h}\right)^2 + \frac{1}{4}\left(\frac{a}{h}\right) + \frac{1}{4}\left(\frac{b}{h}\right) + \frac{1}{24}\right]$$
$$+2\left(\frac{e}{h}\right)\left[\frac{2}{3}\left(\frac{b}{h}\right)\left(\frac{a}{h}\right)^3 - \frac{1}{2}\left(\frac{b}{h}\right)\left(\frac{a}{h}\right) - \frac{1}{4}\left(\frac{b}{h}\right)^2\right]$$
$$+2\left[\frac{1}{3}\left(\frac{b}{h}\right)^2\left(\frac{a}{h}\right)^3 - \frac{1}{2}\left(\frac{b}{h}\right)^2\left(\frac{a}{h}\right)^2 + \frac{1}{4}\left(\frac{b}{h}\right)^2\left(\frac{a}{h}\right) + \frac{1}{12}\left(\frac{b}{h}\right)^3\right]$$

$$k_\eta = e t h\left(\frac{h^2}{12} + e^2\right) + \frac{t(2be + b^2)}{4}\left(\frac{h^2}{2} + 2e^2 + 2be + b^2\right)$$
$$+2(e+b)ta\left[\frac{h^2}{4} + \frac{ha}{2} + \frac{a^2}{3} + (e+b)^2\right] - z_c J_o$$

$$k_\zeta = 0$$

Paper 1794 October, 1958 EM 4

Journal of the
ENGINEERING MECHANICS DIVISION
Proceedings of the American Society of Civil Engineers

DYNAMIC EFFECT OF A MOVING LOAD ON A RIGID FRAME

R. C. DeHart,[1] M. ASCE
(Proc. Paper 1794)

SYNOPSIS

A procedure for determining the response of a rigid frame structure subjected to a distributed load moving at a constant velocity is described in this paper. It is demonstrated that a single impact factor is not applicable to all parts of the frame. In addition, tables are presented which facilitate the handling of a distributed load of variable intensity.

INTRODUCTION

In an earlier paper(1) written by the author, the basic dynamic response equations for a pin ended rigid frame were developed and an analysis made of the response of a rigid frame subjected to time dependent horizontally applied loads. This same technique is now utilized to study the case in which the load is moving at a constant rate across the top of the frame. Finally a comparison is made between the moment caused by a statically applied load and a moving load having the same intensity. Tables for simplifying the computations required if the integration of equation (8) is to be done numerically are also given.

List of Symbols

μ^u is mass of the column per unit length.

μ^v is mass of the beam per unit length.

L^u is column length.

L^v is beam length.

Note: Discussion open until March 1, 1959. To extend the closing date one month, a written request must be filed with the Executive Secretary, ASCE. Paper 1794 is part of the copyrighted Journal of the Engineering Mechanics Division, Proceedings of the American Society of Civil Engineers, Vol. 84, No. EM 4, October, 1958.

1. Structural Research Analyst, Armed Forces Special Weapons Project. Washington 25, D. C.

E is modulus of elasticity.

I is moment of inertia.

ω_i is the vibratory frequency of the frame in the i^{th} mode.

$$k_i^v = \sqrt[4]{\frac{\omega_i^2 \mu^v}{EI^v}}$$

$$k_i^u = \sqrt[4]{\frac{\omega_i^2 \mu^u}{EI^u}}$$

For unsymmetrical modes

$$\frac{c_i^u}{c_i^v} = 2\sqrt{\frac{I^v}{I^u}\frac{\mu^v}{\mu^u}} \left[\frac{\tan k_i^v \frac{L^v}{2}}{-\sin k_i^u L^u + D_i \sinh k_i^u L^u} \right]$$

$$D_i = \frac{-\cos k_i^u L^u + k_i^v \frac{L^v}{2} \sqrt[4]{\frac{I^v}{I^u}\frac{\mu^u}{\mu^v}\frac{\mu^v}{\mu^u}} \sin k_i^u L^u}{-k_i^v \frac{L^v}{2} \sqrt[4]{\frac{I^v}{I^u}\frac{\mu^u}{\mu^v}\frac{\mu^v}{\mu^u}} \sinh k_i^u L^u - \cosh k_i^u L^u}$$

For symmetrical modes

$$\frac{c_i^u}{c_i^v} = \sqrt{\frac{I^v}{I^u}\frac{\mu^v}{\mu^u}} \frac{\cot k_i^v \frac{L^v}{2}}{\sin k_i^u L^u}$$

Equations of Motion

For the loading and frame arrangement displayed in Figure 1 the expression for the generalized coordinate is[1]

$$q_i^v = A_i \sin \omega_i t + B_i \cos \omega_i t + \frac{k_i^v}{2\omega_i \bar{T}_i \mu^v} \int_0^t Q_i^v(\tau) \sin \omega_i (t - \tau)\, d\tau$$

$$\bar{T}_i = \frac{T_i}{(\dot{q}_i^v)^2} \frac{k_i^v}{\mu^v} \qquad (1)$$

$$\bar{T}_i = \bar{T}_i^u + \bar{T}_i^v + \bar{T}_i^T$$

T_i is the kinetic energy in the i^{th} mode.

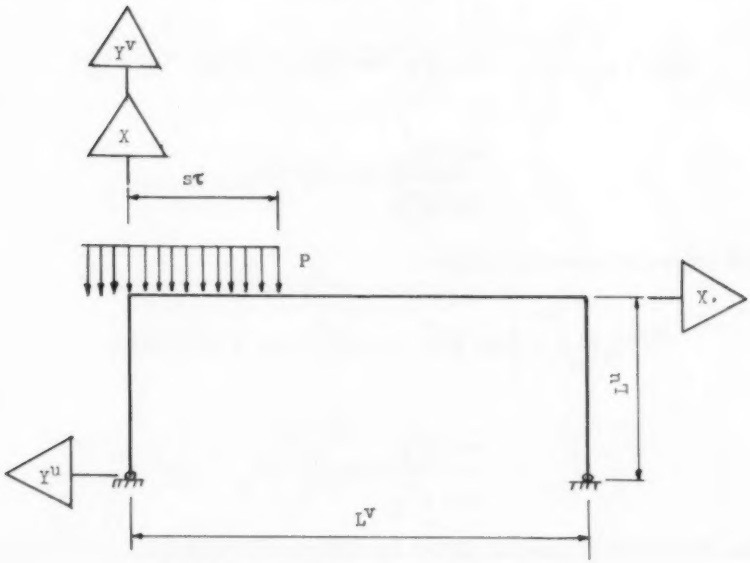

Figure 1. Loading and Frame Arrangement

$\overline{T}_i^u$ is the quantity obtained when the integral of equation (36), Reference 1, is evaluated without the $\frac{1}{k_i^u}$ factor included and is multiplied by

$$\left(\frac{c_i^u}{c_i^v}\right)^2 \frac{\mu^u}{\mu^v}\frac{k_i^v}{k_i^u}$$

$\overline{T}_i^v$ is obtained from equation (35), Reference 1, without the $\frac{1}{k_i^v}$ multiplier included.

$$\overline{T}_i^T = \left[1/2\, k_i^v L^v \frac{\overline{\mu}}{k_i^v} (Y_i^u)^2 (x - L^u)\right]$$

The generalized force for the unsymmetrical modes is

$$Q_i^v(\tau) = \int_0^{s\tau} P y_i^v dx$$

or

$$Q_1^{\nu}(\tau) = \int_0^{s\tau} p \left[- \tan k_1^{\nu}\frac{L^{\nu}}{2} \left(\cos k_1^{\nu}x - \cosh k_1^{\nu}x\right) + \sin k_1^{\nu}x - \frac{\tan k_1^{\nu}\frac{L^{\nu}}{2}}{\tanh k_1^{\nu}\frac{L^{\nu}}{2}} \sinh k_1^{\nu}x \right] dx \tag{2}$$

And for the symmetrical modes is

$$Q_1^{\nu}(\tau) = \int_0^{s\tau} p \left[\cot k_1^{\nu}\frac{L^{\nu}}{2} \left(\cos k_1^{\nu}x - \cosh k_1^{\nu}x\right) + \sin k_1^{\nu}x + \frac{\cot k_1^{\nu}\frac{L^{\nu}}{2}}{\coth k_1^{\nu}\frac{L^{\nu}}{2}} \sinh k_1^{\nu}x \right] dx \tag{3}$$

The integration of equation (2) for the unsymmetrical modes results in the following:

$$Q_1^{\nu} = \frac{P}{k_1^{\nu}} \left[- \tan k_1^{\nu}\frac{L^{\nu}}{2} \left(\sin k_1^{\nu}s\,\tau - \sinh k_1^{\nu}s\,\tau\right) - \frac{\tan k_1^{\nu}\frac{L^{\nu}}{2}}{\tanh k_1^{\nu}\frac{L^{\nu}}{2}} \cosh k_1^{\nu}s\,\tau - \cos k_1^{\nu}s\tau + \frac{\tan k_1^{\nu}\frac{L^{\nu}}{2}}{\tanh k_1^{\nu}\frac{L^{\nu}}{2}} + 1 \right] \tag{4}$$

Substituting equation (4) in (1) yields

$$q_1^{\nu} = \frac{k_1^{\nu}}{2\omega_1 T_1 \mu^{\nu}} \int_0^t \frac{p}{k_1^{\nu}} \left[- \tan k_1^{\nu}\frac{L^{\nu}}{2} \left(\sin k_1^{\nu}s\,\tau - \sinh k_1^{\nu}s\,\tau\right) - \frac{\tan k_1^{\nu}\frac{L^{\nu}}{2}}{\tanh k_1^{\nu}\frac{L^{\nu}}{2}} \cosh k_1^{\nu}s\,\tau - \cos k_1^{\nu}s\tau + \frac{\tan k_1^{\nu}\frac{L^{\nu}}{2}}{\tanh k_1^{\nu}\frac{L^{\nu}}{2}} + 1 \right] \sin \omega_1 (t - \tau)\, d\tau \tag{5}$$

Upon integration of equation (4), the following is obtained:

$$q_i^v = \frac{P}{2\omega_i \overline{M}_{i\mu}^v} \left[\tan k_i^v \frac{L^v}{2} \left(\frac{-k_i^v s \sin \omega_i t + \omega_i \sin k_i^v s t}{(k_i^v s)^2 - \omega_i^2} \right) \right.$$

$$+ \tan k_i^v \frac{L^v}{2} \left(\frac{\omega_i \sinh k_i^v s t - k_i^v s \sin \omega_i t}{(k_i^v s)^2 + \omega_i^2} \right)$$

$$- \frac{\tan k_i^v \frac{L^v}{2}}{\tanh k_i^v \frac{L^v}{2}} \left(\frac{\cosh k_i^v s t - \cos \omega_i t}{(k_i^v s)^2 + \omega_i^2} \right) \omega_i \qquad (6)$$

$$\left. + \left(\frac{\cos k_i^v s t - \cos \omega_i t}{(k_i^v s)^2 - \omega_i^2} \right) \omega_i + \left(1 + \frac{\tan k_i^v \frac{L^v}{2}}{\tanh k_i^v \frac{L^v}{2}} \right) \left(\frac{1 - \cos \omega_i t}{\omega_i} \right) \right]$$

Similarly for symmetrical modes:

$$q_i^v = \frac{P}{k_i^v} \left[- \cot k_i^v \frac{L^v}{2} \left(\frac{\omega_i \sin k_i^v s t - k_i^v s \sin \omega_i t}{(k_i^v s)^2 - \omega_i^2} \right) \right.$$

$$- \cot k_i^v \frac{L^v}{2} \left(\frac{\omega_i \sinh k_i^v s t - k_i^v s \sin \omega_i t}{(k_i^v s)^2 + \omega_i^2} \right)$$

$$+ \frac{\cot k_i^v \frac{L^v}{2}}{\coth k_i^v \frac{L^v}{2}} \left(\frac{\cosh k_i^v s t - \cos \omega_i t}{(k_i^v s)^2 + \omega_i^2} \right) \omega_i \qquad (7)$$

$$\left. + \left(\frac{\cos k_i^v s t - \cos \omega_i t}{(k_i^v s)^2 - \omega_i^2} \right) \omega_i + \left(1 - \frac{\cot k_i^v \frac{L^v}{2}}{\coth k_i^v \frac{L^v}{2}} \right) \left(\frac{1 - \cos \omega_i t}{\omega_i} \right) \right]$$

Equations (6) and (7) are applicable only for the time required for the load to traverse the beam. This time period will be referred to as the first era. During the second era, the entire beam is loaded and the expression for q_i^v for symmetrical modes becomes

$$q_i^v = A_i \sin \omega_i t + B_i \cos \omega_i t + \frac{Q_i}{2\omega_i^2 \overline{T}_i \frac{\mu^v}{k_i^v}} \qquad (8)$$

For the unsymmetrical modes equation (8) applies except Q_i is zero during the second era.

Values for q_i^v and $\dot{q}_i^v$ are obtained at the end of the first era. This information permits the determination of the constants A_i and B_i.

TABLE 2

Values of A_i, B_i, and Time to Second Era Maximums and Minimums

Mode	A_i	B_i	Time to Initial* Second Era, Maximum q_i (& Moment)	Time to Initial* Second Era, Minimum q_i (& Moment)
First Symmetrical	- 0.2808	- 0.2615	0.332 Seconds	0.432 Seconds
Second "	+ 0.001425	- 0.003024	0.322	0.346
Third "	- 0.003610	- 0.001624	0.305	0.318
Fourth "	Not determined since moment contribution is essentially nil.			
First Unsymmetrical	+ 0.2172	- 0.5698	0.576 Seconds	1.201 Seconds
Second "	Not determined since moment contribution is essentially nil.			
Third "	+ 0.001411	+ 0.0007239	0.345	0.347
Fourth "	- 0.0005884	+ 0.0004948	0.305	0.312

* For unsymmetrical modes, time to second era maximum and minimum q_i (and moment) is time to maximum second era negative and positive moment, respectively.

These constants for the various modes are displayed in Table 2 along with the time at which the initial second era maximum and minimum q_i values occur. Later maximum and minimum q_i values would be the same since damping has not been considered.

Determination of Bending Moment

The following relation between bending moment M_i, generalized coordinate q_i^v and mode shape y_i^v will be utilized.

$$-EI^v \frac{\partial^2 Y_i^v}{\partial x^2} = M_i$$

where E is the modulus of elasticity

I is the moment of inertia

$$Y_i^v = q_i^v y_i^v$$

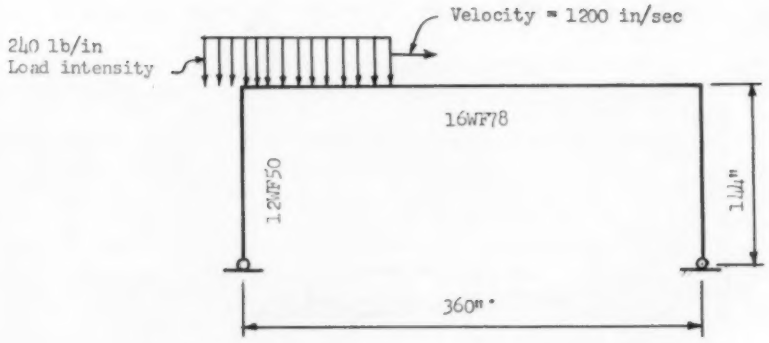

Figure 2. Bent Dimensions and Load Intensity

The coordinate system and loading are displayed in Figure 2. The bent under consideration is the one treated in Reference 1 from which most of the basic information listed below is extracted.

$$\mu^u = \mu^v = 0.333 \frac{\text{lb. sec}^2}{\text{in}^2}$$

$$I^u = 394 \text{ in}^4$$

$$I^v = 1043 \text{ in}^4$$

For the unsymmetrical modes

$k_1^v \frac{L^v}{2} = 1.03$ $k_1^u L^u = 1.05$ $\bar{T}_1 = 12.6$ $\omega_1 = 9.98$ rad/sec

$k_2^v \frac{L^v}{2} = 3.16$ $k_2^u L^u = 3.22$ $\bar{T}_2 = 21.3$ $\omega_2 = 94.1$ rad/sec

$k_3^v \frac{L^v}{2} = 3.98$ $k_3^u L^u = 4.07$ $\bar{T}_3 = 15.8$ $\omega_3 = 150$ rad/sec

$k_4^v \frac{L^v}{2} = 7.04$ $k_4^u L^u = 7.18$ $\bar{T}_4 = 20.1$ $\omega_4 = 468$ rad/sec

$k_5^v \frac{L^v}{2} = 10.1$ $k_5^u L^u = 10.3$ $\bar{T}_5 = 73.3$ $\omega_5 = 969$ rad/sec

For the symmetrical modes

$k_1 \frac{vL^v}{2} = 1.83 \quad k_1 \frac{uL^u}{L} = 1.87 \quad T_1 = 1.12 \quad \omega_1 = 31.8$ rad/sec

$k_2 \frac{vL^v}{2} = 3.59 \quad k_2 \frac{uL^u}{L} = 3.66 \quad T_2 = 77.0 \quad \omega_2 = 122$ rad/sec

$k_3 \frac{vL^v}{2} = 4.97 \quad k_3 \frac{uL^u}{L} = 5.07 \quad T_3 = 3.13 \quad \omega_3 = 234$ rad/sec

$k_4 \frac{vL^v}{2} = 6.67 \quad k_4 \frac{uL^u}{L} = 6.82 \quad T_4 = 187 \quad \omega_4 = 422$ rad/sec

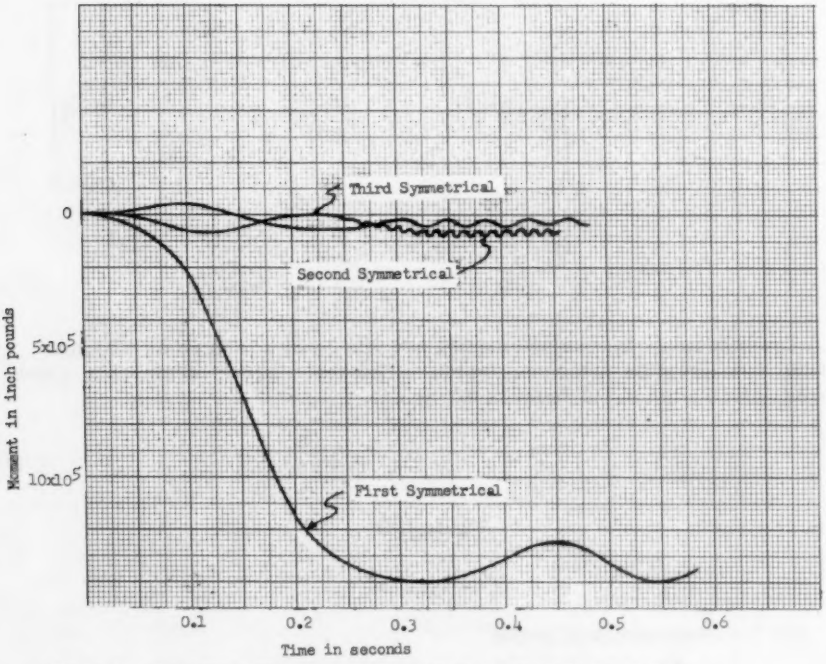

Figure 3. Time Dependent Moment for Symmetrical Modes--Left End of Beam

Time dependent moment for the left end of the beam for the first three symmetrical modes and the first, third, and fourth unsymmetrical modes are given in Figures 3 and 4, respectively. The fourth symmetrical, and second and fifth unsymmetrical modes were, for all practical purposes, not excited. It is apparent that bending moment contributed by higher modes oscillates rapidly relative to the oscillation of bending moment arising from the lower modes. A change in a detail such as the amount of end restraint at the column footing produces a greater change in the frequency of one mode than another.

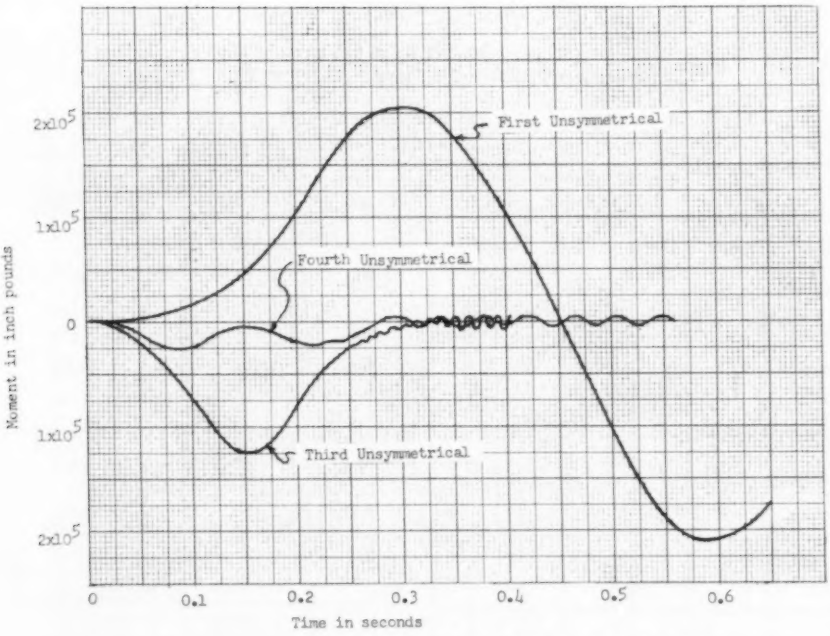

Figure 4. Time Dependent Moment for Unsymmetrical Modes--Left End of Beam

For example, the influence of changing from the pin ended frame used as an example here, to a fixed ended frame of identical proportions, is given in Table 1. On the other hand, small changes in the frequency of a mode make only small changes in the moment contributed by the mode.

It, therefore, appears to be impossible, in the practical case, to determine the exact phasing of the modes. This immediately leads to the concept that, except for perhaps the first symmetrical and unsymmetrical modes, the maximum positive and negative moment from each mode can occur simultaneously. This procedure would give the upper bound for both positive and negative values of moment. For the five unsymmetrical and four symmetrical modes examined, the upper bound for moment at the left end, the center, and the right end of the beam would be 1,700,000 in. lb, 2,370,000 in lb, and 1,700,000 in. lb, respectively. All of these upper bounds occur in the second time era.

Comparable maximum values for the case in which a static load of 240 pounds per linear inch is applied on the full length of the beam, are 1,500,000 in. lb, 2,370,000 in. lb, and 1,500,000 in. lb. If more modes were used, it is obvious that the center moment, under the moving load conditions, would probably be somewhat more than the static center moment.

The conclusion may now be drawn for the bent studied herein that, at the center of the beam, the dynamic bending moment arising from a uniformly distributed load moving at constant velocity is, for all practical purposes, identical to the maximum static bending moment produced at the center of

TABLE 1

Influence of End Conditions on
Frequency of One Bay Single Story Bent

Mode	Pin End Frecuency	Fixed End Frecuency	% Difference
First Symmetrical	31.8 RAD/SEC	33.7 RAD/SEC	6
Second "	122.	170.	39
Third "	234.	246.	5
Fourth "	422.	508.	20
First Unsymmetrical	9.98	21.1	111
Second "	94.1	102.	8
Third "	150.	200.	33
Fourth "	373.	391.	5

the beam by a uniform load having the same intensity. This is the same conclusion that Inglis[2] came to in his study of a simple beam subjected to the loading conditions described above.

On the other hand, under these dynamic loading conditions, the increase over static bending moment at the ends of the beam is approximately 11%. This obviously indicates that impact factors, if they are to be used to account for the difference between dynamic loading and static loading, will vary for different portions of the structure under examination here.

Of further interest is the fact that, had sidesway been eliminated, excitation of the first unsymmetrical mode would be greatly reduced, and the left and right end upper bound bending moments would be nearly the same as for the static load case. One would, therefore, conclude that in this instance the moving load produces a bending moment essentially no different than the maximum static bending moment arising from the application of a uniformly distributed load to the beam.

It should not be overlooked, however, that the velocity with which the load traverses the beam relative to the frequency of the various modes of vibration, particularly the first symmetrical and unsymmetrical modes, determines the magnitude of the dynamic response.

Numerical Integration of Equations of Motion

Attention is now given to the development of information necessary if the equations of motion are to be integrated by numerical means. It is convenient to use the Lagrange equation of motion written for the i^{th} mode, in the following form:

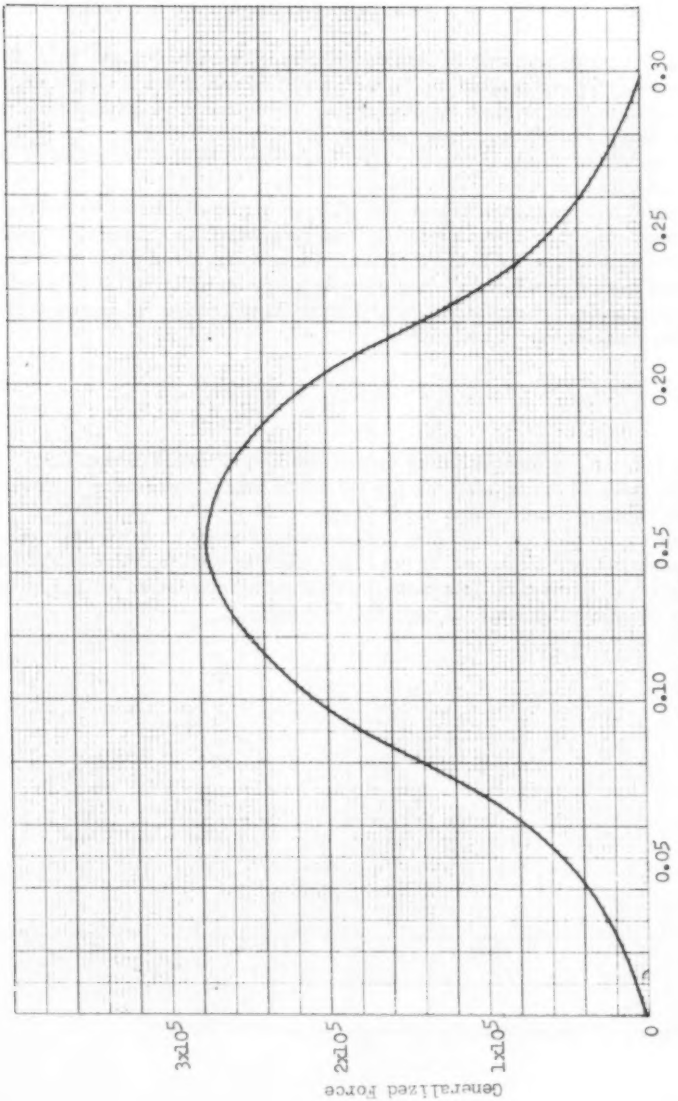

Figure 5. Generalized Force--Time Relations for Second Unsymmetrical Mode

$$2\bar{T}_i \frac{\overset{v}{\approx}}{k_i^v} \ddot{q}_i^v + 2\bar{U}_i (k_i^v)^3 EI^v = Q_i^v \tag{9}$$

The quantity $2\bar{T}_i \frac{\overset{v}{\approx}}{k_i^v} \ddot{q}_i^v$ is usually referred to as the generalized mass for the i^{th} mode and will be denoted by M_g. The quantity $2\bar{U}_i (k_i^v)^3 EI^v$ may be thought of as corresponding to the spring constant for a single degree of freedom system, and will be denoted by K_g. Obviously, no particular terminology is necessary for these factors.

Since $\bar{U}_i$ and $\bar{T}_i$ have equal values, all quantities, with the exception of Q_i, are readily obtainable.

Q_i is defined by equations (2) and (3). For an arbitrary distributed load (time dependent and space dependent) Q_i^v can be plotted as a function of time utilizing the values given in Table 3. These values are for $\int y_i^v \, dz$ for various lengths of the beam where y_i^v is the mode shape equation for the beam. A typical Q_i^v versus time curve appears in Figure 5. Equation (8) is now written, using the terminology given above,

$$M_g \ddot{q}_i^v + K_g q_i^v = Q_i^v \tag{10}$$

Equation (10) can be integrated by numerical or graphical means and values of the moment contributed by the i^{th} mode determined from the relation between bending moment and mode shape.

If the load is of constant intensity, there appears to be no advantage in numerical integration. However, if the load intensity varies, for example as given by Figure 6, numerical integration would be an attractive means of accomplishing the integration of the equations of motion.

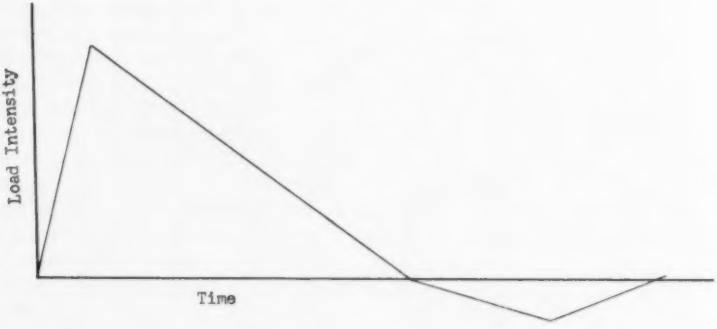

Figure 6. Load Intensity Time Relations

TABLE 3

Value of $\int_0^{ML} Y_i(x)\,dx$

$k_i^v \frac{L^v}{2}$	M = 0.1		M = 0.2		M = 0.3		M = 0.4		M = 0.5	
	Unsymmetrical	Symmetrical	Unsymmetrical	Symmetrical	Unsymmetrical	Symmetrical	Unsymmetrical	Symmetrical	Unsymmetrical	Symmetrical
0.40	-.000285	.005650	-.000858	.02099	-.001605	.04378	-.002107	.07138	-.002243	.1012
0.42	-.000352	.006220	-.001124	.02308	-.001918	.04786	-.002511	.07813	-.002716	.1112
0.44	-.000430	.006803	-.001376	.02527	-.002318	.05228	-.003082	.08552	-.003327	.1214
0.46	-.000514	.007377	-.001690	.02758	-.002838	.05700	-.003715	.09290	-.003947	.1319
0.48	-.000624	.007974	-.001948	.02961	-.003379	.06161	-.004436	.1005	-.004883	.1429
0.50	-.000708	.008553	-.002372	.03215	-.004015	.06655	-.005194	.1084	-.006038	.1541
0.52	-.000858	.009214	-.002752	.03443	-.004772	.07157	-.006216	.1166	-.006731	.1656
0.54	-.001032	.009966	-.003201	.03683	-.005584	.07673	-.007246	.1249	-.007878	.1776
0.56	-.001229	.01072	-.003722	.03933	-.006430	.08184	-.008490	.1337	-.009120	.1889
0.58	-.001332	.01118	-.004327	.04195	-.007468	.08724	-.009798	.1423	-.01058	.2022
0.60	-.001585	.01197	-.005063	.04465	-.008643	.09295	-.011.3	.1514	-.01233	.2150
0.62	-.001863	.01278	-.005788	.04732	-.01003	.09849	-.01304	.1604	-.01413	.2280
0.64	-.002032	.01333	-.006669	.05007	-.011.7	.1042	-.01500	.1697	-.01600	.2407
0.66	-.002381	.01417	-.007575	.05278	-.01315	.1099	-.01714	.1793	-.01862	.2548
0.68	-.002782	.01501	-.008621	.05557	-.01501	.1160	-.01956	.1890	-.02128	.2685
0.70	-.003067	.01564	-.009918	.05858	-.01705	.1221	-.02228	.1988	-.02415	.2825
0.72	-.003547	.01652	-.01118	.06144	-.01930	.1282	-.02522	.2087	-.02747	.2967
0.74	-.004048	.01749	-.01269	.06449	-.02186	.1342	-.02839	.2188	-.03088	.3110
0.76	-.004488	.01807	-.01426	.06736	-.02463	.1405	-.03217	.2288	-.03495	.3255
0.78	-.005153	.01897	-.01612	.07044	-.02774	.1468	-.03622	.2392	-.03942	.3402

TABLE 3 (Cont'd)

$k_i^v \frac{L^v}{2}$	M = 0.1		M = 0.2		M = 0.3		M = 0.4		M = 0.5	
	Unsymmetrical	Symmetrical	Unsymmetrical	Symmetrical	Unsymmetrical	Symmetrical	Unsymmetrical	Symmetrical	Unsymmetrical	Symmetrical
0.80	-.005687	.01968	-.01811	.07435	-.03123	.1530	-.04031	.2493	-.04423	.3551
0.82	-.006485	.02060	-.02034	.07731	-.03494	.1594	-.04565	.2602	-.04954	.3701
0.84	-.007156	.02134	-.02261	.08027	-.03900	.1658	-.05114	.2703	-.05543	.3852
0.86	-.008132	.02227	-.02533	.08323	-.04375	.1723	-.05465	.2918	-.06201	.4006
0.88	-.008975	.02303	-.02835	.08619	-.04876	.1790	-.06379	.2924	-.06924	.4159
0.90	-.009886	.02380	-.03148	.08914	-.05431	.1856	-.07012	.3033	-.07760	.4320
0.92	-.01121	.02474	-.03513	.09227	-.06052	.1922	-.07906	.3141	-.08631	.4476
0.94	-.01236	.02553	-.03908	.09540	-.06732	.1989	-.08794	.3252	-.09505	.4628
0.96	-.01366	.02634	-.04334	.09858	-.07471	.2057	-.09753	.3364	-.1063	.4893
0.98	-.01454	.02705	-.04826	.1017	-.08317	.2125	-.1080	.3472	-.1192	.4953
1.00	-.01704	.02808	-.05345	.1048	-.09230	.2192	-.1197	.3585	-.1309	.5111
1.02	-.01884	.02890	-.05953	.1080	-.1025	.2260	-.1338	.3700	-.1457	.5274
1.04	-.02087	.02971	-.06605	.1112	-.1137	.2326	-.1487	.3812	-.1605	.5432
1.06	-.02311	.03053	-.07325	.1144	-.1259	.2395	-.1649	.3926	-.1788	.5598
1.08	-.02565	.03135	-.08136	.1172	-.1395	.2463	-.1833	.4039	-.2000	.5764
1.10	-.02848	.03216	-.09044	.1204	-.1564	.2531	-.2043	.4153	-.2207	.5923
1.12	-.03160	.03299	-.1006	.1236	-.1723	.2600	-.2258	.4267	-.2463	.6093
1.14	-.03516	.03381	-.1123	.1268	-.1922	.2668	-.2527	.4383	-.2744	.6258
1.16	-.03914	.03463	-.1254	.1300	-.2139	.2737	-.2790	.4497	-.3044	.6425
1.18	-.04367	.03544	-.1372	.1332	-.2381	.2805	-.3146	.4616	-.3376	.6589

TABLE 3 (Cont'd)

$k_i^V \frac{I^V}{2}$	M = 0.1		M = 0.2		M = 0.3		M = 0.4		M = 0.5	
	Unsymmetrical	Symmetrical	Unsymmetrical	Symmetrical	Unsymmetrical	Symmetrical	Unsymmetrical	Symmetrical	Unsymmetrical	Symmetrical
1.20	- .04879	.03625	- .1533	.1366	- .2648	.2873	- .3485	.4744	- .3803	.6761
1.22	- .05465	.03706	- .1714	.1397	- .2980	.2942	- .3902	.4846	- .4230	.6928
1.24	- .06100	.03782	- .1918	.1428	- .3344	.3011	- .4371	.4962	- .4724	.7096
1.26	- .06837	.03857	- .2182	.1459	- .3764	.3081	- .4875	.5074	- .5322	.7266
1.28	- .07724	.03936	- .2448	.1490	- .4238	.3149	- .5560	.5195	- .5999	.7436
1.30	- .08758	.04013	- .2757	.1521	- .4787	.3217	- .6237	.5309	- .6797	.7609
1.32	- .09895	.04085	- .3159	.1552	- .5417	.3285	- .7069	.5425	- .7701	.7779
1.34	- .1134	.04160	- .3590	.1583	- .6204	.3353	- .8152	.5546	- .8776	.7950
1.36	- .1300	.04228	- .4157	.1614	- .7143	.3420	- .9354	.5662	- 1.012	.8034
1.38	- .1512	.04302	- .4778	.1645	- .8284	.3487	- 1.086	.5780	- 1.173	.8299
1.40	- .1740	.04370	- .5620	.1673	- .9698	.3555	- 1.274	.5898	- 1.380	.8474
1.42	- .2132	.04436	- .6691	.1700	- 1.152	.3622	- 1.513	.6016	- 1.633	.8650
1.44	- .2553	.04502	- .8005	.1728	- 1.390	.3689	- 1.824	.6133	- 1.878	.8825
1.46	- .3135	.04567	- .9894	.1756	- 1.720	.3757	- 2.249	.6250	- 2.440	.9001
1.48	- .3980	.04670	- 1.262	.1783	- 2.198	.3831	- 2.870	.6369	- 3.110	.9176
1.50	- .5295	.04773	- 1.692	.1810	- 2.946	.3905	- 3.962	.6487	- 4.181	.9352
1.52	- .7651	.04875	- 2.481	.1838	- 4.286	.3979	- 5.598	.6606	- 6.075	.9528
1.54	-1.346	.04899	- 4.263	.1866	- 7.363	.4054	- 9.659	.6725	- 8.854	.9703
1.56	-7.437	.04923	-23.70	.1893	-41.08	.4108	-53.97	.6837	-58.79	.9879
1.58	4.823	.04947	15.42	.1920	26.82	.4162	35.13	.6965	38.09	1.005

TABLE 3 (Cont'd)

$k_1^v \frac{L^v}{2}$	M = 0.1		M = 0.2		M = 0.3		M = 0.4		M = 0.5	
	Unsymmetrical	Symmetrical	Unsymmetrical	Symmetrical	Unsymmetrical	Symmetrical	Unsymmetrical	Symmetrical	Unsymmetrical	Symmetrical
1.60	1.609	.04972	5.066	.1948	8.794	.4217	11.52	.7086	12.48	1.023
1.62	.9869	.05006	3.130	.1971	5.448	.4281	7.132	.7205	7.723	1.043
1.64	.7247	.05040	2.320	.1994	4.007	.4345	5.265	.7328	5.726	1.063
1.66	.5913	.05074	1.874	.2016	3.237	.4410	4.251	.7449	4.629	1.082
1.68	.5365	.05108	1.583	.2039	2.746	.4473	3.609	.7571	3.915	1.102
1.70	.4338	.05142	1.391	.2062	2.418	.4536	3.164	.7694	3.439	1.122
1.72	.3938	.05176	1.250	.2085	2.173	.4599	2.852	.7816	3.096	1.142
1.74	.3572	.05210	1.143	.2108	1.987	.4663	2.608	.7940	2.829	1.162
1.76	.3291	.05244	1.060	.2130	1.839	.4725	2.414	.8065	2.627	1.181
1.78	.3107	.05278	.9921	.2153	1.726	.4787	2.268	.8188	2.462	1.201
1.80	.2964	.05314	.9373	.2176	1.635	.4849	2.145	.8314	2.330	1.221
1.82	.2797	.05312	.8954	.2191	1.557	.4909	2.042	.8443	2.221	1.243
1.84	.2660	.05310	.8556	.2206	1.492	.4969	1.960	.8569	2.131	1.265
1.86	.2579	.05308	.8255	.2221	1.437	.5030	1.887	.8698	2.052	1.287
1.88	.2506	.05306	.7964	.2236	1.388	.5096	1.824	.8828	1.983	1.309

TABLE 3 (Cont'd)

$k_i^v \frac{L^v}{2}$	M = 0.1		M = 0.2		M = 0.3		M = 0.4		M = 0.5	
	Unsymmetrical	Symmetrical	Unsymmetrical	Symmetrical	Unsymmetrical	Symmetrical	Unsymmetrical	Symmetrical	Unsymmetrical	Symmetrical
1.90	.2412	.05304	.7742	.2252	1.349	.5149	1.770	.8960	1.929	1.331
1.92	.2359	.05302	.7545	.2267	1.316	.5208	1.727	.9091	1.891	1.353
1.94	.2286	.05300	.7344	.2282	1.284	.5268	1.688	.9222	1.852	1.375
1.96	.2248	.05308	.7196	.2297	1.260	.5325	1.657	.9355	1.814	1.397
1.98	.2139	.5306	.7064	.2312	1.237	.5382	1.626	.9493	1.775	1.419
2.00	.2157	.05294	.6940	.2327	1.214	.5438	1.595	.9628	1.737	1.441
2.02	.2136	.05248	.6849	.2329	1.204	.5495	1.582	.9776	1.723	1.468
2.04	.2114	.05238	.6759	.2332	1.193	.5552	1.570	.9924	1.709	1.495
2.06	.2092	.05183	.6669	.2334	1.183	.5611	1.557	1.007	1.696	1.522
2.08	.2071	.05108	.6610	.2336	1.172	.5664	1.544	1.022	1.682	1.549
2.10	.2050	.05027	.6550	.2338	1.162	.5718	1.532	1.037	1.668	1.576
2.12	.2028	.05004	.6490	.2341	1.152	.5772	1.519	1.052	1.654	1.602
2.14	.2006	.04909	.6431	.2343	1.141	.5825	1.506	1.066	1.640	1.629
2.16	.1985	.04803	.6393	.2345	1.131	.5877	1.493	1.081	1.627	1.656
2.18	.1964	.04762	.6356	.2348	1.120	.5928	1.481	1.096	1.613	1.683
2.20	.1942	.04627	.6318	.2350	1.110	.5980	1.468	1.111	1.599	1.710
2.22	.1936	.04497	.6305	.2330	1.109	.6028	1.467	1.129	1.598	1.746
2.24	.1930	.04348	.6293	.2300	1.107	.6076	1.466	1.147	1.598	1.783
2.26	.1924	.04194	.6280	.2289	1.106	.6123	1.465	1.165	1.597	1.819
2.28	.1918	.04023	.6268	.2268	1.105	.6170	1.466	1.183	1.597	1.856

TABLE 3 (Cont'd)

$k_i^v \frac{L^v}{2}$	M = 0.1		M = 0.2		M = 0.3		M = 0.4		M = 0.5	
	Unsymmetrical	Symmetrical	Unsymmetrical	Symmetrical	Unsymmetrical	Symmetrical	Unsymmetrical	Symmetrical	Unsymmetrical	Symmetrical
2.30	.1912	.03843	.6256	.2248	1.104	.6217	1.464	1.202	1.596	1.892
2.32	.1906	.03636	.6243	.2228	1.102	.6264	1.463	1.220	1.595	1.928
2.34	.1900	.03421	.6230	.2207	1.101	.6312	1.462	1.238	1.595	1.965
2.36	.1894	.03269	.6218	.2187	1.100	.6349	1.461	1.256	1.594	1.001
2.38	.1888	.03040	.6206	.2166	1.098	.6386	1.460	1.274	1.594	2.038
2.40	.1882	.02753	.6193	.2146	1.097	.6422	1.459	1.292	1.593	2.074
2.42	.1882	.02480	.6201	.2107	1.100	.6447	1.464	1.317	1.598	2.121
2.44	.1881	.02140	.6209	.2056	1.103	.6472	1.468	1.343	1.604	2.168
2.46	.1881	.01810	.6217	.2021	1.105	.6496	1.473	1.368	1.610	2.216
2.48	.1881	.01324	.6225	.1954	1.108	.6521	1.478	1.394	1.615	2.270
2.50	.1880	.009235	.6233	.1892	1.111	.6546	1.482	1.419	1.620	2.324
2.52	.1880	.004869	.6241	.1834	1.114	.6571	1.487	1.444	1.626	2.378
2.54	.1880	-.0000208	.6249	.1741	1.117	.6596	1.492	1.470	1.632	2.433
2.56	.1880	-.005061	.6257	.1645	1.119	.6620	1.497	1.495	1.637	2.503
2.58	.1879	-.01054	.6263	.1574	1.122	.6645	1.501	1.521	1.642	2.573
2.60	.1879	-.01672	.6273	.1464	1.125	.6670	1.506	1.546	1.648	2.643
2.62	.1881	-.02322	.6293	.1356	1.130	.6643	1.514	1.581	1.658	2.725
2.64	.1883	-.03250	.6312	.1221	1.136	.6616	1.523	1.617	1.668	2.803
2.66	.1884	-.04040	.6332	.1050	1.141	.6589	1.532	1.652	1.677	2.897
2.68	.1886	-.04951	.6351	.1030	1.146	.6562	1.540	1.696	1.687	2.985

TABLE 3 (Cont'd)

$k_i^v \frac{L^v}{2}$	M = 0.1		M = 0.2		M = 0.3		M = 0.4		M = 0.5	
	Unsymmetrical	Symmetrical	Unsymmetrical	Symmetrical	Unsymmetrical	Symmetrical	Unsymmetrical	Symmetrical	Unsymmetrical	Symmetrical
2.70	.1888	- .05897	.6371	.07107	1.152	.6536	1.548	1.740	1.697	3.096
2.72	.1890	- .07199	.6391	.05310	1.157	.6509	1.557	1.784	1.707	3.215
2.74	.1892	- .08419	.6410	.02907	1.161	.6482	1.566	1.828	1.717	3.330
2.76	.1893	- .09733	.6430	.003101	1.167	.6455	1.574	1.887	1.726	3.471
2.78	.1895	- .1123	.6449	- .02414	1.173	.6428	1.582	1.946	1.736	3.629
2.80	.1897	- .1320	.6469	- .05849	1.178	.6401	1.591	2.005	1.746	3.793
2.82	.1898	- .1514	.6494	- .09543	1.185	.6301	1.603	2.075	1.760	3.980
2.84	.1900	- .1660	.6518	- .1406	1.192	.6167	1.614	2.158	1.773	4.195
2.86	.1901	- .2018	.6543	- .1889	1.199	.6036	1.626	2.255	1.786	4.446
2.88	.1902	- .2319	.6567	- .2488	1.206	.5796	1.637	2.345	1.800	4.700
2.90	.1903	- .2703	.6592	- .3169	1.213	.5626	1.649	2.458	1.814	5.035
2.92	.1904	- .3117	.6617	- .3973	1.220	.5320	1.661	2.614	1.827	5.414
2.94	.1905	- .3662	.6641	- .4980	1.227	.4994	1.672	2.783	1.840	5.880
2.96	.1907	- .4284	.6666	- .6200	1.334	.4474	1.684	2.963	1.854	6.397
2.98	.1908	- .5114	.6690	- .7749	1.341	.3995	1.695	3.219	1.868	7.096
3.00	.1909	- .6118	.6715	- .9762	1.248	.3268	1.707	3.536	1.881	7.984
3.02	.1909	- .7525	.6743	-1.236	1.258	.2260	1.722	3.954	1.898	9.135
3.04	.1908	- .9495	.6771	-1.599	1.268	.09067	1.737	4.536	1.916	10.82
3.06	.1908	-1.235	.6798	-2.165	1.278	-.1434	1.752	5.358	1.933	13.14
3.08	.1908	-1.725	.6826	-3.096	1.288	-.5181	1.767	6.747	1.951	17.13

TABLE 3 (Cont'd)

$k_i^v \frac{L^v}{2}$	M = 0.1		M = 0.2		M = 0.3		M = 0.4		M = 0.5	
	Unsymmetrical	Symmetrical	Unsymmetrical	Symmetrical	Unsymmetrical	Symmetrical	Unsymmetrical	Symmetrical	Unsymmetrical	Symmetrical
3.10	.1908	- 2.642	.6854	- 4.880	1.298	- 1.235	1.782	9.562	1.968	25.08
3.12	.1907	- 5.330	.6882	- 10.05	1.308	- 3.309	1.796	17.42	1.985	47.42
3.14	.1907	-75.50	.6910	-145.1	1.318	-57.68	1.811	222.1	2.003	632.0
3.16	.1907	6.768	.6937	13.33	1.328	6.145	1.826	-18.04	2.020	- 52.97
3.18	.1906	3.380	.6965	6.746	1.338	3.472	1.841	- 8.065	2.038	- 25.08
3.20	.1906	2.311	.6993	4.749	1.348	2.823	1.856	- 4.553	2.055	- 15.24
3.22	.1901	1.796	.7022	3.691	1.358	2.277	1.875	- 3.321	2.078	- 11.68
3.24	.1897	1.476	.7051	3.095	1.367	2.039	1.894	- 2.398	2.100	- 9.078
3.26	.1893	1.272	.7080	2.701	1.377	1.880	1.913	- 1.794	2.122	- 7.373
3.28	.1899	1.128	.7109	2.415	1.387	1.777	1.932	- 1.357	2.145	- 6.148
3.30	.1885	1.020	.7138	2.209	1.396	1.694	1.952	1.045	2.168	- 5.313
3.32	.1881	.9371	.7167	2.049	1.406	1.632	1.971	- .7832	2.190	- 4.541
3.34	.1877	.8721	.7196	1.929	1.416	1.604	1.990	- .5509	2.212	- 3.906
3.36	.1873	.8140	.7225	1.826	1.426	1.565	2.009	- .3831	2.235	- 3.490
3.38	.1869	.7693	.7254	1.742	1.435	1.535	2.028	- .2411	2.258	- 3.100
3.40	.1865	.7318	.7283	1.666	1.445	1.509	2.047	- .1330	2.280	- 2.759
3.42	.1855	.7001	.7311	1.632	1.458	1.502	2.073	- .01917	2.310	- 2.494
3.44	.1844	.6725	.7338	1.599	1.472	1.495	2.099	.06881	2.340	- 2.256
3.46	.1834	.6487	.7366	1.565	1.486	1.487	2.125	.1536	2.371	- 2.032
3.48	.1824	.6277	.7393	1.531	1.499	1.480	2.151	.2008	2.401	- 1.847

TABLE 3 (Cont'd)

$k_i^v \frac{L^v}{2}$	M = 0.1		M = 0.2		M = 0.3		M = 0.4		M = 0.5	
	Unsymmetrical	Symmetrical	Unsymmetrical	Symmetrical	Unsymmetrical	Symmetrical	Unsymmetrical	Symmetrical	Unsymmetrical	Symmetrical
3.50	.1814	.6092	.7421	1.498	1.512	1.473	2.176	.2938	2.431	-1.667
3.52	.1803	.5929	.7449	1.464	1.526	1.466	2.202	.3510	2.461	-1.519
3.54	.1793	.5780	.7476	1.430	1.540	1.459	2.228	.4030	2.491	-1.386
3.56	.1783	.5645	.7504	1.396	1.533	1.451	2.254	.4512	2.512	-1.264
3.58	.1772	.5530	.7531	1.363	1.566	1.444	2.280	.5035	2.552	-1.137
3.60	.1762	.5425	.7559	1.329	1.580	1.437	2.306	.5529	2.582	-1.018
3.62	.1740	.5340	.7584	1.319	1.598	1.440	2.340	.6006	2.619	- .9248
3.64	.1717	.5256	.7608	1.309	1.615	1.443	2.374	.6376	2.657	- .7178
3.66	.1695	.5175	.7633	1.299	1.633	1.446	2.407	.6738	2.694	- .7548
3.68	.1672	.5093	.7657	1.289	1.650	1.449	2.441	.7051	2.732	- .6614
3.70	.1650	.5034	.7682	1.278	1.668	1.452	2.475	.7376	2.769	- .5916
3.72	.1627	.4974	.7707	1.268	1.687	1.455	2.509	.7672	2.816	- .5409
3.74	.1605	.4918	.7731	1.258	1.703	1.458	2.543	.8047	2.863	- .4579
3.76	.1583	.4862	.7756	1.248	1.721	1.461	2.576	.8335	2.911	- .3774
3.78	.1560	.4818	.7780	1.238	1.738	1.464	2.610	.8613	2.958	- .3205
3.80	.1538	.4774	.7805	1.228	1.756	1.467	2.644	.9011	3.005	- .2672
3.82	.1508	.4743	.7820	1.225	1.781	1.474	2.691	.9228	3.061	- .2140
3.84	.1472	.4712	.7835	1.223	1.805	1.480	2.738	.9445	3.117	- .1506
3.86	.1437	.4682	.7849	1.220	1.830	1.486	2.786	.9662	3.173	- .1205
3.88	.1394	.4651	.7864	1.217	1.855	1.493	2.833	.9879	3.229	- .07643

TABLE 3 (Cont)

$k_i^v \frac{L^v}{2}$	M = 0.1		M = 0.2		M = 0.3		M = 0.4		M = 0.5	
	Unsymmetrical	Symmetrical	Unsymmetrical	Symmetrical	Unsymmetrical	Symmetrical	Unsymmetrical	Symmetrical	Unsymmetrical	Symmetrical
3.90	.1350	.4620	.7879	1.214	1.880	1.500	2.880	1.010	3.285	-.03280
3.92	.1306	.4589	.7894	1.212	1.904	1.506	2.937	1.031	3.361	.000719
3.94	.1263	.4558	.7909	1.209	1.929	1.512	2.995	1.053	3.437	.04604
3.96	.1210	.4528	.7923	1.206	1.954	1.519	3.052	1.075	3.514	.08318
3.98	.1157	.4497	.7938	1.204	1.978	1.526	3.110	1.096	3.590	.1196
4.00	.1104	.4466	.7953	1.201	2.003	1.532	3.167	1.118	3.666	.1325
4.02	.1041	.4451	.7945	1.202	2.039	1.541	3.237	1.137	3.748	.1879
4.04	.09721	.4436	.7937	1.203	2.075	1.550	3.307	1.155	3.836	.2205
4.06	.08986	.4421	.7929	1.204	2.110	1.559	3.378	1.174	3.930	.2520
4.08	.08203	.4406	.7921	1.205	2.146	1.568	3.468	1.193	4.030	.2824
4.10	.07344	.4390	.7912	1.205	2.182	1.577	3.558	1.212	4.136	.3117
4.12	.06416	.4375	.7904	1.206	2.227	1.586	3.648	1.230	4.247	.3404
4.14	.05433	.4360	.7896	1.207	2.272	1.595	3.739	1.249	4.367	.3686
4.16	.04372	.4345	.7888	1.208	2.318	1.604	3.855	1.268	4.511	.3897
4.18	.03160	.4330	.7880	1.219	2.363	1.613	3.971	1.286	4.652	.4168
4.20	.01866	.4315	.7872	1.210	2.408	1.622	4.087	1.305	4.802	.4336
4.22	.00501	.4306	.7829	1.213	2.486	1.633	4.210	1.324	4.961	.4690
4.24	-.01024	.4297	.7801	1.216	2.530	1.644	4.332	1.343	5.135	.4942
4.26	-.02704	.4289	.7766	1.218	2.593	1.655	4.499	1.363	5.325	.5188
4.28	-.04578	.4280	.7723	1.221	2.666	1.666	4.666	1.382	5.510	.5479

TABLE 3 (Cont'd)

$k_i^v \frac{L^v}{2}$	M = 0.1		M = 0.2		M = 0.3		M = 0.4		M = 0.5	
	Unsymmetrical	Symmetrical	Unsymmetrical	Symmetrical	Unsymmetrical	Symmetrical	Unsymmetrical	Symmetrical	Unsymmetrical	Symmetrical
4.30	- .06617	.4271	.7648	1.224	2.744	1.677	4.848	1.401	5.736	.5714
4.32	- .08881	.4262	.7561	1.227	2.826	1.688	5.043	1.420	6.008	.5904
4.34	- .1144	.4253	.7486	1.230	2.918	1.699	5.260	1.439	6.283	.6133
4.36	- .1432	.4245	.7371	1.232	3.022	1.710	5.475	1.459	6.564	.6360
4.38	- .1756	.4236	.7236	1.235	3.136	1.721	5.772	1.478	6.933	.6617
4.40	- .2124	.4227	.7086	1.238	3.265	1.732	6.079	1.497	7.320	.6804
4.42	- .2530	.4220	.6923	1.242	3.410	1.745	6.422	1.516	7.758	.7020
4.44	- .3033	.4214	.6704	1.246	3.572	1.758	6.818	1.536	8.261	.7235
4.46	- .3578	.4208	.6479	1.251	3.762	1.772	7.275	1.555	8.842	.7446
4.48	- .4407	.4201	.6031	1.255	4.033	1.785	7.946	1.575	9.715	.7760
4.50	- .5042	.4194	.5834	1.259	4.249	1.798	8.448	1.594	10.34	.7866
4.52	- .5979	.4188	.5369	1.263	4.560	1.811	9.213	1.613	11.31	.8071
4.54	- .7141	.4182	.4782	1.267	4.956	1.824	10.16	1.633	12.52	.8276
4.56	- .8667	.4175	.4100	1.272	5.437	1.838	11.35	1.652	14.03	.8479
4.58	-1.060	.4168	.3114	1.276	6.072	1.851	12.90	1.672	16.01	.8681
4.60	-1.330	.4162	.1745	1.280	6.920	1.864	14.99	1.691	18.68	.8882
4.62	-1.707	.4154	- .00818	1.285	8.156	1.880	18.00	1.713	22.52	.9080
4.64	-2.294	.4147	- .3127	1.291	10.04	1.896	22.80	1.734	28.48	.9278
4.66	-3.349	.4140	- .8526	1.296	13.39	1.913	31.07	1.756	38.97	.9475
4.68	-5.680	.4132	-2.068	1.302	20.86	1.929	49.57	1.778	62.45	.9673

TABLE 3 (Cont'd)

$k_i^v \frac{L^v}{2}$	M = 0.1		M = 0.2		M = 0.3		M = 0.4		M = 0.5	
	Unsymmetrical	Symmetrical	Unsymmetrical	Symmetrical	Unsymmetrical	Symmetrical	Unsymmetrical	Symmetrical	Unsymmetrical	Symmetrical
4.70	-15.54	.4124	- 7.218	1.307	52.38	1.945	127.7	1.800	161.6	.9871
4.72	26.68	.4117	14.73	1.312	-81.66	1.961	-204.8	1.821	-260.5	1.009
4.74	7.664	.4110	4.889	1.318	-21.53	1.977	- 55.60	1.843	- 71.05	1.027
4.76	4.630	.4102	3.300	1.323	-11.90	1.994	- 31.76	1.865	- 40.79	1.046
4.78	3.405	.4094	2.670	1.329	- 7.974	2.010	- 22.01	1.886	-28.42	1.066
4.80	2.728	.4087	2.328	1.334	- 5.834	2.026	- 16.70	1.908	-21.69	1.086
4.82	2.314	.4076	2.108	1.341	- 4.492	2.046	- 13.38	1.934	-17.48	1.107
4.84	2.021	.4065	1.973	1.348	- 3.557	2.067	- 11.09	1.960	-14.57	1.127
4.86	1.815	.4054	1.864	1.355	- 2.875	2.087	- 9.421	1.986	-12.45	1.148
4.88	1.653	.4043	1.787	1.362	- 2.361	2.107	- 8.152	2.012	-10.85	1.169
4.90	1.531	.4032	1.728	1.368	- 1.954	2.128	- 7.149	2.038	- 9.577	1.190
4.92	1.423	.4021	1.682	1.375	- 1.624	2.148	- 6.340	2.063	- 8.600	1.210
4.94	1.343	.4010	1.640	1.382	- 1.350	2.168	- 5.671	2.089	- 7.707	1.231
4.96	1.276	.3999	1.610	1.389	- 1.116	2.188	- 5.109	2.115	- 6.997	1.252
4.98	1.216	.3988	1.586	1.396	- .9192	2.209	- 4.631	2.141	- 6.394	1.272
5.00	1.168	.3977	1.566	1.403	- .7441	2.229	- 4.217	2.167	- 5.871	1.293

BIBLIOGRAPHY

1. DeHart, R. C., Response of a Rigid Frame to a Distributed Transient Load, ASCE Proc. Vol. 82, No. ST5, (Sept. 1956.)

2. Inglis, C. E., A Mathematical Treatise on Vibrations in Railway Bridges, Cambridge University Press, London, 1934.

Paper 1822 October, 1958 EM 4

Journal of the
ENGINEERING MECHANICS DIVISION
Proceedings of the American Society of Civil Engineers

LARGE DEFLECTION THEORY OF ELASTO-PLASTIC PLATES

Thein Wah,[1] A.M. ASCE
(Proc. Paper 1822)

SYNOPSIS

Closed form solutions are obtained for the deflections, residual deflections, residual membrane tensions, and other quantities of engineering interest for infinitely long clamped rectangular plates with large deflections, under uniform pressure. The analysis assumes infinite rigidity, in the plane of the plate, of the boundary supports. Charts are provided for convenience in solving the equations.

INTRODUCTION

The so-called plastic design of beams and frames has received considerable attention in recent years. In extending these methods to plate analysis several difficulties arise, not the least of which is that the small deflection theory of plates due to Lagrange(1) yields a limit strength much lower than that actually developed by plates of practical proportions. This is because, as the plate continues to deflect, membrane tensions arise in the middle plane of the plate which add to its load-carrying capacity. A good estimate of the ultimate loads on plates, neglecting membrane action, can be obtained by the rupture-line theory of Johansen.(2,3) While it may be permissible to neglect membrane action in certain practical applications, all plates develop membrane forces for large enough deflections. Any realistic plastic analysis must, therefore, take into account the effect of membrane tensions in the middle plane of the plate.

The basic equations for plates in the large deflection region have been derived by von Karman.(1) An exact solution of these quations in the elastic case was obtained by Levy.(4) When one attempts to make an elasto-plastic

Note: Discussion open until March 1, 1959. To extend the closing date one month, a written request must be filed with the Executive Secretary, ASCE. Paper 1822 is part of the copyrighted Journal of the Engineering Mechanics Division, Proceedings of the American Society of Civil Engineers, Vol. 84, No. EM 4, October, 1958.

1. Southwest Research Inst., San Antonio, Tex.

analysis of rectangular plates using the von Karman equations as the starting point, the mathematical difficulties are prohibitive. One serious difficulty is that rectangular plates with clamped edges yield at the middle points of the edges, and then the plasticity spreads gradually to the corners and to the center of the plate. Thus, at any given stage in the analysis, the boundaries may be partly elastic and partly plastic. Thus, in addition to the inherent mathematical difficulties of von Karman's non-linear equations, one has to consider the complex situation of mixed boundary conditions.

The particular difficulty associated with mixed boundary conditions can be avoided if the plate is assumed to be infinitely long. It is then possible to consider an elementary strip of unit width (Fig. 1) and length ℓ, and von Karman's equations reduce to a single linear differential equation:(1)

$$\frac{d^4w}{dx^4} = \frac{q}{D} + \frac{N_x}{D}\frac{d^2w}{dx^2} \qquad (1)$$

where $D = \frac{Eh^3}{12(1-\nu^2)}$ is flexural stiffness of the plate, q is the load on the plate (assumed uniform in the present analysis) and N_x is the membrane tension which, in this case, is constant throughout the plate. As one is considering an elementary strip, the boundaries may be assumed to yield throughout at the same time and the complexity of mixed boundary conditions thereby avoided. Furthermore, the plastic-hinge concept, so effectively utilized in the case of beams, may be readily extended to the plate problem.

Clarkson(5,6) has solved the above equation for the elasto-plastic range by a power series method, in which he uses two terms of the series to obtain the final solution. In the present paper, the basic concepts of Clarkson are adopted, but a closed form and therefore "exact" solution is obtained, within the limits of the assumptions stated below:

1. The stress-strain law. The relation between stress and strain for first loading, unloading, and reloading is given in Figure 2. The analysis may therefore be expected to apply to materials which exhibit little or no strain hardening, or have a large range of pure yielding.

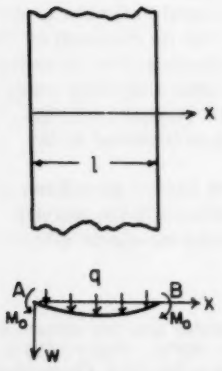

Fig. 1

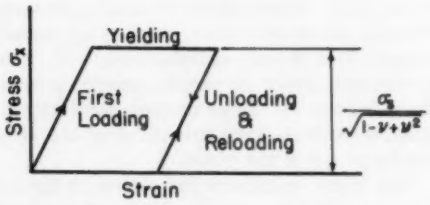

Fig. 2

2. The yield condition. The Hencky-Mises yield condition[7] is adopted in the analysis. For a biaxial stress condition this becomes

$$\sigma_x^2 + \sigma_y^2 - \sigma_x \sigma_y + 3\tau_{xy}^2 = \sigma_s^2 \qquad (2)$$

where σ_s is the yield stress in pure tension. For the infinitely long clamped plate considered here $\sigma_y = \nu \sigma_x$, $\tau_{xy} = 0$

(see page 2 of Reference 2). Equation (2) thus simplifies to

$$\sigma_x = \frac{\sigma_s}{(1-\nu+\nu^2)^{\frac{1}{2}}} \qquad (3)$$

3. Moment-curvature relation. The moment-curvature relationship is similar in form to the stress-strain law. This involves the assumption that a cross section of the plate behaves elastically until it has yielded right through, that is, until the distribution of stresses is as shown in Fig. 3. From there on its resisting moment remains constant at M_p and the section forms a plastic hinge exactly as assumed in the plastic theory of beams. The plate is free to rotate about the hinge with no resulting change in stress at that section. M_p will be called the "fully plastic moment" and differs from its value in the beam theory only insofar as it is modified by the presence of a membrane tension, and Poisson's ratio.

Referring to Fig. 3, one has

$$M_p = \frac{\sigma_s \quad (h^2 - h_1^2)}{\sqrt{1-\nu+\nu^2} \quad 4}$$

and

$$N_x = \frac{\sigma_s \; h_1}{\sqrt{1-\nu+\nu^2}}$$

eliminating h_1 between these two equations

$$M_p = \frac{\sigma_s \; h^2}{4\sqrt{1-\nu+\nu^2}} \left\{ 1 - \frac{(1-\nu+\nu^2) \; N_x^2}{\sigma_s^{\,2} h^2} \right\} \qquad (4)$$

The first plastic hinges form at the edges of the plate, where the bending moment is the maximum. As the load is increased, a plastic hinge forms along the center line of the plate. The load corresponding to the formation of a center-line plastic hinge is called the "limit load." (Actually the plate will continue to carry load beyond the "limit load," until the whole width of the plate is plastified. But this phase is beyond the scope of the present paper).

4. Other assumptions are the same as in large-deflection plate theory in the elastic range. Briefly, the material is supposed to be homogeneous, isotropic and to obey Hooke's law until it yields. The deflections may be many times the thickness of the plate but small compared to its lateral dimensions.

Solution of Differential Equation

On integrating equation (1) twice with respect to **x**, one has

$$\frac{d^2w}{dx^2} = \frac{qx^2}{2D} + \frac{N_x}{D}w + c_1 x + c_2$$

where c_1 and c_2 are constants of integration. Referring to Fig. 1, and making use of the relationship,

$$\frac{d^2w}{dx^2} = -\frac{M(x)}{D}$$

the constants of integration are easily determined and the above equation becomes

$$\frac{d^2w}{dx^2} - \frac{N_x w}{D} = -\frac{qlx}{2D} + \frac{qx^2}{2D} + \frac{Mo}{D} \qquad (5)$$

The general solution of this equation is (see page 12, Reference 2)

$$W = c_1 \sinh \frac{2ux}{l} + c_2 \cosh \frac{2ux}{l} + \frac{ql^3x}{8u^2D} - \frac{ql^2x^2}{8u^2D} - \frac{ql^4}{16u^4D} - \frac{Mol^2}{4u^2D} \qquad (6)$$

from which

$$\frac{dw}{dx} = c_1 \frac{2u}{l} \cosh \frac{2ux}{l} + c_2 \frac{2u}{l} \sinh \frac{2ux}{l} + \frac{ql^3}{8u^2D} - \frac{ql^2x}{4u^2D} \qquad (7)$$

where

$$u^2 = \frac{N_x l^2}{4D} \qquad (8)$$

u being the "tension parameter" and c_1 and c_2 are arbitrary constants.

The boundary conditions, valid in both the elastic and plastic ranges are:

$$w = 0 \text{ at } x = 0 \text{ and } x = l$$

$$\frac{dw}{dx} = o \text{ at } x = l/2$$

On substituting these conditions and then transferring the origin of coordinates to the center of the plate (Fig. 4) one finds:

$$w = c_2\left(\frac{\cosh \frac{2ux}{l}}{\cosh u} - 1\right) + \frac{ql^4}{32u^2D} - \frac{ql^2x^2}{8u^2D} \qquad (9)$$

$$\frac{dw}{dx} = \frac{c_2}{\cosh u} \frac{2u}{l} \sinh \frac{2ux}{l} - \frac{ql^2x}{4u^2D} \qquad (10)$$

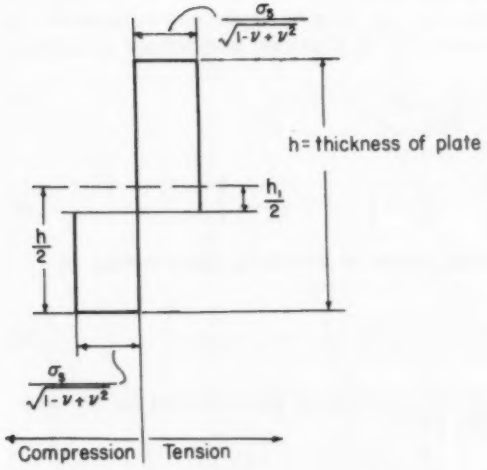

Fig. 3

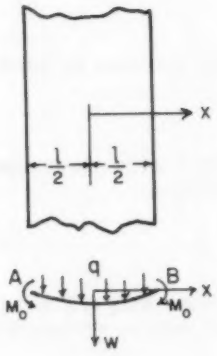

Fig. 4

where

$$c_2 = \frac{ql^4}{16u^4D} + \frac{Mol^2}{4u^2D}$$

The condition for the calculation of $u^2 = \frac{N_x l^2}{4D}$ is obtained by considering the change in the distance between the supports A and B (Fig. 4). Assuming that this change is zero, i.e., the edges are rigid enough to present any "pull in," this condition may be started as follows:

$$\int_0^{\frac{l}{2}} \frac{(1-\nu^2)}{Eh} N_x dx = \frac{1}{2} \int_0^{\frac{l}{2}} \left(\frac{dw}{dx}\right)^2 dx$$

which becomes

$$\frac{N_x(1-\nu^2)\,l}{E\,h} = \int_0^{\frac{l}{2}} \left(\frac{dw}{dx}\right)^2 dx$$

On substituting the value of N_x from equation (8), this reduces to

$$\frac{u^2h^2}{3l} = \int_0^{\frac{l}{2}} \left(\frac{dw}{dx}\right)^2 dx \qquad (11)$$

On page 12 of Reference 2, it is shown that for the elastic case where the boundary slope is zero, M_o has the value

$$M_o = -\frac{q\,l^2}{4u^2} + \frac{q\,l^2}{4u} \coth u \qquad (12)$$

When a plastic hinge is formed at the edges, the end moment is the fully plastic moment M_p given by equation (4). M_p may be expressed in terms of the "plate strength parameter" B introduced by Clarkson and defined as follows:

$$B = \frac{1 - \nu^2}{\sqrt{1-\nu+\nu^2}} \frac{\sigma_s l^2}{E h^2} \tag{13}$$

M_p may then be written

$$|M_p| = \frac{3hD}{l^2}\left\{ B - \frac{u^4}{9B} \right\} \tag{14}$$

Thus, after the formation of plastic hinges at the edges, the constant c_2 becomes

$$c_2 = \frac{ql^4}{16u^4D} + \frac{3h}{4u^2}\left\{ B - \frac{u^4}{9B} \right\} \tag{15}$$

Substituting (15) and (10) into (11) and integrating, the condition for no "pull in" may be written in the following form:

$$P^2 + 4P\frac{\Phi_2}{\Phi_1}\left\{\frac{9B}{u^4} - \frac{1}{B}\right\} + 4\frac{\Phi_3}{\Phi_1}\left\{\frac{9B^2}{u^4} + \frac{u^4}{9B^2} - 2\right\} - \frac{6}{3\Phi_1} = 0 \tag{16}$$

in which

$$\Phi_1 = \frac{5}{4}\frac{\tanh u}{u^9} + \frac{1}{6u^6} - \frac{1}{4u^8\cosh^2 u} - \frac{1}{u^8}$$

$$\Phi_2 = \frac{\tanh u}{2u^3} - \frac{1}{3u^2} - \frac{1}{6u^2\cosh^2 u}$$

$$\Phi_3 = \frac{\tanh u}{u} - \frac{1}{\cosh^2 u}$$

$$P = \frac{ql^4}{Dh} = \frac{12(1-\nu^2)l^4 q}{Eh^4} \quad \text{the "non-dimensional load"} \tag{17}$$

Equation (16) is a quadratic for P for given values of u and B. Figures 5 and 6 give a plot of P against B for various values of u. In Fig. 5, P is plotted on a logarithmic scale. Table I contains the same information as given in Figures 5 and 6.

The deflections after the formation of edge plastic hinges may be obtained by substituting the value of c_2 from equation (15) into equation (9). Thus one finds:

$$w = \left\{\frac{ql^4}{16u^4D} + \frac{3h}{4u^2}\left(B - \frac{u^4}{9B}\right)\right\}\left\{\frac{\cosh\frac{2ux}{l}}{\cosh u} - 1\right\} + \frac{ql^4}{32u^2D} - \frac{ql^2x^2}{8u^2D} \tag{18}$$

The maximum deflection may be obtained by letting $x = 0$ in (18). It is convenient to express this in non-dimensional form as follows:

$$\frac{w_m}{h} = \frac{P}{16u^2}\left(\frac{1-\cosh u}{u^2\cosh u} + \frac{1}{2}\right) + 3/4\left(B - \frac{u^4}{9B}\right)\left(\frac{1-\cosh u}{u^2\cosh u}\right) \tag{19}$$

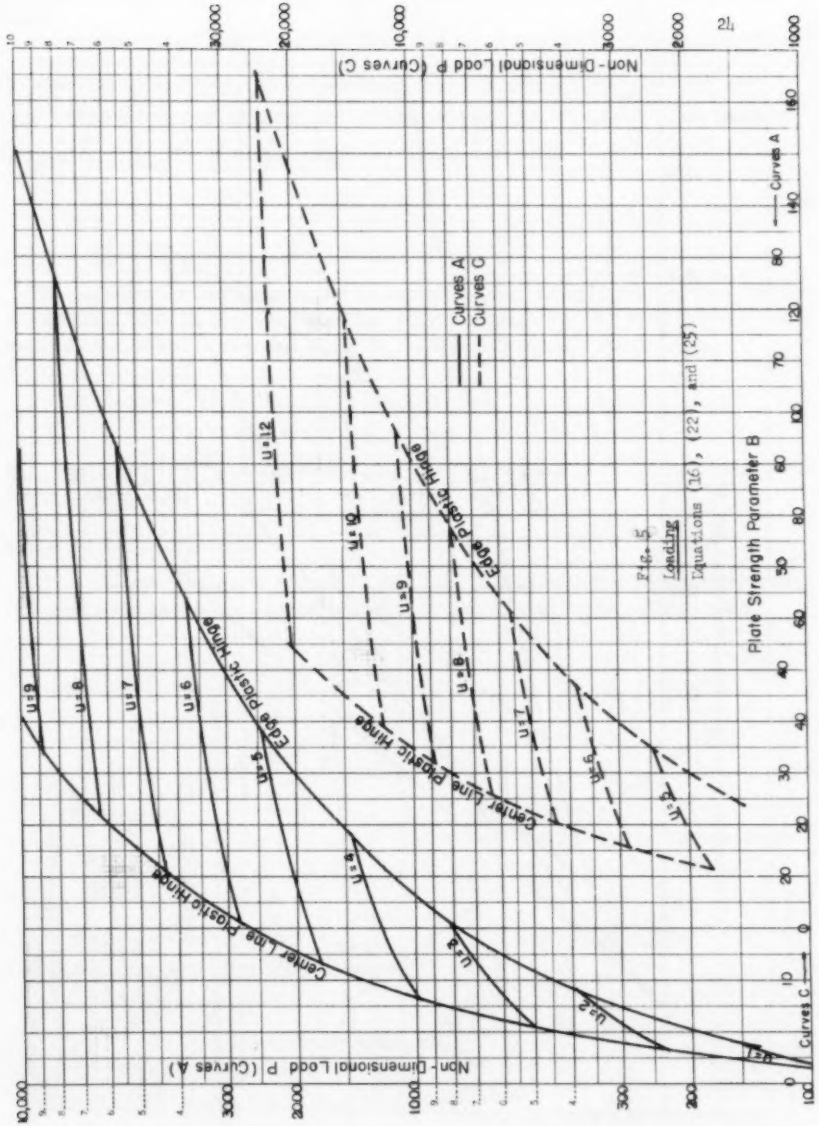

Fig. 5

Loading Equations (16), (22), and (25)

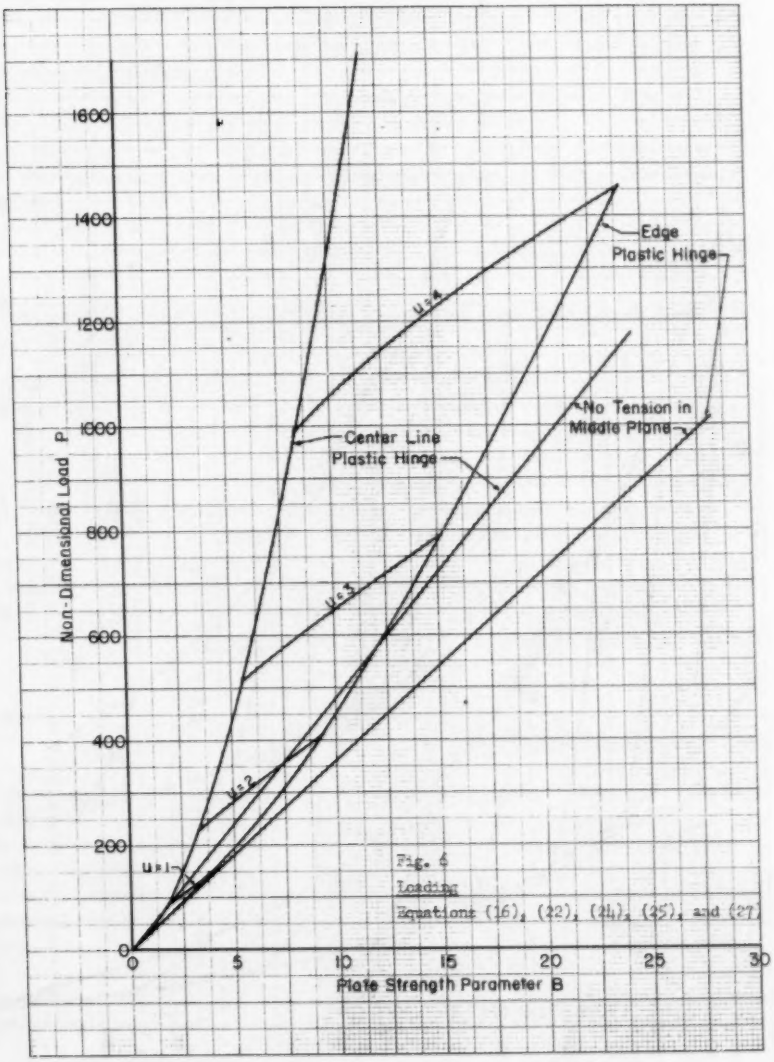

Fig. 6
Loading
Equations (16), (22), (24), (25), and (27)

If corresponding values of B, u, and P are substituted in (19), the maximum deflection may be obtained. In Table I are shown values of $\frac{w_m}{h}$ this calculated.

An inspection of Table I shows that, for all practical purposes, the non-dimensional deflection $\frac{w_m}{h}$ is independent of P and B, and may be considered as a function of u alone. When average values of $\frac{w_m}{h}$ are plotted against u (Fig. 7), it is seen that the linear relation

$$\frac{w_m}{h} = 0.361\, u \tag{20}$$

closely expresses the relation between u and $\frac{w_m}{h}$.

The end slopes corresponding to any load after plastic hinges have formed at the edges can be obtained similarly from equation (10). It is convenient to express the value of the end slope in "non-dimensional" form thus:

$$\alpha = -\frac{dw}{dx} \cdot \frac{l}{h}\bigg|_{x=\frac{1}{2}} = \frac{P}{8u^2}\left\{1 - \frac{\tanh u}{u}\right\} + \frac{3}{2}\,\frac{\tanh u}{u}\left(\frac{u^4}{9B} - B\right) \tag{21}$$

Fig. 8 gives a plot of α against P for various values of u. P is plotted on a logarithmic scale.

Onset of Edge Plasticity

The load when plastic hinges form at the edges may be determined from the condition that the elastic fixed-end moment equals the fully plastic

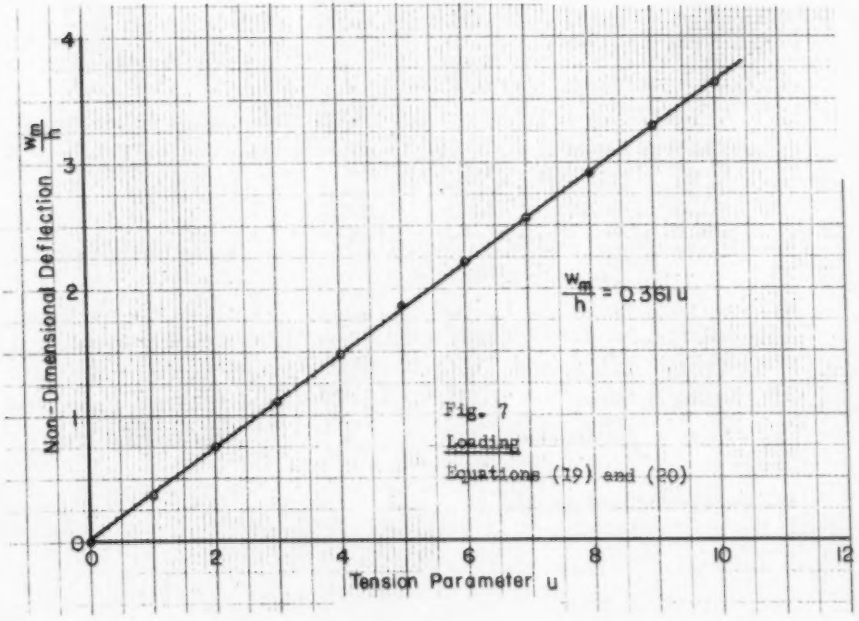

Fig. 7
Loading
Equations (19) and (20)

TABLE I (LOADING)

u	B	P	w_m/h	α	Remarks
1	1.54	82.6	0.367	0.744	Center Plastic Hinge
	4.10	156.2	.369	0	Edge Plastic Hinge
			.368 a		
2	3.25	223.1	.747	1.743	Center Plastic Hinge
	5.00	282.1	.756	1.208	
	9.14	396.9	.739	0	Edge Plastic Hinge
			.747 a		
3	5.46	505.8	1.108	2.765	Center Plastic Hinge
	10.00	648.5	1.118	1.491	
	15.00	784.5	1.098	0.118	
	15.42	804.2	1.107	0	Edge Plastic Hinge
			1.108 a		
4	8.21	981.5	1.472	3.972	Center Plastic Hinge
	10.00	1050.5	1.482	3.475	
	15.00	1213.9	1.494	2.203	
	20.00	1354.6	1.488	0.977	
	23.95	1455.4	1.472	0	Edge Plastic Hinge
			1.482 a		
5	11.60	1730.5	1.826	5.238	Center Plastic Hinge
	15.00	1867.8	1.844	4.361	
	20.00	2037.0	1.856	3.190	
	25.00	2185.0	1.858	2.074	
	26.30	2221.0	1.857	1.787	
	30.00	2318.9	1.851	0.971	
	34.38	2426.6	1.836	0	Edge Plastic Hinge
			1.847 a		
6	15.66	2819.8	2.179	6.543	Center Plastic Hinge
	20.00	3004.6	2.199	5.494	
	25.00	3184.0	2.212	4.403	
	26.30	3226.9	2.215	4.131	
	30.00	3342.4	2.219	3.371	
	40.00	3618.9	2.213	1.372	
	46.89	3786.1	2.197	0	Edge Plastic Hinge
			2.205 a		
7	20.40	4317.6	2.530	7.873	Center Plastic Hinge
	25.00	4525.1	2.549	6.824	
	26.30	4577.8	2.554	6.548	
	30.00	4717.8	2.564	5.793	
	40.00	5045.0	2.577	3.889	
	50.00	5324.2	2.575	2.071	
	61.52	5603.6	2.555	0	Edge Plastic Hinge
			2.554 a		

a - average for constant u

TABLE I (LOADING) - Cont'd)

u	D	P	w_m/h	α	Remarks
8	25.61	6290.9	2.880	9.217	Center Plastic Hinge
	26.30	6316.4	2.883	9.108	
	30.00	6491.6	2.897	8.313	
	40.00	6886.3	2.922	6.402	
	50.00	7213.9	2.934	4.660	
	60.00	7500.3	2.934	2.990	
	78.25	7947.4	2.911	0	Edge Plastic Hinge
			2.905 a		
9	31.91	8810.0	3.231	10.575	Center Plastic Hinge
	40.00	9192.7	3.257	8.981	
	50.00	9581.5	3.277	7.240	
	60.00	9915.2	3.288	5.626	
	70.00	10212.0	3.294	4.077	
	80.00	10480.4	3.287	2.562	
	90.00	10725.0	3.277	1.062	
	97.10	10885.5	3.267	0	Edge Plastic Hinge
			3.272 a		
10	38.68	11938.9	3.582	11.939	Center Plastic Hinge
	40.00	12009.9	3.586	11.678	
	50.00	12479.0	3.613	9.872	
	60.00	12870.7	3.631	8.247	
	70.00	13214.1	3.641	6.747	
	80.00	13523.1	3.646	5.297	
	90.00	13805.4	3.646	3.883	
	100.00	14065.6	3.641	2.491	
	110.00	14305.8	3.632	1.109	
	118.05	14485.3	3.621	0	Edge Plastic Hinge
			3.624 a		
12	54.23	20304.4	4.274	14.688	Center Plastic Hinge
	60.00	20613.8	4.296	13.703	
	70.00	21083.5	4.319	12.141	
	80.00	21494.4	4.333	10.704	
	90.00	21863.8	4.343	9.347	
	100.00	22202.0	4.350	8.047	
	120.00	22806.8	4.356	5.548	
	140.00	23337.7	4.351	3.127	
	160.00	23808.3	4.337	0.745	
	166.28	24059.9	4.355	0	Edge Plastic Hinge
			4.331 a		

a = average for constant u

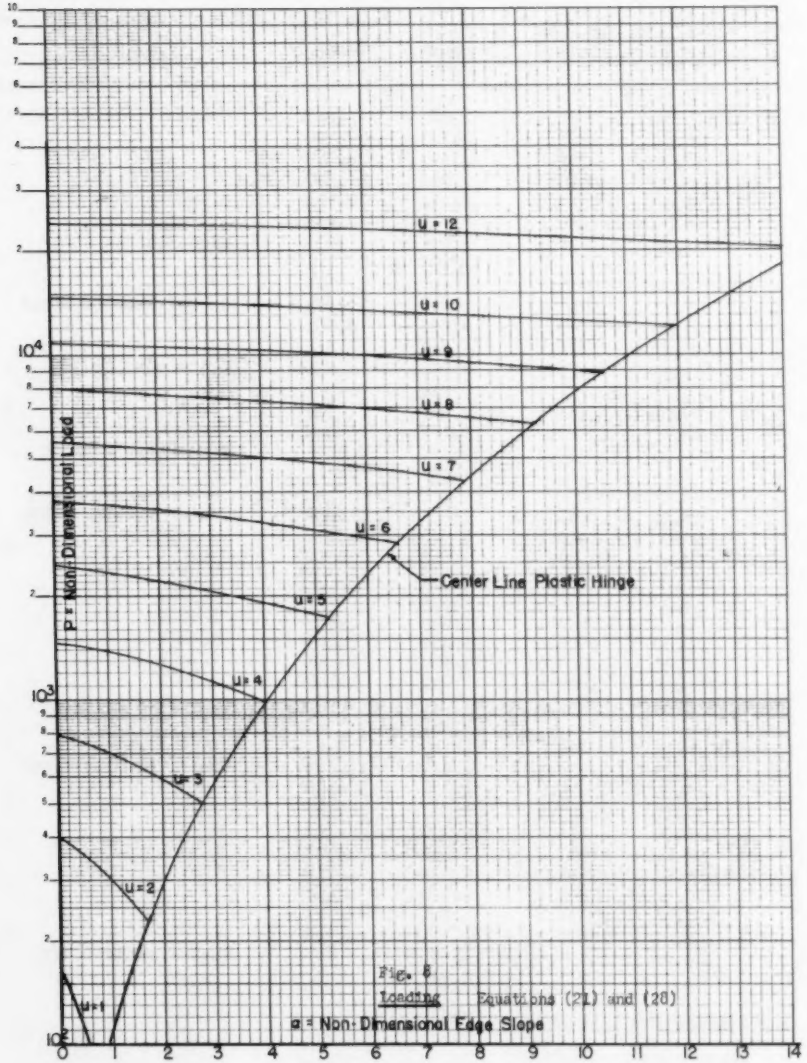

Fig. 6

Loading Equations (21) and (28)

moment. Thus, from equations (12 and 14):

$$-\frac{ql^2}{4u^2} + \frac{ql^2}{4u}\coth u = \frac{3Dh}{l^2}\left(B - \frac{u^4}{9B}\right)$$

or

$$P_E = \frac{12\,u^2 \tanh u}{u - \tanh u}\left(B - \frac{u^4}{9B}\right) \qquad (22)$$

where $P_E = \frac{ql^4}{Dh}$

The relation between B and u when edge plastic hinges form can be derived by substituting the value of P from (22) into (16). In this way one finds:

$$B^4\left\{\frac{27}{4}\Phi_1\frac{u^4\tanh^2 u}{(u-\tanh u)^2} + \frac{81}{4}\Phi_2\frac{\tanh u}{u^2(u-\tanh u)} + \frac{27}{16}\frac{\Phi_3}{u^4}\right\}$$

$$-B^2\left\{\frac{9}{2}\Phi_2\frac{u^2\tanh u}{u-\tanh u} + \frac{3}{2}\Phi_1\frac{u^8\tanh^2 u}{(u-\tanh u)^2} + \frac{3}{8}\Phi_3 + 1\right\}$$

$$+\frac{u^{12}}{12}\Phi_1\frac{\tanh^2 u}{(u-\tanh u)^2} + \frac{\Phi_2}{4}\frac{u^6\tanh u}{u-\tanh u} + \frac{u^4\Phi_3}{48} = 0 \qquad (23)$$

where ϕ_1, ϕ_2, and ϕ_3, are the same as in equation (16).

Equation (23) gives related values of B and u which must be substituted in equation (22) to obtain the non-dimensional load P corresponding to edge plasticity. Figs. 5 and 6 are shown a plot of equation (22). Table I gives the values from which the curves were drawn.

It may be noted here that when there is no tension in the middle plane of the plate, i.e., u = 0, equation (23) no longer applies, and B is independent of u. On setting u = 0 in equation (22), there follows

$$P_E = 36B \qquad (24)$$

This is the non-dimensional load for the formation of edge plastic hinges if the tension in the middle plane is neglected as in classical plate (or beam) theory. Fig. 6 shows a graph of equation (24) and clearly indicates the great increase in the stiffness of the plate due to membrane tension.

Onset of Center Plasticity

The load of P corresponding to the formation of a center-line plastic hinge may be obtained by equating the bending moment at the center to the fully plastic moment. Differentiating equation (18) and letting x = 0, there follows:

$$-D\left.\frac{d^2w}{dx^2}\right|_{x=0} = -\frac{ql^2}{4u^2\cosh u} + \frac{ql^2}{4u^2} - \frac{3hD}{l^2\cosh u}\left(B - \frac{u^4}{9B}\right)$$

Setting this equal to $M_p = \frac{3hD}{l^2}\left(B - \frac{u^4}{9B}\right)$ and simplifying, there finally results:

$$P_L = 12u^2 \left(B - \frac{u^4}{9B}\right) \left(\frac{\cosh u+1}{\cosh u-1}\right) \qquad (25)$$

This is the "limit load" on the plate as here defined.

The relation between B and u when a center-line plastic hinge forms may be obtained by substituting P from (25) into (16). The result may be written as a quadratic equation for B^2:

$$B^4 \left\{ \frac{27}{4} \Phi_1 u^4 \frac{(\cosh u+1)^2}{(\cosh u-1)^2} + \frac{81}{4} \frac{\Phi_2}{u^2} \frac{(\cosh u+1)}{(\cosh u-1)} + \frac{27}{16} \frac{\Phi_3}{u^4} \right\}$$
$$-B^2 \left\{ \frac{9}{2} \Phi_2 u^2 \frac{(\cosh u+1)}{(\cosh u-1)} + \frac{3}{2} \Phi_1 u^8 \frac{(\cosh u+1)^2}{(\cosh u-1)^2} + \frac{3}{8} \Phi_3 + 1 \right\}$$
$$+ \frac{u^{12}}{12} \Phi_1 \frac{(\cosh u+1)^2}{(\cosh u-1)^2} + \frac{\Phi_2}{4} u^6 \frac{(\cosh u+1)}{(\cosh u-1)} + \frac{u^4 \Phi_3}{48} = 0 \qquad (26)$$

Figs. 5 and 6 show a plot of equation (25), corresponding values of B and u being obtained from equation (26).

It may be noted that when there is no tension in the middle plane of the plate, equation (26) no longer applies. Setting u = 0 in equation (25) yields:

$$P_L = 48B \qquad (27)$$

This is the non-dimensional load for the formation of a center-line plastic hinge when the tension in the middle plane is neglected. Fig. 6 shows a graph of equation (27).

The non-dimensional edge slope when a plastic hinge forms at the center-line may be obtained by substituting the value of P from equation (25) into equation (21). One finds then:

$$\alpha_L = \frac{3}{2} \left(B - \frac{u^4}{9B}\right) \left(\frac{u+u \cosh u-2 \sinh u}{u (\cosh u-1)}\right) \qquad (28)$$

Fig. (8) shows a plot of equation (28)

Unloading

When unloading takes place after the formation of plastic hinges at the edges, the end rotations remain constant at the maximum value reached during first loading. Otherwise the beam behaves elastically. Thus the maximum end rotation reached prior to unloading provides the additional boundary condition required for a unique solution.

It is evident that the basic differential equation for unloading is (5). The boundary conditions (Fig. 4):

$$w = 0 \quad \text{at} \quad x = o \quad \text{and} \quad x = l$$

$$\frac{dw}{dx} = o \text{ at } x = \frac{l}{2}$$

are still valid. If these are substituted in the solution (6) and the origin transferred to the center line (Fig. 4) one obtains equations (9) and (10). The value of the constant c_2 is the same as before, and M_o is now determined from the condition

$$\frac{l}{h}\left(\frac{dw}{dx}\right)\Big|_{x=\frac{l}{2}} = -\alpha$$

Substituting from equation (10), one finds

$$M_o = -\left\{\alpha + \frac{\bar{P}}{8u^2}\left(\frac{\tanh u}{u} - 1\right)\right\}\frac{2uDh}{l^2\tanh u} \qquad (29)$$

The notation $\bar{P}$ is used to distinguish the load reached during the unloading process from the load P reached during the loading process. The deflection during any stage of the unloading may be obtained by substituting (29) into (9). One thus finds:

$$w = \left\{\frac{\bar{P}\,h}{16u^3\tanh u} - \frac{\alpha\,h}{2u\tanh u}\right\}\left\{\frac{\cosh\frac{2ux}{l}}{\cosh u} - 1\right\} + \frac{\bar{P}\,h}{32u^2} - \frac{\bar{P}x^2h}{8u^2l^2} \qquad (30)$$

It is to be noted that α has to be substituted from equation (21) and that the value of u to be used in determining α corresponds to P and not $\bar{P}$. The maximum non-dimensional deflection can be obtained from (30) by setting $x = 0$.

$$\frac{w_m}{h} = \frac{\bar{P}}{16u^2}\left\{\frac{1-\cosh u}{u\sinh u} + \frac{1}{2}\right\} - \frac{\alpha}{2}\left\{\frac{1-\cosh u}{u\sinh u}\right\} \qquad (31)$$

The value of u in equations (29) and (31) is obtained by using the condition of no "pull in" as given in equations (11). One thus finds:

$$\bar{P}^2\left\{-\frac{9}{256u^7\tanh u} - \frac{3}{256u^6\sinh^2 u} + \frac{3}{64u^8} + \frac{1}{120u^6}\right\}$$

$$-\bar{P}\alpha\left\{\frac{3}{8u^6} - \frac{3}{16u^5\tanh u} - \frac{3}{16u^4\sinh^2 u}\right\} + \alpha^2\left\{\frac{3}{4u^3\tanh u} - \frac{3}{4u^2\sinh^2 u}\right\}$$

$$-1 = 0 \qquad (32)$$

Fig. 9 gives a plot of $\bar{P}$ against α for various values of u. Table II gives the same information. This table also gives the values of $\frac{w_m}{h}$ calculated from equation (31). An inspection of these figures shows that $\frac{w_m}{h}$ may, for all practical purposes, be expressed as a function of u alone. Fig. 10 shows a plot of average values of $\frac{w_m}{h}$ for a constant u, against u. It is seen that the relation is almost exactly linear and may be expressed by the equation

$$\frac{w_m}{h} = 0.361\,u \qquad (33)$$

It is a remarkable and unexpected result that equations (20) and (33) are identical.

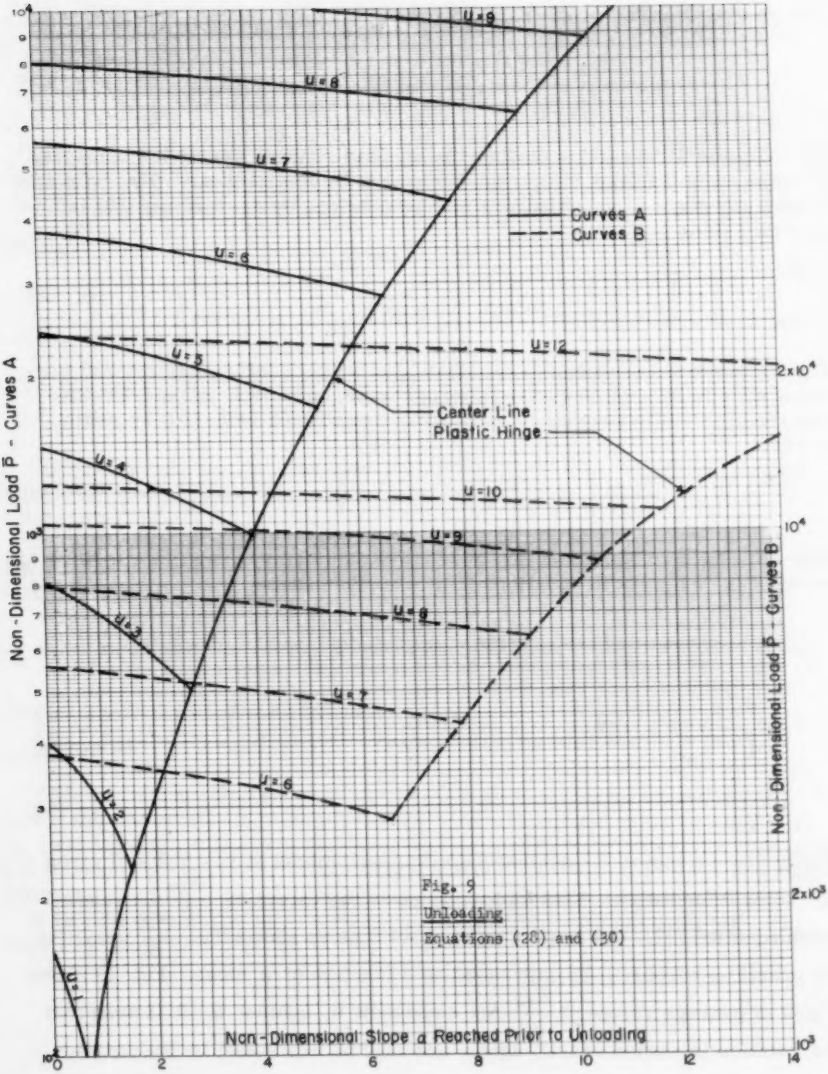

Fig. 9
Unloading
Equations (26) and (30)

TABLE II (UNLOADING)

u	α	$\bar{P}$	w_m/h	Remarks
1	.744	82.6	.368	Center Plastic Hinge
	0.00	156.2	.370	Edge Plastic Hinge
			.369 a	
2	1.743	223.1	.747	Center Plastic Hinge
	1.00	302.6	.754	
	0.00	396.9	.739	Edge Plastic Hinge
			.750 a	
3	2.765	505.8	1.11	Center Plastic Hinge
	2.00	591.6	1.12	
	1.00	706.7	1.12	
	0.00	804.2	1.11	Edge Plastic Hinge
			1.12 a	
4	3.972	981.9	1.472	Center Plastic Hinge
	3.00	1114.1	1.489	
	2.00	1238.9	1.494	
	1.00	1352.8	1.489	
	0.00	1456.2	1.473	Edge Plastic Hinge
			1.484 a	
5	5.238	1730.7	1.826	Center Plastic Hinge
	5.00	1768.7	1.832	
	4.00	1921.4	1.849	
	3.00	2063.1	1.857	
	2.00	2194.4	1.858	
	1.00	2315.5	1.851	
	0.00	2426.6	1.836	Edge Plastic Hinge
			1.844 a	
6	6.543	2819.7	2.178	Center Plastic Hinge
	6.0	2917.0	2.190	
	5.0	3087.4	2.206	
	4.0	3247.2	2.216	
	3.0	3396.7	2.219	
	2.0	3536.3	2.217	
	1.0	3666.0	2.210	
	0.0	3786.1	2.196	Edge Plastic Hinge
			2.204 a	

a = average for constant u

TABLE II (UNLOADING) - Cont'd

u	α	$\bar{P}$	w_m/h	Remarks
7	7.873	4317.3	2.529	Center Plastic Hinge
	7.00	4491.0	2.546	
	6.00	4680.0	2.561	
	5.00	4858.5	2.571	
	4.00	5026.9	2.577	
	3.00	5185.5	2.578	
	2.00	5334.4	2.574	
	1.00	5473.7	2.567	
	0.00	5603.6	2.555	Edge Plastic Hinge
			2.562 a	
8	9.217	6291.5	2.880	Center Plastic Hinge
	9.00	6340.3	2.885	
	8.00	6558.8	2.902	
	7.00	6766.7	2.916	
	6.00	6964.4	2.926	
	5.00	7152.2	2.932	
	4.00	7330.3	2.935	
	3.00	7498.7	2.934	
	2.00	7657.7	2.930	
	1.00	7807.2	2.922	
	0.00	7947.4	2.911	Edge Plastic Hinge
			2.916 a	
9	10.575	8809.0	3.231	Center Plastic Hinge
	10.00	8950.4	3.241	
	9.00	9188.0	3.257	
	8.00	9415.4	3.270	
	7.00	9632.7	3.279	
	6.00	9840.1	3.286	
	5.00	10029.7	3.288	
	4.00	10226.1	3.291	
	3.00	10404.9	3.289	
	2.00	10577.3	3.285	
	1.00	10734.6	3.277	
	0.00	10885.5	3.267	Edge Plastic Hinge
			3.272 a	
10	11.939	11938.9	3.582	Center Plastic Hinge
	11.00	12189.7	3.597	
	10.00	12446.8	3.612	
	9.00	12693.7	3.623	
	8.00	12930.7	3.633	
	7.00	13158.0	3.640	
	6.00	13375.7	3.644	
	5.00	13583.9	3.646	
	4.00	13782.8	3.646	
	3.00	13972.3	3.643	
	2.00	14152.6	3.638	
	1.00	14323.8	3.631	
	0.00	14485.7	3.622	Edge Plastic Hinge
			3.627 a	

a = average for constant u

TABLE II (UNLOADING) - Cont'd

u	α	$\bar{P}$	w_m/h	Remarks
12	14.688	20304.4	4.274	Center Plastic Hinge
	14.00	20521.0	4.294	
	13.00	20827.5	4.308	
	12.00	21124.0	4.320	
	11.00	21410.6	4.330	
	10.00	21687.6	4.339	
	9.00	21954.9	4.345	
	8.00	22212.9	4.350	
	7.00	22461.4	4.354	
	6.00	22700.6	4.355	
	5.00	22930.6	4.355	
	4.00	23151.5	4.353	
	3.00	23363.1	4.350	
	2.00	23565.8	4.345	
	1.00	23759.4	4.338	
	0.00	23943.9	4.330	Edge Plastic Hinge
			4.338 a	

a = average for constant u

Unloaded Plate

Certain important quantities when the plate is completely unloaded may be obtained from the above equations by letting $\bar{P} = 0$.

The maximum residual deflection is obtained by letting $\bar{P} = 0$ in (31). There follows:

$$\left(\frac{w_m}{h}\right)_{\text{residual}} = \frac{\alpha\,(\cosh u - 1)}{2u \sinh u} \tag{34}$$

In equation (34) α is the maximum non-dimensional edge slope reached prior to unloading and u is the residual value of the tension parameter after complete unloading. The relation between these two quantities is obtained by setting $\bar{P} = 0$ in equation (32). Thus:

$$\alpha^2 = \frac{4u^3}{3} \quad \frac{\tanh u \sinh^2 u}{\sinh^2 u - u \tanh u} \tag{35}$$

Equations (34) and (35) are plotted in Fig. (11). Table III shows the figures from which these curves have been drawn.

Example

In Figure 12 are shown two curves taken from Mr. Clarkson's paper.[6] One is a plot of non-dimensional deflection against non-dimensional load and the other non-dimensional residual deflection against non-dimensional load. The curves are for a plate of strength parameter 26.3. On the same chart

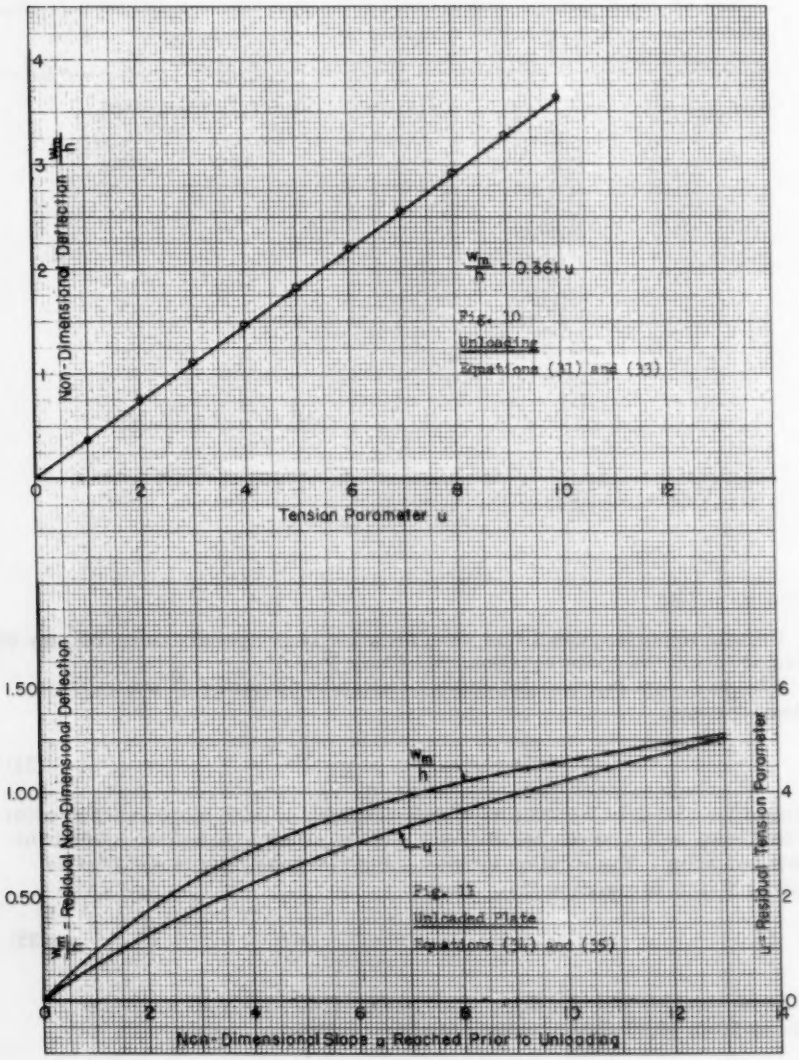
Non-Dimensional Deflection $\frac{w_m}{h}$
$\frac{w_m}{h} = 0.36 + u$
Fig. 10
Unloading
Equations (11) and (13)
Tension Parameter u
$\frac{w_m}{h}$ = Residual Non-Dimensional Deflection
$\frac{w_m}{h}$
$\frac{w_m}{h} = u$
Fig. 11
Unloaded Plate
Equations (34) and (35)
u = Residual Tension Parameter
Non-Dimensional Slope g Reached Prior to Unloading

TABLE III (UNLOADED PLATE)

RESIDUAL DEFLECTION & TENSION

α Reached Prior to Unloading	Residual u	Residual $\frac{w_m}{h}$
1.506	1.0	.348
2.411	1.5	.511
3.471	2.0	.661
4.695	2.5	.797
6.076	3.0	.917
7.502	3.5	1.01
9.259	4.0	1.11
11.03	4.5	1.20
12.92	5.0	1.27
14.897	5.5	1.34
16.97	6.0	1.41

are shown circled points representing results obtained by interpolation from curves given in the present paper. (Some of these values were also calculated and are shown in Tables I and II). The agreement between the two solutions is clearly close.

To obtain, for example, the load corresponding to the formation of a plastic hinge at the center line, Figure 5 is used. For B = 26.3, it is seen that P_L = 6400 and u = 8.1. From Figure 7, the non-dimensional deflection is found to be 2.95. For permanent set information read in Figure 5, P = 4600 for u = 7. Entering Figure 8 with these values, α = 6.6. With α = 6.6, Figure 11 gives the residual non-dimensional deflection as 0.95.

CONCLUSIONS

The question naturally arises as to the applicability of these results for plates with length-width ratios other than infinity. Levy and Greenman[8] have made a study of this problem for the elastic case by using the exact solution of von Karman's equations for a clamped rectangular plate with length-width ratio of 1.5. Their conclusion is that, for the elastic range, the maximum stresses and center deflection for a plate of such proportions differ less than 3 percent from the corresponding values for infinitely long

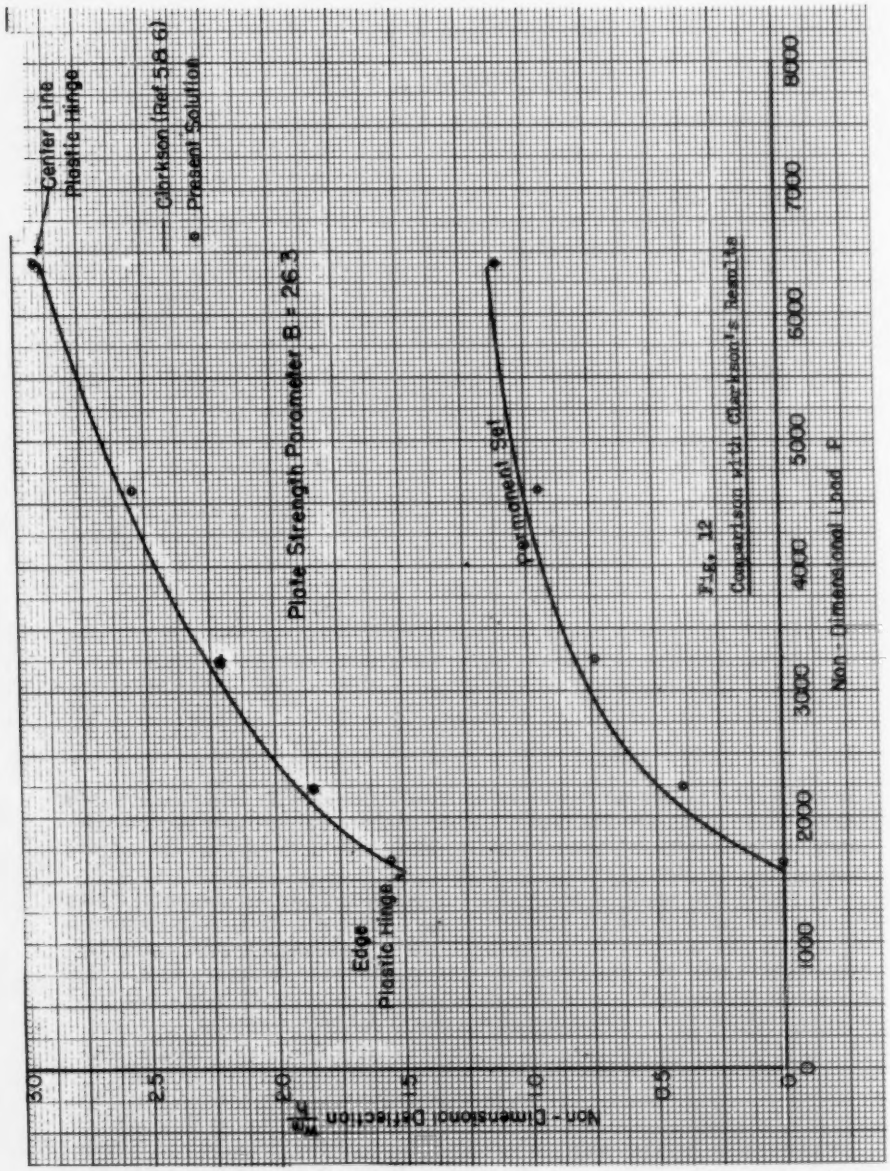
Center Line
Plastic Hinge
Clarkson (Ref 58 6)
Present Solution
Plate Strength Parameter B = 26.3
Edge
Plastic Hinge
Permanent Set
Fig. 12
Comparison with Clarkson's Results
Non - Dimensional Deflection
Non - Dimensional Load P
0
0.5
1.0
1.5
2.0
2.5
3.0
1000
2000
3000
4000
5000
6000
7000
8000

plates. While this does not give quantitative figures for the elasto-plastic case, it would seem a safe assumption that for design purposes, a plate of length-width ration ≥ 3 may be assumed to be infinitely long. Clarkson[5] has come to a similar conclusion.

The formulas derived in this paper are entirely theoretical and based on several idealizations which cannot be exactly duplicated in practice. In particular, the boundary conditions (whether, for example, the edges can be assumed to be infinitely rigid in the plane of the plate) will have an effect on the results. It is to be noted that while infinitely long plates will not develop membrane stress if the condition of "no pull in" is replaced by one of free edge displacement, a plate of finite aspect ratio always develops large membrane stress whether or not the supports are immovable. Furthermore, in many practical applications, such as in ship bulkheads, where a panel of plating may be regarded as being in an infinite field of such panels, the rigidity of the edges is effectively infinite from considerations of symmetry. The present solution may be expected to yield reasonably good results for such cases. Solutions for many other boundary conditions can evidently be obtained by the method presented in this paper.

ACKNOWLEDGMENT

A large portion of the work contained in this paper was carried out under Project No. 5-780-2 (IR), sponsored by Southwest Research Institute, San Antonio, Texas, under the Associates Plan. The numerical results were obtained by means of the electronic digital computer operated by the Institute.

The basic inspiration for this paper came from Mr. J. Clarkson's two articles[5,6] and the author wishes to acknowledge this debt. The author is grateful to Mr. Martin Goland and Dr. Edward Wenk, Jr., Director of the Institute and Chairman of the Department of Engineering Mechanics, respectively, for their encouragement and for giving him the opportunity to carry out this work.

The author is greatly indebted to Mr. Victor W. H. Chu, Research Engineer at the Institute, for his careful scrutiny of the manuscript. Mrs. Julia K. Childs, Research Engineer, kindly prepared the figures and charts.

REFERENCES

1. Timoshenko, S., Theory of Plates and Shells, McGraw-Hill Co., Inc. 1940.
2. Johansen, K., Moments of Rupture of Cross-Reinforced Slabs, First Congress Int. Assoc. of Bridge & Structural Engineering 1932, p. 277.
3. Hognestad, E., Yield-Line Theory for Ultimate Flexural Strength of Reinforced Concrete Slabs., Journal of the A. C. I. March 1953, p 637.
4. Levy, S., Bending of Rectangular Plates with Large Deflections, NACA Report No. 737, 1942.
5. Clarkson, J., A New Approach to the Design of Plates to Withstand Lateral Pressure, Quarterly Trans. of the Inst. of Naval Architects, Oct. 1956, pp 445.

6. Clarkson, J., The Strength of Approximately Flat Long Rectangular Plates Under Lateral Pressure, N. E. Coast Inst. of Engineers and Shipbuilders, November 1957, p. 21.

7. See, for example, Prager, W. and Hodge, Jr., P. G., Theory of Perfectly Plastic Solids, John Wiley, New York, 1951, p. 22.

8. "Bending with Large Deflection of a Clamped Rectangular Plate with Length-Width Ratio of 1.5 Under Normal Pressure," NACA TN No. 853.

APPENDIX

Notation

B	-	$\frac{1-\nu^2}{\sqrt{1-\nu+\nu^2}} \frac{\sigma_s l^2}{E h^2}$	"Plate Strength Parameter"
D	-	$\frac{Eh^3}{12(1-\nu^2)}$	Plate Stiffness
E	-	Modulus of Elasticity	
N_x	-	Membrane Tension	
P	-	$\frac{ql^4}{Dh} = \frac{12(1-\nu^2)l^4 q}{Eh^4}$	"Non-dimensional Load"
P_E	-	Non-dimensional Load at Formation of Plastic Hinges at Edges	
P_L	-	Non-dimensional Limit Load	
h	-	Thickness of Plate	
l	-	Length of Plate	
q	-	Uniformly Distributed Load per Unit Length	
u	-	$\left(\frac{N_x l^2}{4D}\right)^{\frac{1}{2}}$	Tension Parameter
w	-	Deflection of Plate	
w_m	-	Maximum Deflection of Plate	
x,y	-	Coordinate Axes	
α	-	"Non-dimensional Edge Slope"	
ν	-	Poisson's Ratio	
σ_s	-	Yield Stress in Tension	
σ_x	-	Stress in x Direction	
σ_y	-	Stress in y Direction	
τ_{xy}	-	Shearing Stress	

Paper 1831 October, 1958 EM 4

Journal of the

ENGINEERING MECHANICS DIVISION

Proceedings of the American Society of Civil Engineers

CONTENTS

DISCUSSION
(Proc. Paper 1831)

DEMONSTRATIONS OF PLASTIC BEHAVIOR OF STEEL FRAMES[a]

Closure by H. M. Nelson, D. T. Wright and J. W. Dolphin

H. M. NELSON,[1] D. T. WRIGHT,[2] J. M. ASCE and J. W. DOLPHIN.[3]—The writers are very glad to have the contribution on the effects of shear force on plastic moments from Mr. Sobotka. Particularly so because it shows that the difficult problem of shear effects has been approached, independently, by the method that Baker, Horne and Heyman[1] also favoured and which the writers think is the best yet available for practical use.

However, their equation (1) i.e.

$$\frac{M_p'}{M_p} = 1 - \frac{M_w}{M_p}\left[1 - \sqrt{1-3(\tau_w/\sigma_y)^2}\right] \qquad (1)$$

by Mr. Sobotka's approach becomes simply

$$M_p' = M_w\sqrt{1-3(\tau_w/\sigma_y)^2}$$

and they do not see the point of rewriting this in the much more complicated form of the contributer's equation (9).

The interaction diagram obtained from (1) above is, of course, identical with that in the discussion and it is useful to have this diagram formally presented. For design work a different diagram is required for each rolled section, and in practice the authors favour equation (1) or the empirical rule (3) suggested by the Lehigh team.

The writers find that in their paper they ascribed this "lower-bound" approach to Horne. . In fact it appears to have been first published by Heyman and Dutton in Welding and Metal Fabrication 1954 and subsequently by Longbottom and Heyman in the Proceedings of the Institution of Civil Engineers, Part III, August 1956.

It may be of interest to add the following additional reference:

The full plastic moments of sections subjected to shear force and axial load. M. R. Horne, British Weld. Jr. 5 (1958) April.

---

a. Proc. Paper 1390, October, 1957, by H. M. Nelson, D. T. Wright and J. W. Dolphin.

1. Lecturer in Civ. Eng., The Univ. of Glasgow, Scotland
2. Asst. Prof. of Civ. Eng., Queen's Univ., Canada
3. Prof. and Head of Dept. of Civ. Eng., Royal Military College, Canada

ANALYSIS OF CONTINUOUS BEAMS BY FOURIER SERIES[a]

Closure by Seng-Lip Lee

SENG-LIP LEE,[1] A. M. ASCE.—Mr. Medwadowski states that the advantage of having the deflection function and its derivatives continuous over intermediate supports given by the Fourier series analysis results also by employing Heaviside's step-function. That the latter is not quite true can be shown by means of the following illustration.

Consider the continuous beam shown in Fig. a. In order to determine the maximum value of R_1 produced by a moving uniformly distributed load extending over a distance of 1/2 1, Eq. (e) yields

$$R_1 = \frac{\omega}{9} \sum_{n=1}^{\infty} \frac{1}{n^4} \left(51 \sin \frac{n\pi}{3} - 45 \sin \frac{2n\pi}{3}\right) \int_{s\ell}^{(s+\frac{1}{2})\ell} \sin \frac{n\pi x}{\ell}\, dx \qquad (D\text{-}1)$$

or

$$R_1 = \frac{\omega \ell}{9\pi} \sum_{n=1}^{\infty} \frac{1}{n^5} \left(51 \sin \frac{n\pi}{3} - 45 \sin \frac{2n\pi}{3}\right) \left[\cos n\pi s - \cos n\pi (s+\tfrac{1}{2})\right]$$

The location of the load corresponding to the maximum value of R_1 is given by

$$\frac{dR_1}{ds} = 0$$

or

$$\sum_{n=1}^{\infty} \frac{1}{n^4} \left(51 \sin \frac{n\pi}{3} - 45 \sin \frac{2n\pi}{3}\right) \left[\sin n\pi (s+\tfrac{1}{2}) - \sin n\pi s\right] = 0$$

Taking only the first two terms of the series yields

$$1 - 4 \sin \pi s - \tan \pi s = 0$$

The solution of which yields S = 0.0639. The corresponding value of R_1 is

$$(R_1)_{max.} = \frac{\omega \ell}{9\pi} \sum_{n=1}^{\infty} \frac{1}{n^5} \left(51 \sin \frac{n\pi}{3} - 45 \sin \frac{2n\pi}{3}\right) (\cos 0.0639 n\pi - \cos 0.5639 n\pi)$$

$$= 0.386\, \omega \ell$$

---

a. Proc. Paper 1399, October, 1957, by Seng-Lip Lee.

1. Associate Prof. of Civ. Eng., Northwestern Univ., Evanston, Ill.

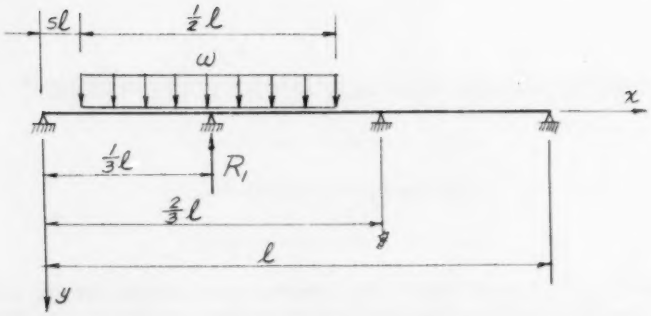

Fig.a Maximum value of R_1 due to uniformly distributed load extending over a distance of $\frac{1}{2}\ell$.

If Heaviside's step-function were used in this case, Eq. (D-1) would be replaced by

$$R_1 = \frac{27\omega}{5\ell^3}\int_{s\ell}^{(s+\frac{1}{2})\ell} \left\{ 8\left[-\frac{2}{3}x^3 + H_1(x-\tfrac{\ell}{3})^3 + \frac{10}{27}\ell^2 x\right] - 7\left[-\tfrac{1}{3}x^3 + H_2(x-\tfrac{2}{3}\ell)^3 + \tfrac{8}{27}\ell^2 x\right]\right\} dx \qquad (D\text{-}2)$$

where

$$H_1 = \begin{cases} 0 & 0 \le x \le \frac{1}{3}\ell \\ 1 & \frac{1}{3}\ell \le x \le \ell \end{cases}$$

$$H_2 = \begin{cases} 0 & 0 \le x \le \frac{2}{3}\ell \\ 1 & \frac{2}{3}\ell \le x \le \ell \end{cases}$$

Although Eq. (D-2) gives R_1 in a single expression, the integrand is actually discontinuous at x = 1/3 1 and x = 2/3 1. In this problem, it is obvious that S = 1/2 < 2/3 for which Eq. (D-2) takes the form

$$R_1 = \frac{27\omega}{5\ell^3}\left[8\int_{s\ell}^{(s+\frac{1}{2})\ell}\left(-\frac{2}{3}x^3 + \frac{10}{27}\ell^2 x\right)dx + 8\int_{\frac{1}{3}\ell}^{(s+\frac{1}{2})\ell}(x-\tfrac{\ell}{3})^3\,dx - 7\int_{s\ell}^{(s+\frac{1}{2})\ell}\left(-\tfrac{1}{3}x^3 + \tfrac{8}{27}\ell^2 x\right)dx\right]$$

For S + 1/2 < 2/3, Eq. (D-2) yields a longer expression for R_1 with additional integrals. In problems where the limits of integration are not known a priori, the choice of one or the other has to be made before differentiating to determine the value of S corresponding to (R_1) max. If the wrong choice were made, the procedure has to be repeated. This difficulty is avoided by the use of (D-1) where the integral is truly continuous between $s\ell \le x \le (s+\frac{1}{2})\ell$. That

the numerical work involved in the solution of the problem under consideration by Eq. (D-1) is less than that if Eq. (D-2) were employed is not difficult to see. Furthermore, in problems where the limits of integration extend over several supports, Eq. (D-2) yields additional integrals whereas the integrand of Eq. (D-1) remains unchanged.

The writer agrees with Mr. Medwadowski that Eq. (15) may be derived from Eq. (11) by the direct substitution of the prescribed deflections of the intermediate supports $y(a_m l) = -d_m$. The reason for using Eq. (13) with the aid of Castigliano's theorem can be explained by the example shown in Fig. b.

To determine the reactions of the springs on the beams loaded as shown, the center reaction R_1 is taken as the redundant quantity. For this case, Eq. (13) takes the form

$$U = \frac{l^5}{4\pi^4 EI}\sum_{n=1}^{\infty}\frac{1}{n^4}C_n^2 + \frac{1}{2}\sum_{r=1}^{3}\frac{R_r^2}{K_r}$$

$$= \frac{l^3}{\pi^4 EI}\sum_{n=1}^{\infty}\frac{1}{n^4}\left(P\sin\frac{n\pi}{4} - R_1\sin\frac{n\pi}{2}\right)^2 + \frac{1}{2K}\sum_{n=1}^{3}R_r^2$$

where $K = k\dfrac{EI}{l^3}$ is the spring constant and the values of R_r, the spring reactions, are shown in Fig. b in terms of R_1. The application of the theorem of minimum energy leads to

$$\frac{dU}{dR_1} = 0$$

or

$$-\sum_{n=1}^{\infty}\frac{1}{n^4}\sin\frac{n\pi}{2}\left(P\sin\frac{n\pi}{4} - R_1\sin\frac{n\pi}{2}\right) + \frac{1}{2k}\left(\frac{3}{2}R_1 - \frac{1}{2}P\right) = 0$$

solving which yields

$$R_1 = \frac{0.688 + 24.0/k}{1 + 72.0/k}P$$

For infinitely stiff springs, $k \to \infty$ for which $R_1 = 0.688P$ whereas for very flexible springs, $k \to 0$ for which $R_1 = \dfrac{P}{3}$.

It should be observed in this case that the energy method makes it unnecessary to consider the deflections at the spring supports and lends itself to a simpler solution, whereas the other approach involves a somewhat lengthier procedure. The above example was a part of the original draft which was subsequently shortened to the form presented.

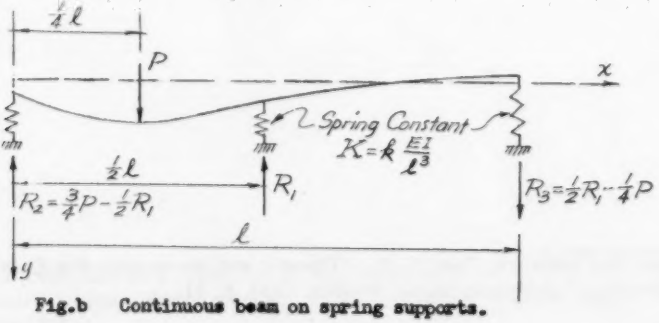

Fig.b Continuous beam on spring supports.

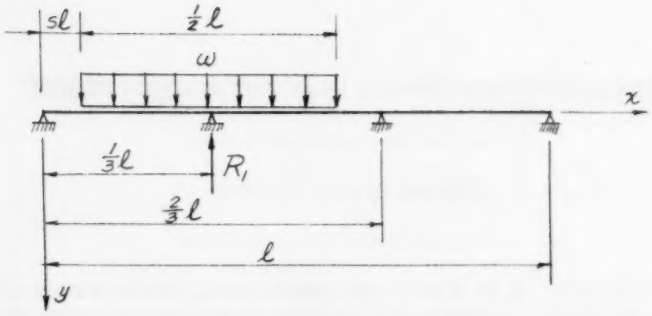

Fig.a Maximum value of R_1 due to uniformly distributed load extending over a distance of $\frac{1}{2}\ell$.

If Heaviside's step-function were used in this case, Eq. (D-1) would be replaced by

$$R_1 = \frac{27\omega}{5\ell^3}\int_{s\ell}^{(s+\frac{1}{2})\ell} \left\{ 8\left[-\frac{2}{3}x^3 + H_1(x-\frac{\ell}{3})^3 + \frac{10}{27}\ell^2 x\right] - 7\left[-\frac{1}{3}x^3 + H_2(x-\frac{2}{3}\ell)^3 + \frac{8}{27}\ell^2 x\right]\right\} dx \qquad (D\text{-}2)$$

where

$$H_1 = \begin{cases} 0 & 0 \le x \le \frac{1}{3}\ell \\ 1 & \frac{1}{3}\ell \le x \le \ell \end{cases}$$

$$H_2 = \begin{cases} 0 & 0 \le x \le \frac{2}{3}\ell \\ 1 & \frac{2}{3}\ell \le x \le \ell \end{cases}$$

Although Eq. (D-2) gives R_1 in a single expression, the integrand is actually discontinuous at x = 1/3 1 and x = 2/3 1. In this problem, it is obvious that S = 1/2 < 2/3 for which Eq. (D-2) takes the form

$$R_1 = \frac{27\omega}{5\ell^3}\left[8\int_{s\ell}^{(s+\frac{1}{2})\ell} (-\frac{2}{3}x^3 + \frac{10}{27}\ell^2 x)\,dx + 8\int_{\frac{1}{3}\ell}^{(s+\frac{1}{2})\ell} (x-\frac{\ell}{3})^3\,dx - 7\int_{s\ell}^{(s+\frac{1}{2})\ell} (-\frac{1}{3}x^3 + \frac{8}{27}\ell^2 x)\,dx\right]$$

For S + 1/2 < 2/3, Eq. (D-2) yields a longer expression for R_1 with additional integrals. In problems where the limits of integration are not known a priori, the choice of one or the other has to be made before differentiating to determine the value of S corresponding to (R_1) max. If the wrong choice were made, the procedure has to be repeated. This difficulty is avoided by the use of (D-1) where the integral is truly continuous between $s\ell \le x \le (s+\frac{1}{2})\ell$. That

the numerical work involved in the solution of the problem under consideration by Eq. (D-1) is less than that if Eq. (D-2) were employed is not difficult to see. Furthermore, in problems where the limits of integration extend over several supports, Eq. (D-2) yields additional integrals whereas the integrand of Eq. (D-1) remains unchanged.

The writer agrees with Mr. Medwadowski that Eq. (15) may be derived from Eq. (11) by the direct substitution of the prescribed deflections of the intermediate supports $y(a_m \ell) = -d_m$. The reason for using Eq. (13) with the aid of Castigliano's theorem can be explained by the example shown in Fig. b.

To determine the reactions of the springs on the beams loaded as shown, the center reaction R_1 is taken as the redundant quantity. For this case, Eq. (13) takes the form

$$U = \frac{\ell^5}{4\pi^4 EI} \sum_{n=1}^{\infty} \frac{1}{n^4} C_n^2 + \frac{1}{2} \sum_{r=1}^{3} \frac{R_r^2}{K_r}$$

$$= \frac{\ell^3}{\pi^4 EI} \sum_{n=1}^{\infty} \frac{1}{n^4} \left(P \sin \frac{n\pi}{4} - R_1 \sin \frac{n\pi}{2} \right)^2 + \frac{1}{2K} \sum_{n=1}^{3} R_r^2$$

where $K = k \frac{EI}{1^3}$ is the spring constant and the values of R_r, the spring reactions, are shown in Fig. b in terms of R_1. The application of the theorem of minimum energy leads to

$$\frac{dU}{dR_1} = 0$$

or

$$-\sum_{n=1}^{\infty} \frac{1}{n^4} \sin \frac{n\pi}{2} \left(P \sin \frac{n\pi}{4} - R_1 \sin \frac{n\pi}{2} \right) + \frac{1}{2k} \left(\frac{3}{2} R_1 - \frac{1}{2} P \right) = 0$$

solving which yields

$$R_1 = \frac{0.688 + 24.0/k}{1 + 72.0/k} P$$

For infinitely stiff springs, $k \to \infty$ for which $R_1 = 0.688P$ whereas for very flexible springs, $k \to 0$ for which $R_1 = \frac{P}{3}$.

It should be observed in this case that the energy method makes it unnecessary to consider the deflections at the spring supports and lends itself to a simpler solution, whereas the other approach involves a somewhat lengthier procedure. The above example was a part of the original draft which was subsequently shortened to the form presented.

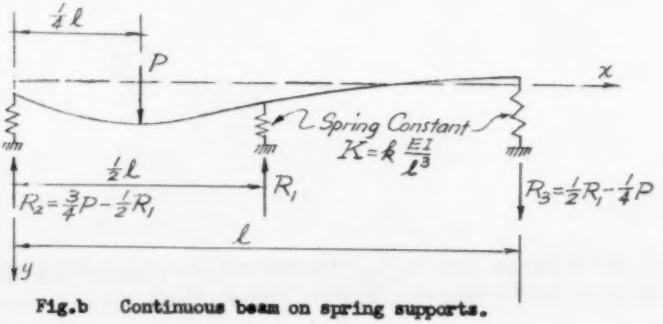

Fig.b Continuous beam on spring supports.

Mr. Medwadowski questions the correctness of the statement that a given load and the reactions of the intermediate supports can be approximated by Fourier series of the type given by Eq. (4). The writer differs with him on this point and wishes to point out that the well known technique of representing load functions by Fourier series has been used by other authors.[2] The laborious part in the analysis of continuous beams lies in the determination of the deflection and slope functions including the influence lines for reactions. To these ends, among others, it has been demonstrated that the Fourier series analysis yields simple solutions which converge rapidly. Once the redundant reactions are known, the shearing force and bending moment functions are best derived by the classical procedure of integrating the load functions.

The writer wishes to thank Mr. Medwadowski for his discussion and pertinent questions in regard to the analysis of continuous beams of constant flexural rigidity by means of Fourier series. He wishes to express his appreciation to Mr. Medwadowski for the opportunity of elaborating on some pertinent points of the paper. He is also grateful to him for mentioning the paper by Saibel and D'Appolonia. The omission was not intentional.

2. See, for instance, Bleich, F., "Theorie und Berechung der Eisernen Brucken," Julius Springer, Berlin, 1924, p. 51.

SEA BOTTOM PRESSURE FIELDS PRODUCED BY YAWED VESSELS[a]

Corrections

CORRECTIONS:—In the second footnote at the bottom of page 1496-1 and continued on bottom of page 1496-2 the phrase that presently reads "at a speed ($\sqrt{gh}$," should read "at a speed less than $1/3\sqrt{gh}$." The factor b/c appearing on the right-hand side of Equation (3b) should be replaced by b/a. The lower limit on the integral of equation (3c) should read o instead of λ. Also in the caption of Figure 2 the ratio a:b:c which now reads "a:b:c = 10.50 = 1:11:1" should read "a:b:c = 10.50:1.11:1."

a. Proc. Paper 1496, January, 1958, by P. M. Fitzpatrick.

1. Hydrodynamics Branch, Research Div., U. S. Navy Mine Defense Lab., Panama City, Fla.

EFFECT OF DEFLECTION ON LATERAL BUCKLING STRENGTH[a]

Corrections by J. W. Clark[1] and A. H. Knoll,[2]

CORRECTIONS.—Page 2, line 2: The reference should be to Pettersson, rather than Pattersson.

Page 11, line following Eq. (17): The variable eliminated should be v, not ν.

Page 11: The number for Eq. (18) should follow the equation immediately above the one that is now marked as Eq. (18).

Page 12, line 3: Change C to C_1.

a. Proc. Paper 1596, April, 1958, by J. W. Clark and A. H. Knoll.

1. Asst. Chf., Eng. Design Div., Alcoa Research Laboratories, New Kensington, Pa.
2. Research Engr. Eng. Design Div., Alcoa Research Laboratories, New Kensington, Pa.

INCREMENTAL COMPRESSION TEST FOR CEMENT RESEARCH[a]

Discussion by Keith Jones

KEITH JONES,[1] M. ASCE—The civil engineering profession is in urgent need of a more complete and detailed understanding of the physical behavior of concrete and its constituent materials with particular regard to the elastic and creep properties of those materials. That need is accentuated by the increasing use of thin-shell and prestressed concrete designs.

The incremental compression test, as devised and described by Mr. Hrennikoff, offers a new avenue of approach to the investigation of the macroscopic properties of cement and concrete. Further investigations by means of this test, particularly if applied to concrete, can be expected to yield information applicable to design. It is probable, though, that the phenomenon of creep is of a basically molecular nature and therefore fully explainable only in terms of molecular movement perhaps related to crystalline behavior.

Previous tests, to the best of this writer's knowledge, have described creep phenomena under long-time sustained loading and the recovery of creep deformation has not been so strikingly evident from those tests. Such tests do, however, more nearly duplicate the conditions actually experienced by concrete in structures. As a more complete understanding of creep and related effects such as a variable Poisson's ratio is gained, criteria may be established which would enable the prediction of long-term structural behavior of any particular concrete based on findings from short-term incremental compression tests similar to those of Mr. Hrennikoff.

The variation of μ during creep as compared with the constancy of that ratio during change of load is, to this writer, the most suprising and perhaps the most significant fact presented in the paper. From Fig. 13 of the author's paper it appears that μ, measured for a particular period of creep, is related to the amount of creep taking place during that period. The top and bottom graphs of Fig. 13 show that, in general, the longer abscissas of creep strain accompany the higher ordinates of μ. In comparison, the constancy of μ during change of load is accompanied by substantially equal changes of load and of strain. It would be interesting to see a chart similar to Fig. 13 applied to a test of a dry specimen similar to Fig. 14 or 15 where the creep strain for each period is smaller and more nearly constant.

A second significant fact is revealed by comparing the area between the loading and unloading curves of moist specimens with that of dry specimens. That hysteresis loop represents a net expenditure of energy which is much greater for moist than for dry specimens. It is probable that a complete

---

a. Proc. Paper 1604, April 1958, by A. Hrennikoff.

1. Engr., Commissioner's Office, Bureau of Reclamation, Denver, Colo.

accounting of the energy represented by the hysteresis loop will eventually be available to aid the rational and mathematical explanation of creep and its attendant phenomena.

Mr. Hrennikoff is to be congratulated on his initiation of a new test aimed at determining the fundamental properties of our most economical, widely used, and least understood structural material. His departure from conventional concepts based on elastic theory where the effects of creep are subordinate and his substitution of tests in which creep is allowed to assume equal importance with elastic deformation may be expected to contribute new and more usable and accurate design criteria as those tests are extended in scope, usage and acceptance.

LIMIT ANALYSIS OF SIMPLY SUPPORTED CIRCULAR SHELL ROOFS[a]

Corrections

CORRECTIONS—Because of errors and omissions which occurred inadvertently in the printing of Proceedings Paper 1706, a listing of necessary corrections as given below is considered advisable to permit proper understanding of the paper:

On page 1706-4, after the 3rd paragraph ending "and these are pictured in Fig. 3", insert the following:

Equilibrium.— A precise theory of cylindrical shells must be concerned with at least 8 stress resultants, namely 3 membrane forces, 2 radial shears, 1 twisting moment and 2 bending moments. However as reported by Timoshenko (Reference 3, page 447) and in ASCE Manual No. 31 (Reference 4, page 43), practical results in the elastic range for the type of shell herein considered indicate that the only significant stress resultants are the 3 membrane forces, N_x, N_ϕ, S, the transverse radial shear, Q, and the transverse bending moment M. We shall here make the assumption that the remaining stress resultants may be neglected in the plastic as well as in the elastic range. Further, the usual assumption that the radial shear does insignificant work is also made herein. Therefore, the radial shear is a reaction, rather than a generalized stress (Reference 11); it does not appear in the yield condition, and it may be eliminated from the working equations.

With the coordinate system of Fig. 1, the equilibrium equations using dimensionless stress resultants are

$$n_\varphi + h\frac{\partial^2 m}{\partial \varphi^2} + P = 0 \qquad (a),$$

$$\sqrt{3}\, r\frac{\partial n_x}{\partial y} + \frac{\partial s}{\partial \varphi} = 0 \qquad (b), \qquad (21)$$

$$\frac{\partial n_\varphi}{\partial \varphi} + \frac{r}{\sqrt{3}}\frac{\partial s}{\partial y} - h\frac{\partial m}{\partial \varphi} = 0 \qquad (c).$$

For the case of the shell with simply supported ends and free edges, the stress resultant boundary conditions are noted below.

(1) Along the free edges $\varphi = \pm \varphi_o$,

$$m = 0 \quad (a), \quad Q = 0 \therefore \frac{\partial m}{\partial \varphi} = 0 \quad (b), \qquad (22)$$

$$n_\varphi = 0 \quad (c), \quad s = 0 \quad (d).$$

a. Proc. Paper 1706, July, 1958, by M. N. Fialkow.

(2) Along the simply supported ends $y = \pm 1$,

$$n_x = 0 \quad (e). \tag{22}$$

On page 1706-7, on the 4th and 6th lines, substitute "$\frac{\partial m}{\partial \varphi}$" in lieu of "$\frac{\sigma m}{\sigma \varphi}$"

On page 1706-7, on the 24th line, in lieu of "Section IV", substitute, "the section on Kinematically Admissible Velocity Fields".

On page 1706-12, delete the last three equations (63) and substitute, the following in lieu thereof:

$$\begin{aligned} "G_A = G(o,o) &= -n_{x_A}(o) - m(o) - n_\varphi(o) \leq 1 \\ H_A = H(o) &= -m(o) \quad -n_\varphi(o) \leq 1 \\ N_A = N(o) &= -n_{x_A}(o) \leq 1 \end{aligned} \tag{63}$$

On page 1706-13, on the 2nd line, in lieu of "Section IV", substitute, "the Section on Kinematically Admissible Velocity Fields".

On page 1706-15, on the 8th line, in lieu of "Section IV" substitute, "the section on Kinematically Admissible Velocity Fields".

On page 1706-15, on the 32nd line, substitute, "$\frac{\partial m}{\partial \varphi}$" in lieu of "$\frac{\sigma m}{\sigma \varphi}$".

On page 1706-18, on the 19th line, in lieu of "Section III", substitute, "the section on Statically Admissible Stress Fields".

On page 1706-20, the 20th line should read "where $A = \frac{1}{1+h}$".

On page 1706-21, in the first of equations (58), the sign of the fourth term in the bracket in the numerator should be +.

On page 1706-22, on the 3rd line from the bottom, change the first word from "Considered" to "Certain".

PROCEEDINGS PAPERS

The technical papers published in the past year are identified by number below. Technical-division sponsorship is indicated by an abbreviation at the end of each Paper Number, the symbols referring to: Air Transport (AT), City Planning (CP), Construction (CO), Engineering Mechanics (EM), Highway (HW), Hydraulics (HY), Irrigation and Drainage (IR), Pipeline (PL), Power (PO), Sanitary Engineering (SA), Soil Mechanics and Foundations (SM), Structural (ST), Surveying and Mapping (SU), and Waterways and Harbors (WW), divisions. Papers sponsored by the Board of Direction are identified by the symbols (BD). For titles and order coupons, refer to the appropriate issue of "Civil Engineering." Beginning with Volume 12 (January 1956) papers were published in Journals of the various Technical Divisions. To locate papers in the Journals, the symbols after the paper numbers are followed by a numeral designating the issue of a particular Journal in which the paper appeared. For example, Paper 1440 is identified as 1440 (HY 5) which indicates that the paper is contained in the fifth issue of the Journal of the Hydraulics Division during 1957.

VOLUME 83 (1957)

OCTOBER: 1387(CP2), 1388(CP2), 1389(EM5), 1390(EM4), 1391(HY5), 1392(HY5), 1393(HY5), 1394(HY5), 1395(HY5), 1396(PO5), 1397(PO5), 1398(PO5), 1399(EM4), 1400(SA5), 1401(HY5), 1402(HY5), 1403(HY5), 1404(HY5), 1405(HY5), 1406(HY5), 1407(SA5), 1408(SA5), 1409(SA5), 1410(SA5), 1411(SA5), 1412(EM4), 1413(EM4), 1414(PO5), 1415(EM4)[C], 1416(PO5)[C], 1417(ST5)[C], 1418(EM4), 1419(PO5), 1420(PO5), 1421(PO5), 1422(SA5)[C], 1423(SA5), 1424(EM4), 1425(CP2).

NOVEMBER: 1426(SM4), 1427(SM4), 1428(SM4), 1429(SM4), 1430(SM4)[C], 1431(ST6), 1432(ST6), 1433(ST6), 1434(ST6), 1435(ST6), 1436(ST6), 1437(ST6), 1438(SM4), 1439(SM4), 1440(ST5), 1441(ST6), 1442(ST6), 1443(SU2), 1444(SU2), 1445(SU2), 1446(SU2), 1447(SU2), 1448(SU2)[C].

DECEMBER: 1449(IR5), 1450(HY6), 1451(HY6), 1452(HY6), 1453(HY6), 1454(HY6), 1455(HY6), 1456(HY6)[C], 1457(PO6), 1458(PO6), 1459(PO6), 1460(PO6)[C], 1461(SA6), 1462(SA6), 1463(SA6), 1464(SA6), 1465(SA6), 1466(SA6)[C], 1467(AT2), 1468(AT2), 1469(AT2), 1470(AT2), 1471(AT2), 1472(AT2), 1473(AT2), 1474(AT2), 1475(AT2), 1476(AT2), 1477(AT2), 1478(AT2), 1479(AT2), 1480(AT2), 1481(AT2), 1482(AT2), 1483(AT2), 1484(AT2), 1485(AT2)[C], 1486(BD2), 1487(BD2), 1488(PO6), 1489(PO6), 1490(BD2), 1491(BD2), 1492(BD2), 1493(BD2).

VOLUME 84 (1958)

JANUARY: 1494(EM1), 1495(EM1), 1496(EM1), 1497(IR1), 1498(IR1), 1499(IR1), 1500(IR1), 1501(IR1), 1502(IR1), 1503(IR1), 1504(IR1), 1505(IR1), 1506(IR1), 1507(IR1), 1508(ST1), 1509(ST1), 1510(ST1), 1511(ST1), 1512(ST1), 1513(WW1), 1514(WW1), 1515(WW1), 1516(WW1), 1517(WW1), 1518(WW1), 1519(ST1), 1520(EM1)[C], 1521(IR1)[C], 1522(IR1)[C], 1523(WW1)[C], 1524(HW1), 1525(HW1)[C], 1526(HW1).

FEBRUARY: 1527(HY1), 1528(PO1), 1529(HY1), 1530(HY1), 1531(HY1), 1532(HY1), 1533(SA1), 1534(SA1), 1535(SM1), 1536(SM1), 1537(SM1), 1538(PO1)[C], 1539(SA1), 1540(SA1), 1541(SA1), 1542(SA1), 1543(SA1), 1544(SM1), 1545(SM1), 1546(SM1), 1547(SM1), 1548(SM1), 1549(SM1), 1550(SM1), 1551(SM1), 1552(SM1), 1553(PO1), 1554(PO1), 1555(PO1), 1556(PO1), 1557(SA1)[C], 1558(HY1)[C], 1559(SM1)[C].

MARCH: 1560(ST2), 1561(ST2), 1562(ST2), 1563(ST2), 1564(ST2), 1565(ST2), 1566(ST2), 1567(ST2), 1568(WW2), 1569(WW2), 1570(WW2), 1571(WW2), 1572(WW1), 1573(WW2), 1574(PL1), 1575(PL1), 1576(ST2)[C], 1577(PL1), 1578(PL1)[C], 1579(WW2)[C].

APRIL: 1580(EM2), 1581(EM2), 1582(HY2), 1583(HY2), 1584(HY2), 1585(HY2), 1586(HY2), 1587(HY2), 1588(HY2), 1589(IR2), 1590(IR2), 1591(IR2), 1592(SA2), 1593(SU1), 1594(SU1), 1595(SU1), 1596(EM2), 1597(PO2), 1598(PO2), 1599(PO2), 1600(PO2), 1601(PO2), 1602(PO2), 1603(HY2), 1604(EM2), 1605(SU1)[C], 1606(SA2), 1607(SA2), 1608(SA2), 1609(SA2), 1610(SA2), 1611(SA2), 1612(SA2), 1613(SA2), 1614(SA2)[C], 1615(IR2)[C], 1616(HY2)[C], 1617(SU1), 1618(PO2)[C], 1619(EM2)[C], 1620(CP1).

MAY: 1621(HW2), 1622(HW2), 1623(HW2), 1624(HW2), 1625(HW2), 1626(HW2), 1627(HW2), 1628(HW2), 1629(ST), 1630(ST3), 1631(ST3), 1632(ST3), 1633(ST3), 1634(ST3), 1635(ST3), 1636(ST3), 1637(ST3), 1638(ST3), 1639(WW3), 1640(WW3), 1641(WW3), 1642(WW3), 1643(WW3), 1644(WW3), 1645(SM2), 1646(SM2), 1647(SM2), 1648(SM2), 1649(SM2), 1650(SM2), 1651(HW2), 1652(HW2)[C], 1653(WW2)[C], 1654(SM2), 1655(SM2), 1656(ST2)[C], 1657(SM2)[C].

JUNE: 1658(AT1), 1659(AT1), 1660(HY3), 1661(HY3), 1662(HY3), 1663(ST2), 1664(HY3), 1665(SA3), 1666(PL2), 1667(PL2), 1668(PL2), 1669(AT1), 1670(PO3), 1671(PO3), 1672(PO3), 1673(PL2), 1674(PL2), 1675(PO3), 1676(PO3), 1677(SA3), 1678(SA3), 1679(SA3), 1680(SA3), 1681(SA3), 1682(SA3), 1683(PO3), 1684(HY3), 1685(SA3), 1686(SA3), 1687(PO3), 1688(SA3)[C], 1689(PO3)[C], 1690(HY3)[C], 1691(PL2)[C].

JULY: 1692(EM3), 1693(EM3), 1694(ST4), 1695(ST4), 1696(ST4), 1697(SU2), 1698(SU2), 1699(SU2), 1700(SU2), 1701(SA4), 1702(SA4), 1703(SA4), 1704(SA4), 1705(SA4), 1706(EM3), 1707(ST4), 1708(ST4), 1709(ST4), 1710(ST4), 1711(ST4), 1712(ST4), 1713(SU2), 1714(SA4), 1715(SA4), 1716(SU2), 1717(SA4), 1718(EM3), 1719(EM3), 1720(SU2), 1721(ST4)[C], 1722(ST4), 1723(ST4), 1724(EM3)[C].

AUGUST: 1725(HY4), 1726(HY4), 1727(SM3), 1728(SM3), 1729(SM3), 1730(SM3), 1731(SM3), 1732(SM3), 1733(PO4), 1734(PO4), 1735(PO4), 1736(PO4), 1737(PO4), 1738(PO4), 1739(PO4), 1740(PO4), 1741(PO4), 1742(PO4), 1743(PO4), 1744(PO4), 1745(PO4), 1746(PO4), 1747(PO4), 1748(PO4), 1749(PO4).

SEPTEMBER: 1750(IR3), 1751(IR3), 1752(IR3), 1753(IR3), 1754(IR3), 1755(ST5), 1756(ST5), 1757(ST5), 1758(ST5), 1759(ST5), 1760(ST5), 1761(ST5), 1762(ST5), 1763(ST5), 1764(ST5), 1765(WW4), 1766(WW4), 1767(WW4), 1768(WW4), 1769(WW4), 1770(WW4), 1771(WW4), 1772(WW4), 1773(WW4), 1774(WW4), 1775(IR3), 1776(IR3), 1777(SA5), 1778(SA5), 1779(SA5), 1780(SA5), 1781(WW4), 1782(SA5), 1783(SA5), 1784(IR3)[C], 1785(WW4)[C], 1786(SA5)[C], 1787(SA5)[C], 1788(SA5), 1789(WW4).

OCTOBER: 1790(EM4), 1791(EM4), 1792(EM4), 1793(EM4), 1794(EM4), 1795(HW3), 1796(HW3), 1797(HW3), 1798(HW3), 1799(HW3), 1800(HW3), 1801(HW3), 1802(HW3), 1803(HW3), 1804(HW3), 1805(HW3), 1806(HY5), 1807(HY5), 1808(HY5), 1809(HY5), 1810(HY5), 1811(EM5), 1812(SM4), 1813(SM4), 1814(ST7), 1815(ST6), 1816(ST6), 1817(ST6), 1818(ST6), 1819(ST6), 1820(ST6), 1821(ST6), 1822(SM4), 1823(PO5), 1824(SM4), 1825(SM4), 1826(SM4), 1827(ST6)[C], 1828(SM4)[C], 1829(HW3)[C], 1830(PO5)[C], 1831(SM4)[C], 1832(HY5)[C].

C. Discussion of several papers grouped by divisions.